APTD-0594

PB196499

FINAL REPORT

APTD - 0594

HOLOGRAPHIC DETERMINATION OF INJECTED LIMESTONE DISTRIBUTION IN UNIT 10 OF THE SHAWNEE POWER PLANT

JUNE 1970

prepared by

B. J. MATTHEWS and R. F. KEMP

UNDER NAPCA CONTRACT CPA 70-4
TRW REPORT NO. 14103-6001-RO-00

TRW
SYSTEMS GROUP
ONE SPACE PARK • REDONDO BEACH • CALIFORNIA

Reproduced by
NATIONAL TECHNICAL
INFORMATION SERVICE
Springfield, Va. 22151

89

FINAL REPORT

HOLOGRAPHIC DETERMINATION OF INJECTED LIMESTONE DISTRIBUTION IN UNIT 10 OF THE SHAWNEE POWER PLANT

JUNE 1970

prepared by

B. J. MATTHEWS and R. F. KEMP

UNDER NAPCA CONTRACT CPA 70-4
TRW REPORT NO. 14103-6001-RO-00

TRW
SYSTEMS GROUP
ONE SPACE PARK • REDONDO BEACH • CALIFORNIA

FOREWORD

This is the final report on the "Holographic Determination of Injected Limestone Distribution in Unit 10 of the Shawnee Power Plant." Work reported in this document was sponsored by the National Air Pollution Control Administration of the Department of Health, Education and Welfare. This report is submitted by TRW Systems Group, TRW Inc., in accordance with the provisions of NAPCA Contract CPA 70-4.

Work on this contract was accomplished by personnel of the Science and Technology Division of TRW Systems Group. The Project Manager was Mr. B. J. Matthews. Dr. R. F. Wuerker served as Consulting Principal Scientist. Mr. R. F. Kemp was a participating Staff Engineer. Technical administration of the contract was by Mr. D. K. Felton of the NAPCA Division of Process Control Engineering.

The authors wish to acknowledge the work and cooperation of the following TRW Systems personnel: Mr. D. E. Gallagher who ably assisted in both the early laboratory experiments at TRW as well as the test programs at the Shawnee Unit 10 boiler; Mr. R. J. Chouinard who provided valuable assistance in readying the pulsed ruby laser for use at the boiler; and, Mr. J. P. Mark who helped in the fabrication of mechanical components for the holocamera. The conduct of testing at the Tennessee Valley Authority's Shawnee Power Plant was aided materially by a number of persons. In particular, the coordination and assistance provided by Messrs. D. T. Clay of NAPCA, and T. D. Womble, E. L. Sanderlin and R. C. Tulis of TVA proved invaluable.

CONTENTS

Page

1. INTRODUCTION 1
   - 1.1 Shawnee Unit 10 Boiler 1
   - 1.2 Dry Limestone Injection Process 4
   - 1.3 Holographic Determination of Injected Linestone Plumes 4
2. PROGRAM SUMMARY 9
   - 2.1 Calibration Studies — Phase I 9
   - 2.2 Field Trials — Phase II and III 10
3. EXPERIMENTAL APPARATUS 12
   - 3.1 Pulsed Ruby Laser Illuminator 12
   - 3.2 Single Beam (Gabor) Holocamera 12
   - 3.3 Two-Beam Holocamera 18
   - 3.4 Reconstruction Apparatus and Techniques 23
     - 3.4.1 Reconstruction of Gabor Holograms 24
     - 3.4.2 Reconstruction of Two-Beam Holograms 25
   - 3.5 Recording Films and Processing 27
4. LABORATORY EXPERIMENTS 28
   - 4.1 Gabor Holograms 28
   - 4.2 Two-Beam Scattered Light Holograms 35
5. SHAWNEE UNIT 10 EXPERIMENTS 38
   - 5.1 Gabor Holograms — Unit 10 Superheater 38
   - 5.2 Scattered Light Holograms — Unit 10 Boiler 38
     - 5.2.1 Operating and Test Conditions 40
     - 5.2.2 Data Reduction from Holographic Reconstructions 42
6. RESULTS AND DISCUSSION 43
   - 6.1 Tests Without Limestone Injection — 140 MW 43
   - 6.2 Tests Without Limestone Injection — 85 MW 47
   - 6.3 Tests With Limestone Injection — 140 MW 48
   - 6.4 Intensity Measurements and Calibration 50
7. CONCLUSIONS 55
8. RECOMMENDATIONS FOR FUTURE WORK 57

REFERENCES R-1

CONTENTS (Continued)

Page

APPENDIXES

A The Technique of Holography A-1

B USAF 1951 Resolving Power Test Target B-1

C Data Summary Sheets Unit 10 Limestone Injection Test Holograms C-1

ILLUSTRATIONS

Page

1 Sketch of Shawnee Unit 10 Boiler 2
2 Photograph of Soot Blower Port 3
3 Photograph of Row of Limestone Injectors 3
4 Program Expenditures for 8-Month Technical Effort 5
5 Activity Summary Network 7
6 TRW Q-Switched Ruby Laser Illuminator 13
7 Ruby Laser Illuminator with Cover Removed 13
8 Schematic of Compact Ruby Laser Illuminator 14
9 Photograph of TRW Pulsed Ruby Laser Power Supply Consoles and Tektronix 535A Oscilloscope 15
10 Schematic of Single Beam Pulsed Ruby Laser Holocamera Test Setup 15
11 Schematic of Single Beam Pulsed Ruby Laser Holocamera Arrangement. 16
12 Pulsed Ruby Laser Setup on the West Side of Unit 10 17
13 Photograph of Shutter and Plate Holder in Front of Port 17
14 Schematic of Two-Beam Scattered Light Holocamera 19
15a Plan View of Two-Beam Holocamera Installation. 21
15b Perspective View of Holocamera Installation at Unit 10 21
16 Ruby Laser Illuminator Installed Adjacent to Unit 10 Boiler 22
17 Holocamera Shutter Assembly 22
18 Single Beam Hologram Recording and Reconstruction Geometries. 24
19 Reconstruction Camera Setup for Maximum Depth of Field . . . 26
20 Single-Beam Holocamera Resolution Measurements. 29
21 Helium-Neon Laser Reconstruction of a Pulsed Ruby Hologram 32
22 Cumulative Volume Fraction Versus Bead Diameter 32
23 Real Image From Hologram No. 1, Series 10-8-69 33
24 Reconstruction Photo of Stream of 40-50 Mesh Glass Beads . . 33
25 Reconstruction Photo of Stream of 40-50 Mesh Glass Beads at 6 Feet From Hologram 34
26 Reconstruction of Images of 40-50 Mesh Glass Beads at 12 Feet from Hologram. 34

ILLUSTRATIONS (Continued)

Page

27 View of Virtual Image of Low-Angle Forward Scattered Light From Cotton Balls at 6 and 12 Feet From Hologram 36

28 Composite Views of a Scattered Light Reconstruction. 37

29 Matrix of Shawnee Unit 10 Holographic Tests 40

30 Schematic of Holocamera Scene Beam Geometries 41

31 Collimated Scene Beam "fingerprint" on Holographic Plate 43

32 Densitometer Trace for Hologram No. 1331 Reconstruction Photograph 45

33a Reconstruction Photo of Hologram 1381 46

33b Reconstruction Photo of Ruby Scene Beam Light at Prism Approximately 33 Feet From Holocamera 46

34 Densitometer Trace for Hologram 1564 Reconstruction Photograph 51

35 Densitometer Traces From a Mapping of Hologram 1570 Projected into a Composite Perspective. 52

36 Photograph of Reconstructed Virtual Image of Fan Beam Scattered Light From Hologram 1570 52

1. INTRODUCTION

The dry limestone process of removing sulfur oxide from power plant stack gases is one of several methods currently under investigation by the National Air Pollution Control Administration (NAPCA). Full-scale testing and evaluation of this process is, at this time, being conducted at the Unit 10 boiler of the Tennessee Valley Authority's (TVA) Shawnee Steam Plant located outside of Paducah, Kentucky.[1, 2, 3] This report is concerned with the application of pulsed ruby laser holography as an instrumentation technique for detecting the penetration and dispersion of limestone plumes injected into the Unit 10 boiler operating at nominal conditions.*

1.1 SHAWNEE UNIT 10 BOILER

The test boiler at the Shawnee plant is a pulverized coal, front-fired unit which, during the holographic studies, was operated at a nominal electrical power output of 140 megawatts. At this power output, Unit 10 burns approximately 56 tons of pulvarized coal per hour injected into the furnace through 16 individual burners. The amount of air consumed in the combustion process (at the nominal output) is in the order of a million pounds per hour.

The holography experiments were conducted at an elevation of 364 feet, 9 inches using one of the limestone injection ports on the north side and an unused soot blower port on the south or front side of the boiler. Flame temperatures in this general vicinity are in excess of 2500°F resulting in a high black body (yellow) luminous output. Combustion gas velocities are estimated to range from 30 to 60 ft/sec at the 365-foot elevation. A perspective sketch, shown in Figure 1, illustrates the general arrangement of the Unit 10 boiler as well as pertinent port locations.

In Figure 1, it will be seen that the internal distance between the front (south) and rear (north) water walls of the boiler is 24 feet at the 365-foot elevation. The internal width (east to west) of the boiler is 46 feet. Not shown in this sketch is a boiler division wall which divides the 46-foot width in half. Note that the main or ground floor of the Shawnee plant is at an elevation of 345 feet. Details of the boiler below that elevation are not shown in Figure 1. The photographs of Figures 2 and 3 show the viewing ports used in the holocamera test setup. Figure 2 illustrates the unused soot blower port (elevation 365) on the front side of the boiler. Figure 3 shows the limestone injection port on the rear side of the boiler at elevation 364 feet, 6 inches. During the holography experiments, the limestone injection tube was removed from the port.

---

*The holographic studies described in this report were conducted under provisions of NAPCA Contract CPA 70-4 in support of the overall dry limestone process evaluation program.

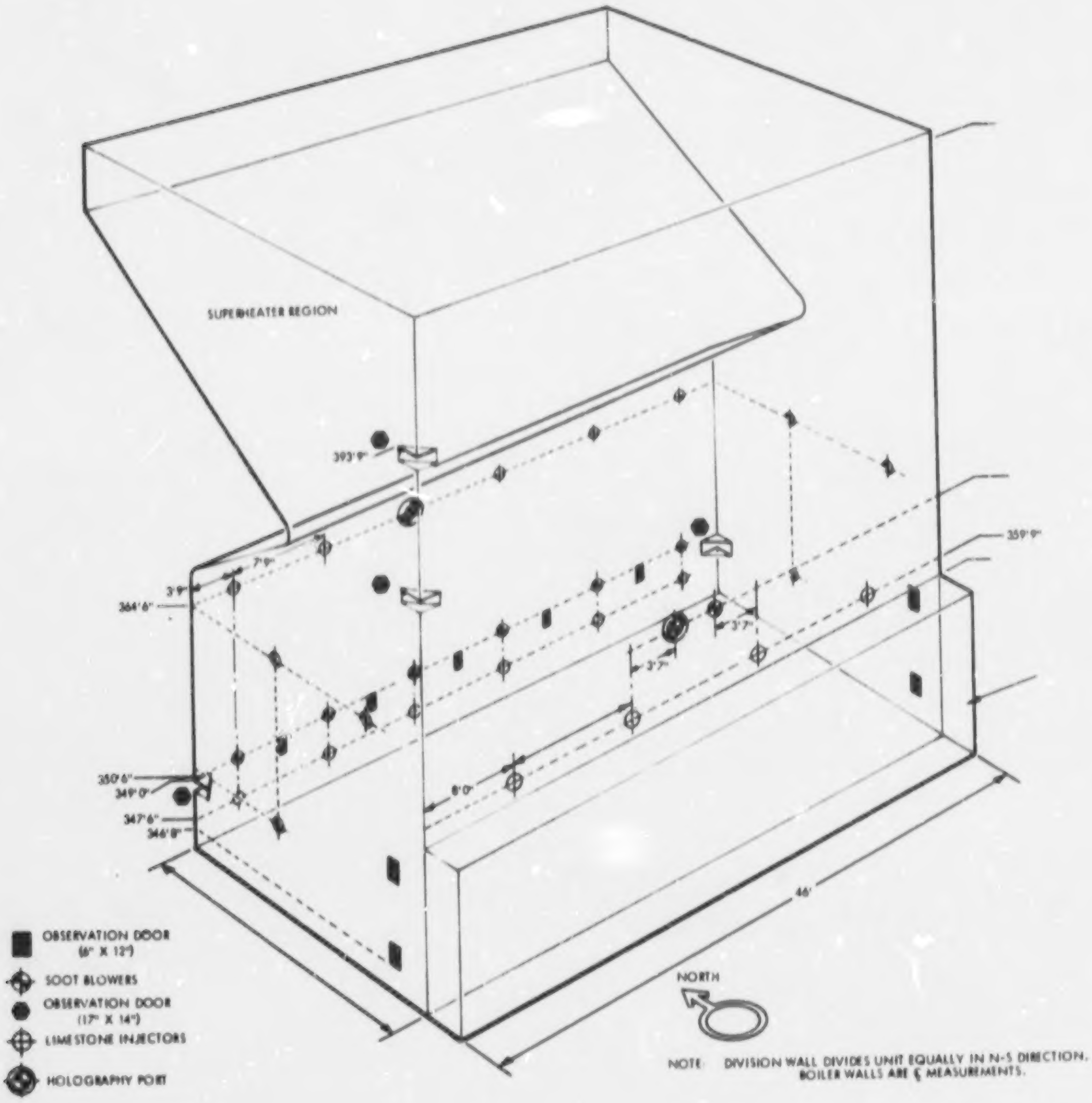

NOTE: DIVISION WALL DIVIDES UNIT EQUALLY IN N-S DIRECTION. BOILER WALLS ARE ℄ MEASUREMENTS.

Figure 1. Perspective sketch of the Shawnee Unit 10 boiler showing basic dimensions and port locations

The injection of limestone is accomplished through a total of 16 injection ports. The ports are located at three different elevations on the boiler. Four of the limestone injectors are located at an elevation of 359 feet, 9 inches on the south or front side of the boiler. All of the remaining 12 limestone injectors are installed on the rear (north) side of the boiler with six located at the elevation 347 feet, 6 inches and six more at elevation 369 feet, 6 inches. Injection of the limestone is accomplished pneumatically. During the holography experiments, described in Sections 5 and 6 of this report, the limestone injection flow rates varied between 1000 and 2750 pounds per hour for individual ports. At the point of injection into the boiler, approximately 70 percent of the limestone is less than 200 mesh (74 micron diameter) size. In contrast, measured fly ash samples (collected at the stack precipitator) reveal that 80 to 95 percent of the fly ash is less than approximately 30 microns in diameter.

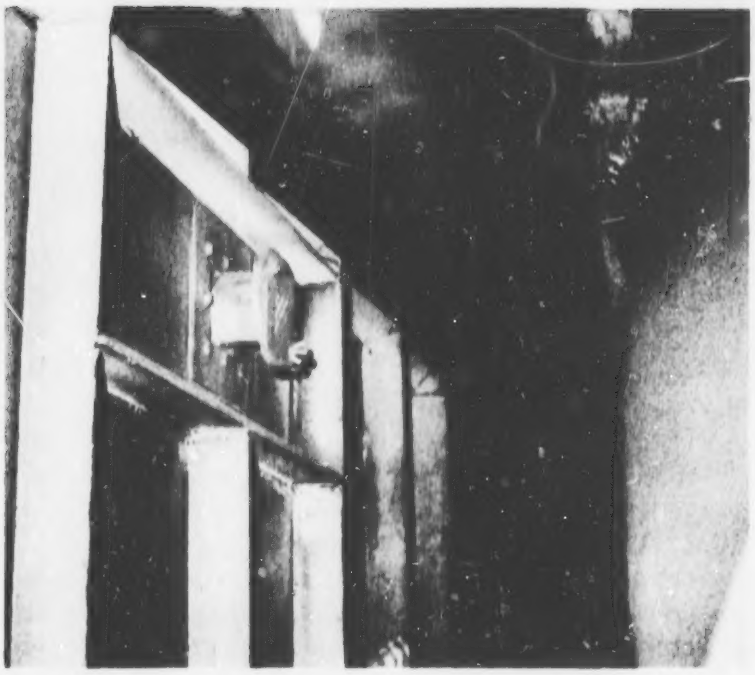

Figure 2. Photograph of soot blower port on south side of Unit 10 used for holography tests (elevation 364 feet, 6 inches)

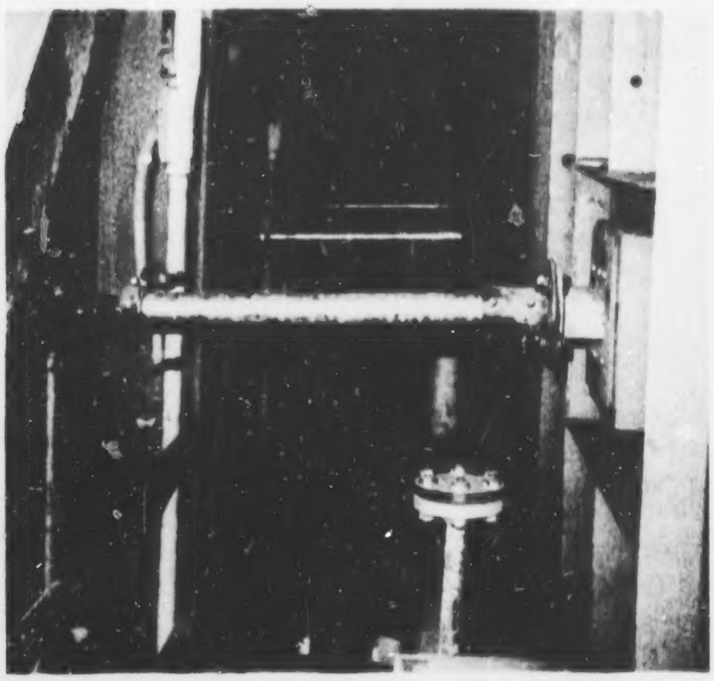

Figure 3. Photograph of row of limestone injectors at elevation 364 feet 9 inches on north side of Unit 10. For holography tests, the injection tube was removed from near port.

1.2 DRY LIMESTONE INJECTION PROCESS

In the dry limestone process under evaluation at Shawnee, finely ground limestone particles are pneumatically injected into the Unit 10 boiler at one or more of three elevations. Upon injection into the boiler combustion gases, the particles sorb sulfur dioxide as they travel through the furnace. Although the sorption process is complex and not completely understood, the following reactions are usually assumed:[4]

(1) $CaCO_3 + \text{Heat} \rightarrow CaO + CO_2$

(2) $CaO + SO_2 + 1/2O_2 \rightarrow CaSO_4$

During the initial calcination, carbon dioxide is removed to make room for the sulfur dioxide and the limestone particle becomes porous. This porosity results in an increase in particle surface area and promotes a more rapid reaction with the sulfur dioxide in the combustion gases. The reaction temperature and particle residence time are critical. A temperature in the order of 2000°F is required for the initial calcination of the limestone particles. The optimum temperature for the lime sulfation reaction is thought to be approximately 1900°F.[5]

1.3 HOLOGRAPHIC DETERMINATION OF INJECTED LIMESTONE PLUMES

Of primary concern to the full-scale evaluation of the dry limestone injection process is the degree of limestone plume penetration, dispersion and continuity. Holography was selected as a candidate instrumentation technique for two reasons. Perhaps the most significant reason is that passive in situ measurements are possible with holography, hence, the recorded quantity is not compromised by remote sampling procedures or the introduction of foreign mechanisms or probes. Also of importance is the fact that holography permits the recording of a volume of information as opposed to more limited methods such as point sampling. Accordingly, an 8-month program was initiated in August 1969, to demonstrate the feasibility and utility of pulsed ruby laser holography for recording injected limestone plumes in the Shawnee Unit 10 boiler.

The holography program, sponsored by NAPCA under contract CPA 70-4, consisted of three phases. During Phase I optical components for a single-beam (Gabor) holographic arrangement were designed, fabricated and assemble for calibration tests. The single-beam holography tests consisted of resolution measurements over distances comparible to the dimensions of the Unit 10 boiler (elevation 365) and superheater (elevation 392) where subsequent field trials were to be conducted. In addition to the single-beam holographic tests made during Phase I, a modified two-beam system was developed and demonstrated. The two-beam holographic arrangement was unique in that objects within the scene volume were not imaged directly onto the photographic plate (hologram). Instead, low angle forward components of the light scattered by objects within the laser scene beam were recorded by the hologram.

Although the two-beam holographic technique was ultimately selected to record portions of the limestone plumes injected into the Unit 10 boiler, considerable work was done in the area of Gabor or single-beam holography. Gabor holography appeared attractive from the standpoint of overall simplicity and the need for installation of only a minimum number of components on the boiler. For these reasons, a Phase II feasibility demonstration trial at the Shawnee Unit 10 superheater (elevation 392) was implemented. The single-beam technique proved inadequate to the task of recording large ensembles of particulate in the superheater because of heavy attenuation of the laser light. Holographic studies continued, however, with the initiation of Phase III and employment of the alternate two-beam holographic technique developed during Phase I. The subsequent Phase III tests were conducted at the 365-foot elevation of the boiler. Holographic recordings of light scattering caused by the presence of limestone clouds or plumes were successfully made. The final portion of Phase III was devoted to developing means of acquiring and evaluating limestone plume data.

Financial expenditures (excluding fee) for the 8-month technical effort for the holography program are shown in Figure 4. The technical activities associated with each of the three phases of work are presented in the event logic network of Figure 5. This latter figure also shows the sequence of reports submitted during the 8-month technical effort as well as the prepar- and submittal of this final report.

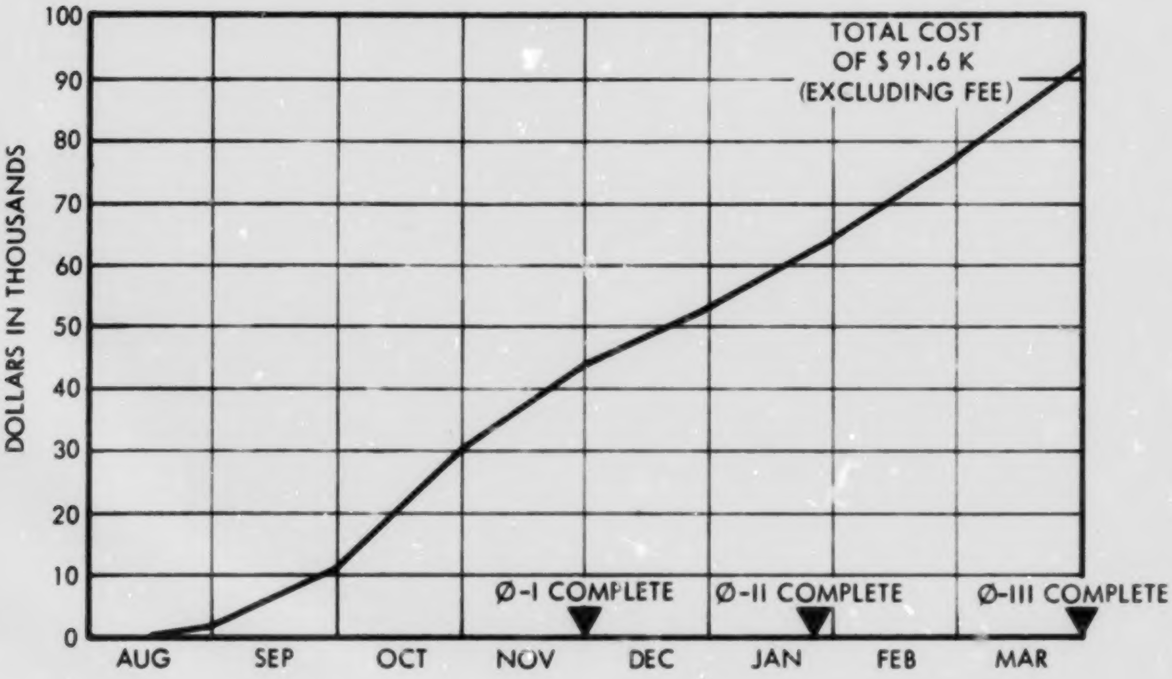

Figure 4. Program expenditures for 8-month technical effort

A

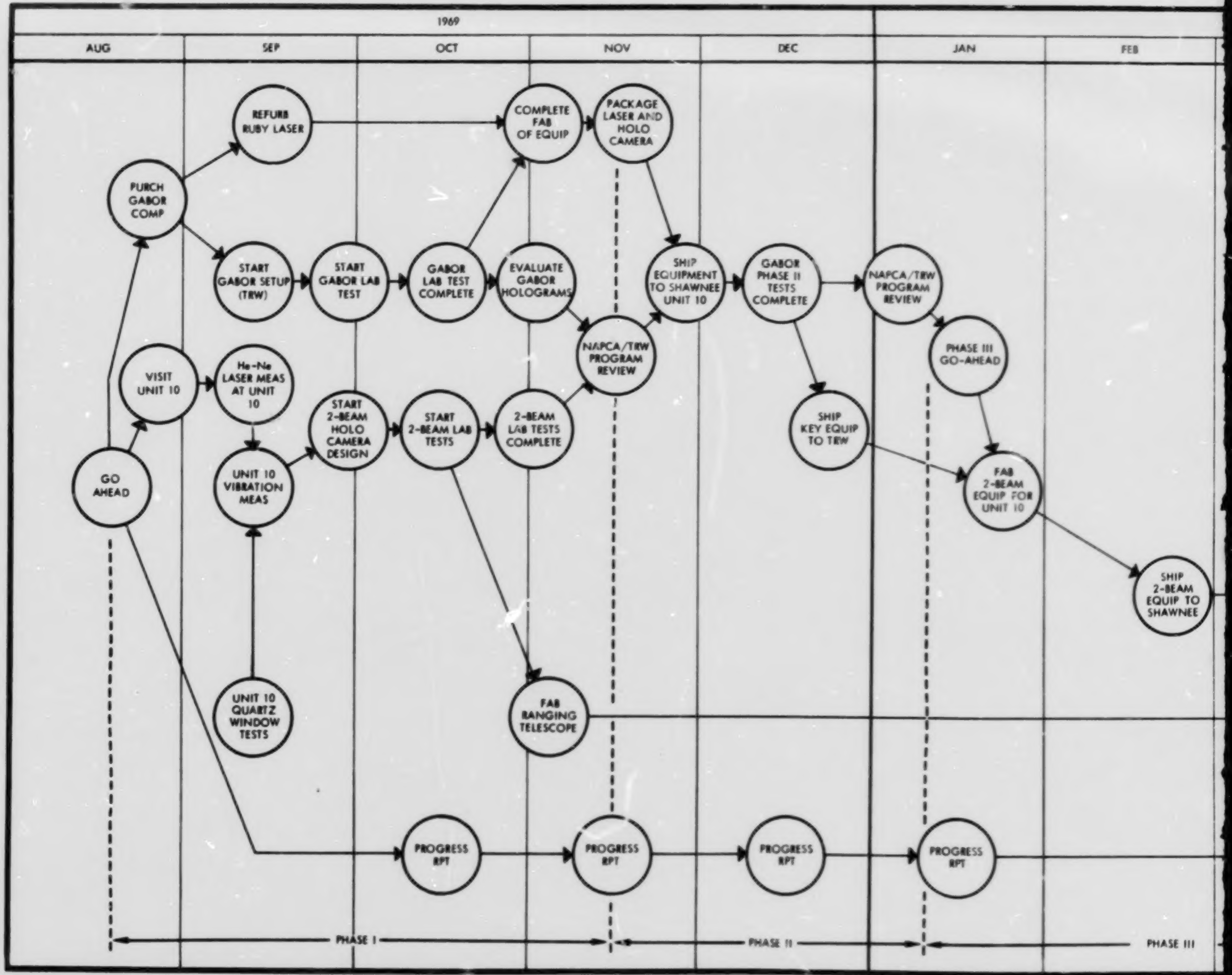
1969
AUG
SEP
OCT
NOV
DEC
JAN
FEB
REFURB RUBY LASER
COMPLETE FAB OF EQUIP
PACKAGE LASER AND HOLO CAMERA
PURCH GABOR COMP
START GABOR SETUP (TRW)
START GABOR LAB TEST
GABOR LAB TEST COMPLETE
EVALUATE GABOR HOLOGRAMS
SHIP EQUIPMENT TO SHAWNEE UNIT 10
GABOR PHASE II TESTS COMPLETE
NAPCA/TRW PROGRAM REVIEW
NAPCA/TRW PROGRAM REVIEW
PHASE III GO-AHEAD
VISIT UNIT 10
He-Ne LASER MEAS AT UNIT 10
START 2-BEAM HOLO CAMERA DESIGN
START 2-BEAM LAB TESTS
2-BEAM LAB TESTS COMPLETE
SHIP KEY EQUIP TO TRW
FAB 2-BEAM EQUIP FOR UNIT 10
GO AHEAD
UNIT 10 VIBRATION MEAS
SHIP 2-BEAM EQUIP TO SHAWNEE
UNIT 10 QUARTZ WINDOW TESTS
FAB RANGING TELESCOPE
PROGRESS RPT
PROGRESS RPT
PROGRESS RPT
PROGRESS RPT
PHASE I
PHASE II
PHASE III

B

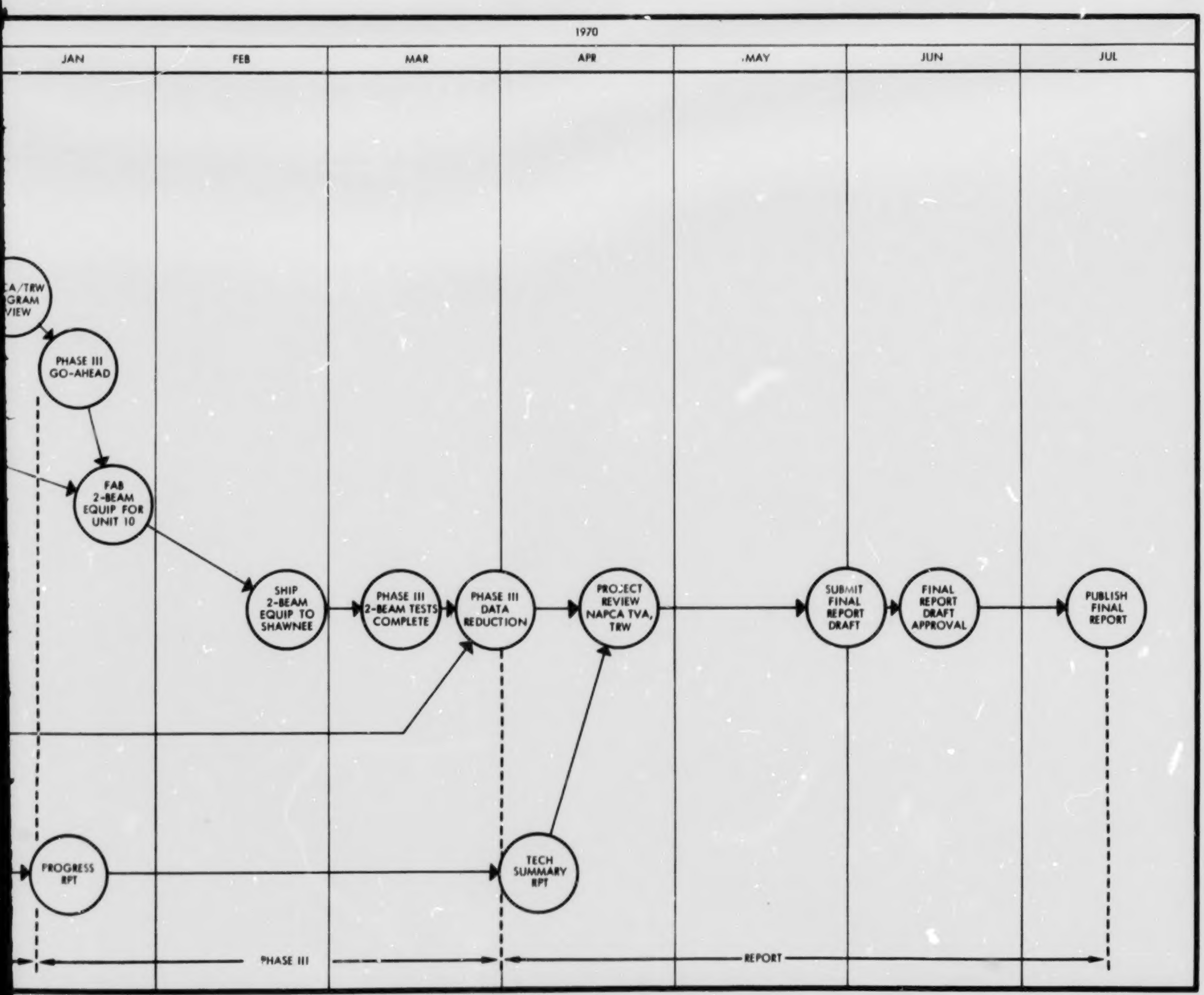
1970
JAN
FEB
MAR
APR
MAY
JUN
JUL
CA/TRW
GRAM
VIEW
PHASE III GO-AHEAD
FAB 2-BEAM EQUIP FOR UNIT 10
SHIP 2-BEAM EQUIP TO SHAWNEE
PHASE III 2-BEAM TESTS COMPLETE
PHASE III DATA REDUCTION
PROJECT REVIEW NAPCA TVA, TRW
SUBMIT FINAL REPORT DRAFT
FINAL REPORT DRAFT APPROVAL
PUBLISH FINAL REPORT
PROGRESS RPT
TECH SUMMARY RPT
PHASE III
REPORT

Figure 5. Activity Summary Network

2. PROGRAM SUMMARY

The three-phase holography program to make in situ recordings of injected limestone plumes in the Shawnee Unit 10 boiler is conveniently discussed in terms of the initial calibration studies made at TRW Systems Group in Redondo Beach, California, and the subsequent field trials at the Shawnee Steam Plant in Kentucky.

2.1 CALIBRATION STUDIES—PHASE I

The Phase I calibration studies at TRW Systems were initiated in August 1969. This work included the preparation of holographic equipment and the experimental verification of techniques for later use at the Shawnee facility. A major effort was directed toward utilizing a single-beam (Gabor) holographic arrangement to record particulate in the superheater region (elevation 392) of Unit 10 during Phase II. There was, however, concern that the expected large quantities of fly ash and injected limestone particulate would attenuate the probing ruby laser beam to the extent that single-beam holography would not be feasible.* For this reason, a two-beam holographic arrangement was designed to overcome this anticipated problem area. Although somewhat more sophisticated in concept, this alternate technique was later used (in Phase III) when the single-beam method subsequently proved inadequate.

Work during Phase I with both the Gabor and the two-beam methods of holography resulted in several significant achievements. Although the single-beam method was eventually discarded in favor of the two-beam system, a considerable amount of testing was accomplished representing an extension of previous technology. For this reason, the single-beam holography results are discussed at length in this report in the belief that this work may provide insight for possible future applications.

Modification of a conventional two-beam holographic arrangement to allow the recording of low-angle forward-scattered light is the most significant aspect of the calibration studies of Phase I. Development of this technique led to the successful recording of limestone plumes in the Unit 10 boiler during Phase III. The pulsed ruby laser holography work and accomplishments of the calibration studies are summarized as follows:

- Components were fabricated and assembled into a single-beam holographic arrangement suitable for "long distance" holography.
- Single-beam holograms of resolution targets and dispersions of glass beads were recorded at intervals of 6 feet from the holographic plate over distances in excess of 48 feet. This is the first known work with Gabor holography at these extreme object distances.

---

*See Appendix A for a discussion on the fundamentals of holography and the singular advantage of a two-beam system for applications where heavy scene beam attenuation is encountered.

- Single-beam holographic resolution measurements at an object distance of 6 feet yielded a resolution equivalent to particles of approximately 50 microns in size. At 50 feet the resolution measurements indicated that particles of only 550 microns could be resolved.

- From the single-beam recordings of glass beads (40 to 120 mesh) it was demonstrated that discrete bead images could be distinguished up to distances of 12 feet. Beyond this distance, reconstruction of distinct bead images was difficult. When the distance exceeded 18 feet, individual bead images were not discernible.

- Using a reconstructed holographic recording of 40 to 50 mesh glass beads located a distance of 6 feet from the film plate, it was demonstrated that individual bead images could be measured and a size distribution determined from the measured data.

- A two-beam holographic arrangement was developed to record light scattered at low angles in the forward direction over distances up to 50 feet. A series of "scattered light holograms" of various objects located in the scene volume were recorded to demonstrate the feasibility of this new technique.

- A ranging telescope was built, calibrated and subsequently used to demonstrate that two-beam holographic images of scattered light could be brought into focus. Distance measurements along the laser beam axis to the edges of the scattered light image were possible and, therefore, the position of the image within the recorded scene could be measured.

2.2 FIELD TRIALS — PHASE II AND III

Phase II of the program was accomplished during December 1969. The TRW pulsed ruby laser and holographic equipment were shipped to the Shawnee Steam Plant in Kentucky. The apparatus was installed on the Unit 10 superheater at the 392-foot elevation. Gabor holograms of fly ash distributions across the 50-foot-wide superheater were attempted. Twenty-nine recordings were made; however, no meaningful reconstructions were obtained. Further attempts to utilize single-beam holography were abandoned. It was concluded that the severe attenuation and multiple scattering by the particulate in the stack gas encoded the single beam of coherent light sufficiently to prevent making holograms which could be reconstructed.

A program review of the initial two phases of work led to a decision in January 1970, to concentrate on adapting a two-beam holographic system for recording injected limestone plumes in the Unit 10 boiler. Equipment modifications were completed at TRW Systems and the Phase III field trials begun at the Shawnee plant in February 1970. The holocamera apparatus was installed at a boiler elevation of 365 feet. Details of the installation are presented in Section 3.3 of this report.

During the 3-week Phase III effort, 79 holograms were recorded both with and without limestone injection into the boiler. Data reduction and evaluation of results were accomplished on 25 of these successful holographic recordings. The significant achievements of Phase III work may be summarized as follows:

- The successful recordings obtained during field trials at Shawnee represent the first major application of holography to the study and monitoring of an industrial process.
- Using the innovation of scattered light holography, the presence of limestone plumes in the boiler was detected. The recordings yield instantaneous scattered light images possessing excellent three-dimensional qualities.
- A hologram recording rate of one plate per minute was achieved using manual methods. Although each recording provided an instantaneous increment of data, repetitive recordings allow the evaluation of time changes in the limestone plume phenomena.
- Photometric techniques were developed to obtain quantitative information from the developed holograms concerning the penetration of the limestone plume into the boiler, dimensions of the plume (along the laser beam axis) and the presence of voids or gas bubbles in the plume.
- Excellent correlation was established between the dimensional data obtained with the photometric measurements and those acquired directly using the calibrated ranging telescope to observe the scattered light images in the hologram.
- In addition to dimensional plume data, an indication of limestone plume density was obtained from the relative light intensity measurements made via the photometric studies. An approach to determining absolute light intensity values from the reconstructed hologram images was conceived which would allow estimates of particle number concentrations of limestone during future holographic studies.

In summary, the feasibility of using holographic techniques to make in situ recording of limestone clouds or plumes in a full-scale operating steam boiler was demonstrated. Techniques were developed to analyze the resulting holograms and acquire quantitative data. This final report describes the experimental apparatus used, the laboratory experiments and the test program conducted at the Shawnee plant. These discussions are presented in Sections 3 through 5, respectively. A discussion of the results obtained during the Phase III field trials with scattered light holography is presented in Section 6. Conclusions and recommendations follow in Section 7 and 8.

3. EXPERIMENTAL APPARATUS

3.1 PULSED RUBY LASER ILLUMINATOR

The source of illumination for the holocamera apparatus was a pulsed ruby laser system designed and built at TRW Systems Group. Photographs of this solid state ruby laser are shown in Figures 6 and 7. The laser emits 1 to 3 joules of 0.6943 micron wavelength (red light) in pulses of 30 to 50 nanoseconds duration. The temporal coherence of the laser was not measured; however, from past experience it is believed to be about 5 centimeters.

A schematic diagram, Figure 8, shows a plan view of the components in the ruby laser. Included in the package are a "folded" arrangement of the oscillator-amplifier Q-switched ruby laser, a monitor diode, a dark-field alignment autocollimator and a helium-neon directional pointing gas laser. Switching of the optical path among these components is accomplished by a arrangement of reflectors operated by the small round knobs on top of the laser cabinet (Figure 6). Reference to Figure 8, and the photograph of Figure 7 illustrates the internal optical path of the laser and the various components of the system.[6]

The laser power supply and control electronics are housed in separate consoles as seen in Figure 9. The right-hand console contains two ignitron-fired 0 to 5 kv, 375 μ F capacitor banks used to energize the helical Xenon flash lamps in the ruby oscillator and amplifier assemblies of the laser. The companion console contains the independent high voltage supply and control circuits for the Kerr cell Q-switch. Also shown in Figure 9 is a Tektronix Type 535A oscilloscope used to record the ruby oscillator output energy monitored by the integrating photodiode.

3.2 SINGLE BEAM (GABOR) HOLOCAMERA

At the beginning of this study (Phases I and II), Gabor holography was tested as a means of detecting limestone clouds. It did not prove feasible; however, a sufficient amount of work was accomplished using the Gabor technique to warrant a description of the apparatus. A brief summary of results using single-beam holography is given subsequently in Sections 4.1 and 5.1.

Gabor holography employs a single-beam of coherent light which is typically passed through a scene and allowed to fall directly on a photographic plate. The plate records the intensity distribution caused by the interference between the beam transmitted through the scene and the light scattered by objects in the beam. Although only a single beam is used, the photographic plate records the superposition of two wave fronts: the transmitted and the scattered light wave fronts.*

---

*The fundamental technique of holography is discussed in Appendix A.

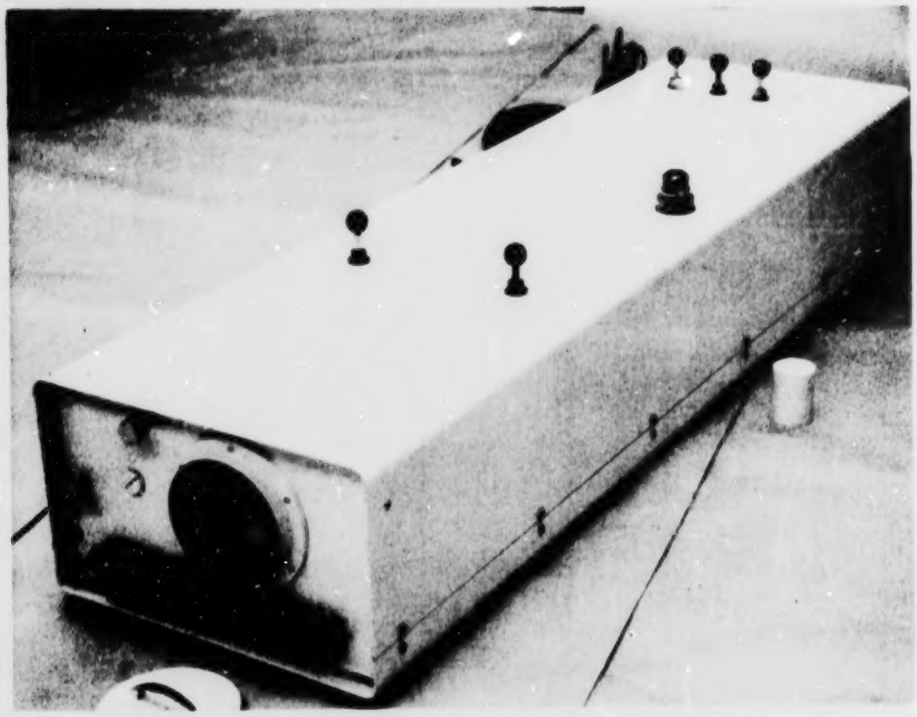

Figure 6. TRW Q-switched ruby laser illuminator

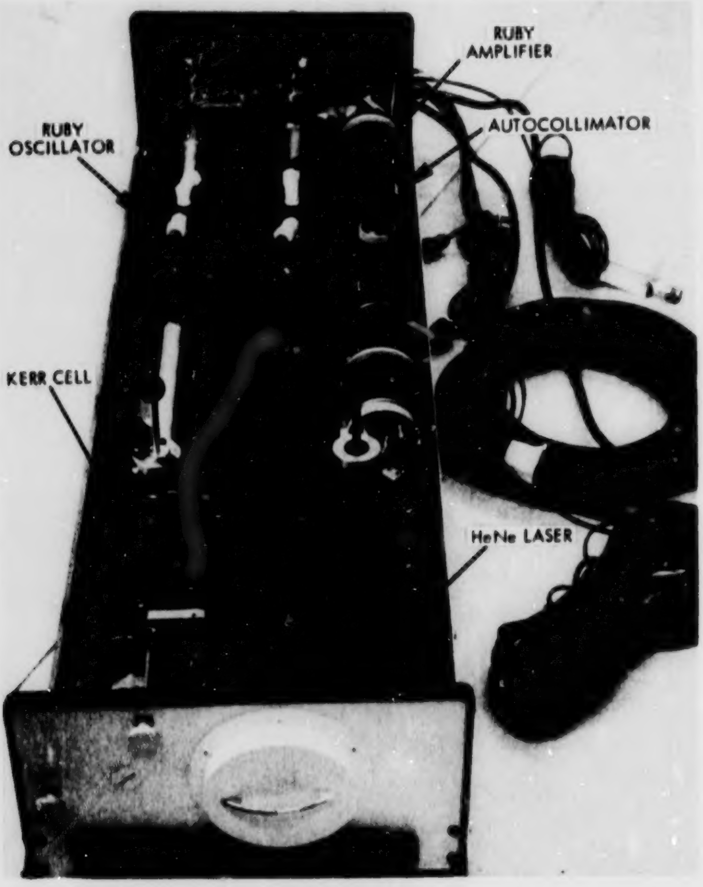

Figure 7. Ruby laser illuminator with cover removed to show location of major components

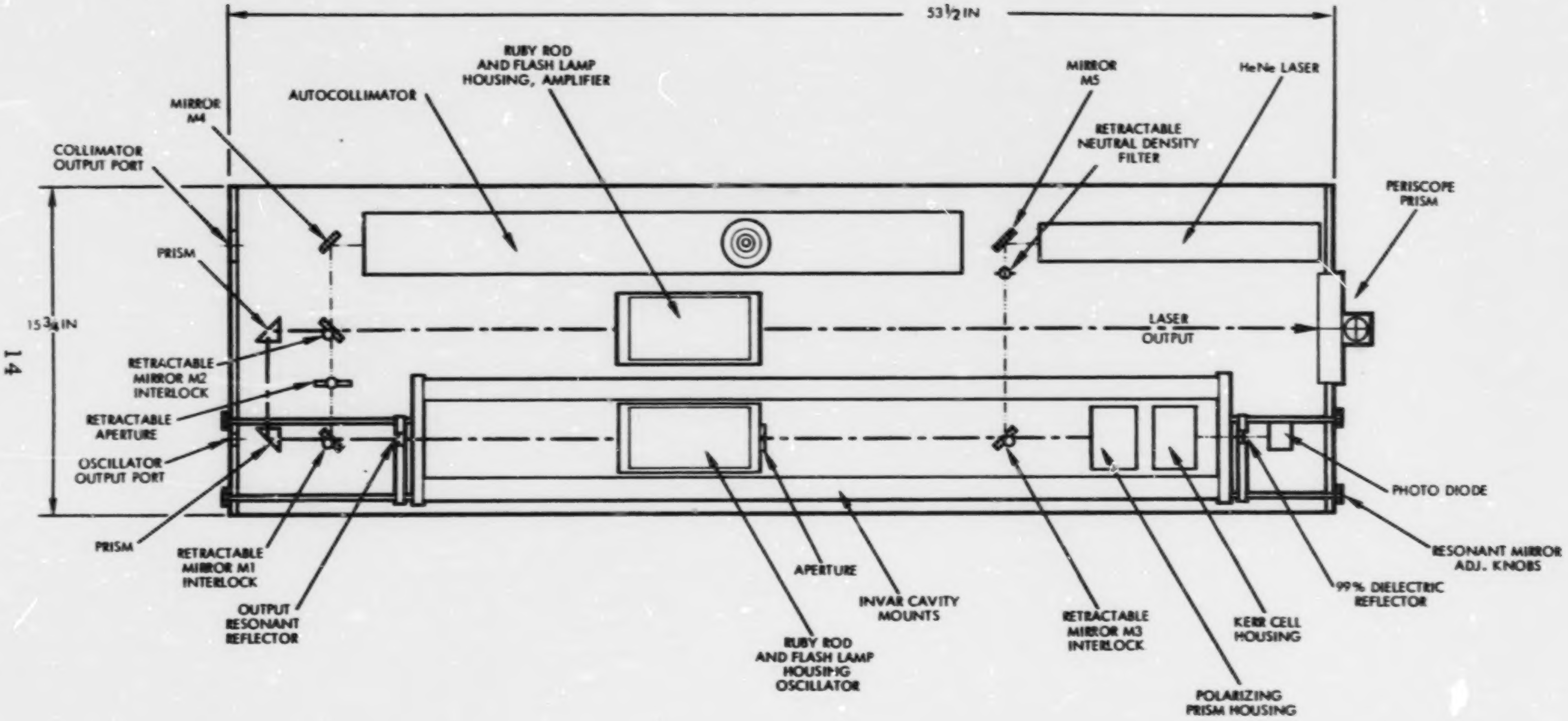
53½ IN
15¾ IN
RUBY ROD AND FLASH LAMP HOUSING, AMPLIFIER
AUTOCOLLIMATOR
MIRROR M4
COLLIMATOR OUTPUT PORT
PRISM
RETRACTABLE MIRROR M2 INTERLOCK
RETRACTABLE APERTURE
OSCILLATOR OUTPUT PORT
PRISM
RETRACTABLE MIRROR M1 INTERLOCK
OUTPUT RESONANT REFLECTOR
RUBY ROD AND FLASH LAMP HOUSING OSCILLATOR
APERTURE
INVAR CAVITY MOUNTS
RETRACTABLE MIRROR M3 INTERLOCK
POLARIZING PRISM HOUSING
KERR CELL HOUSING
99% DIELECTRIC REFLECTOR
RESONANT MIRROR ADJ. KNOBS
PHOTO DIODE
PERISCOPE PRISM
LASER OUTPUT
HeNe LASER
RETRACTABLE NEUTRAL DENSITY FILTER
MIRROR M5

Figure 8. Schematic diagram of compact ruby laser illuminator

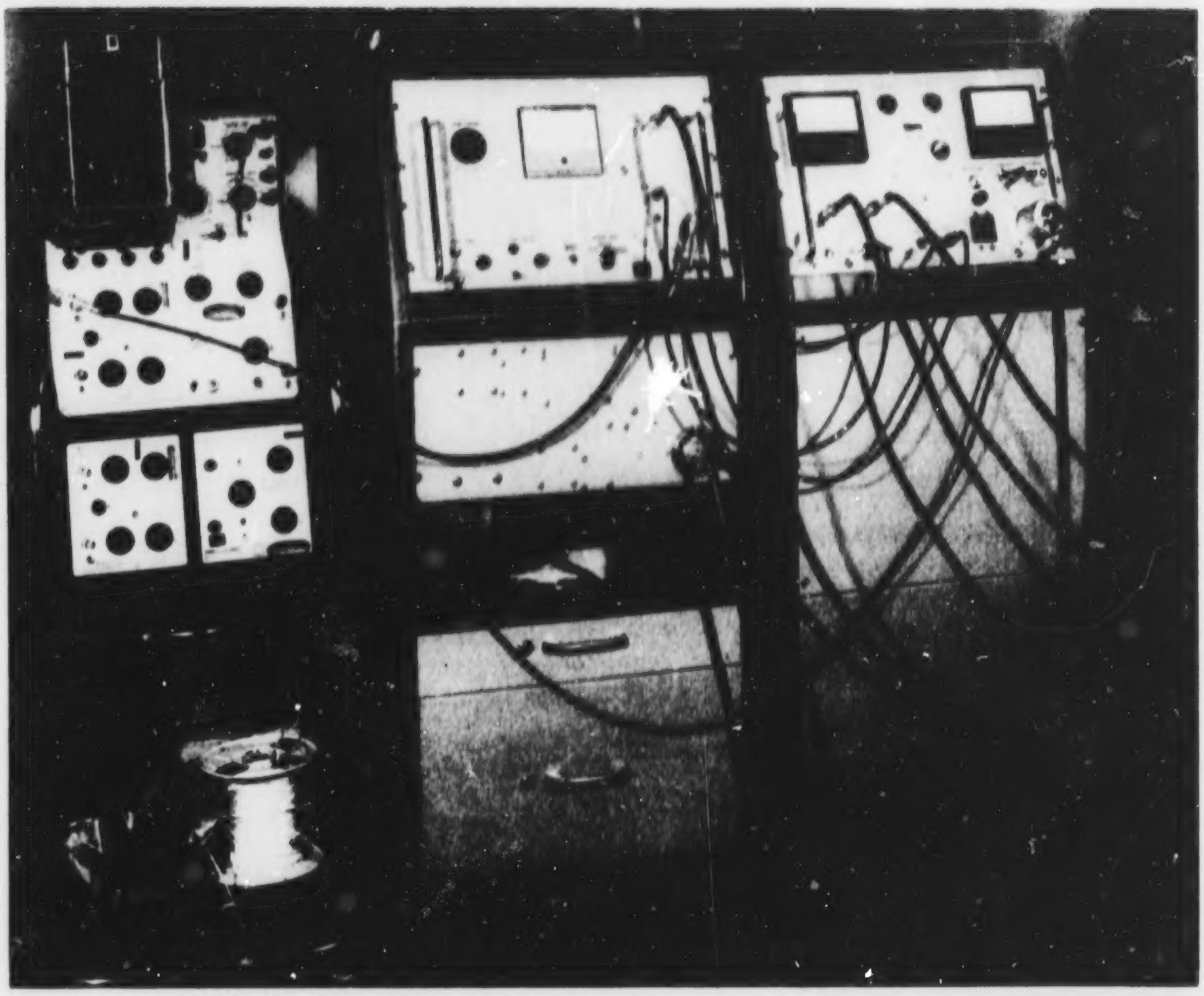

Figure 9. Photograph of TRW pulsed ruby laser power supply consoles and Tektronix 535A oscilloscope

The simplicity of a single beam or Gabor holographic test setup is shown in Figure 10. Such a test arrangement was used at TRW Systems to conduct laboratory measurements of resolution as a function of object distance d from the holographic plate. Results of these measurements are presented in Section 4.1. The Gabor setup has the further feature that it is almost insensitive to the temporal coherence of the ruby laser illuminator.

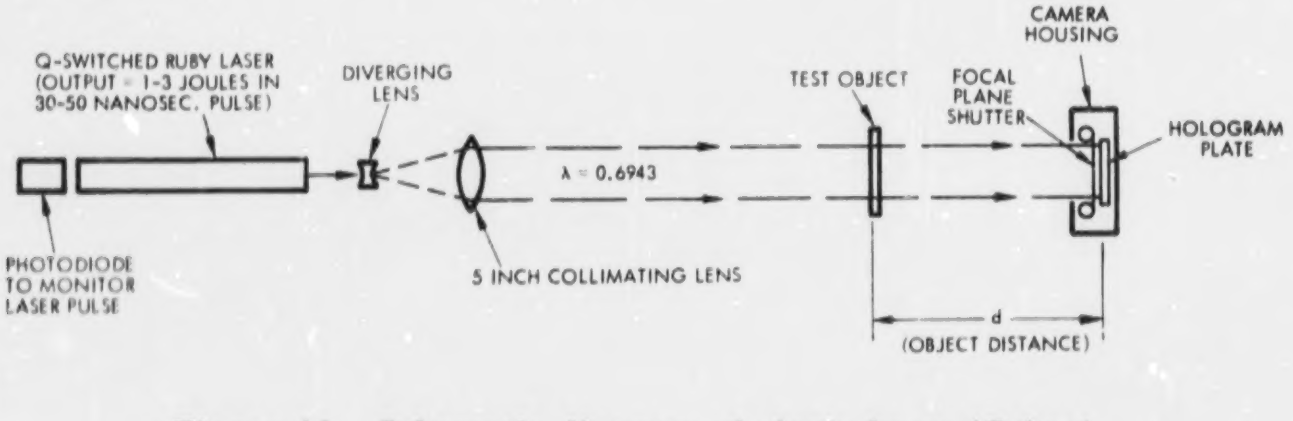

Figure 10. Schematic diagram of single beam (Gabor) pulsed ruby laser holocamera test setup

The illuminator was a Q-switched ruby laser (λ = 0.6943 micron) which provided a 30 to 50 nanosecond pulse of 1 to 3 joules content. From Figure 8, it can be seen that typically a 1-centimeter (0.394-inch) diameter beam from the ruby laser was expanded by a small diverging lens and then collimated with a 5-inch-diameter, 24.75-inch-focal-length lens.[*] A test object was located in the scene light a predetermined distance from the hologram plate. During laboratory experiments, the test object was a USAF 1951 resolution target or a fine spray of titanium glass beads. The overall distance from the hologram plate, located in the "camera housing," to the output (collimating) lens of the laser system was about 55 feet.

Subsequent Unit 10 Gabor holography tests utilized a test setup comparable to that just described. A schematic of equipment placement and pertinent dimensions is shown in Figure 11. Photographs of the pulsed ruby laser and camera shutter mechanism placed before the superheater (elevation = 392 feet) are presented in Figures 12 and 13.

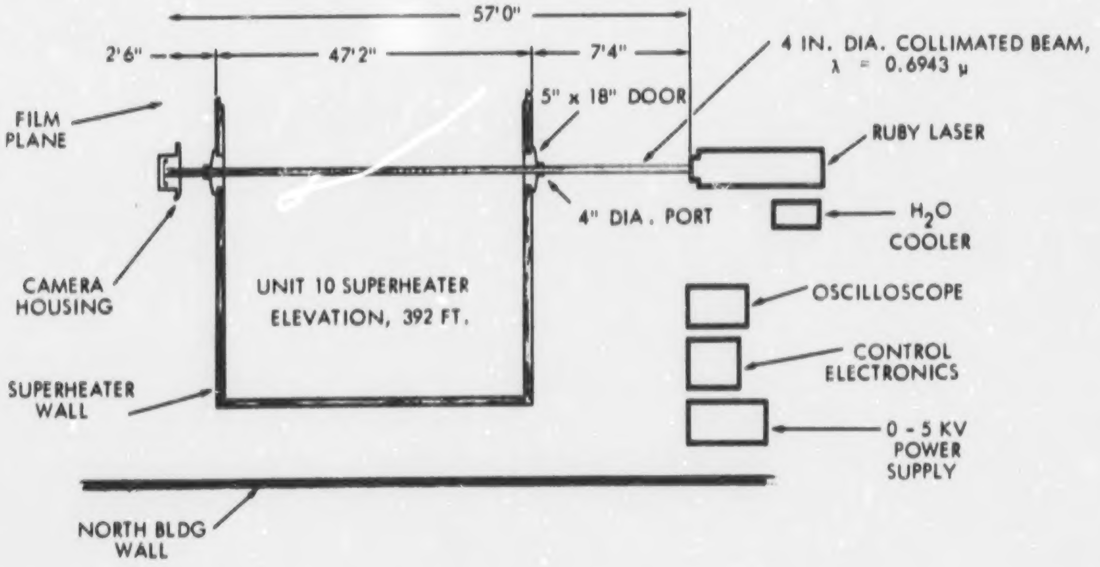

Figure 11. Schematic diagram of single beam pulsed ruby laser holocamera arrangement used on the Shawnee Unit 10 boiler superheater

The ruby laser was located on the west side of the Unit 10 superheater with the "camera" located on the far side of the boiler directly opposite. Alignment of the ruby laser, with the 4-inch-diameter boiler ports and the camera was accomplished visually using the beam from a continuous wave helium-neon gas laser bore sighted to the pulsed ruby laser beam. The gas laser was mounted in line and directly over the

---

[*] Jaegers lens No. 3E 1475.

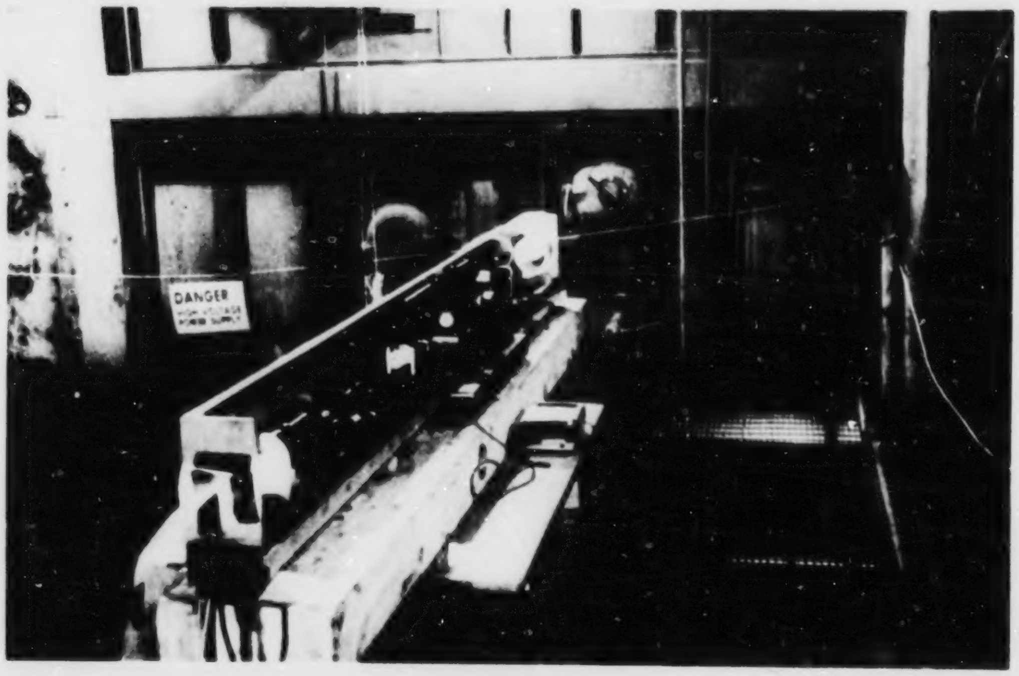

Figure 12. Pulsed ruby laser setup on the west side of the Unit 10 superheater for Phase II Gabor hologram recording tests

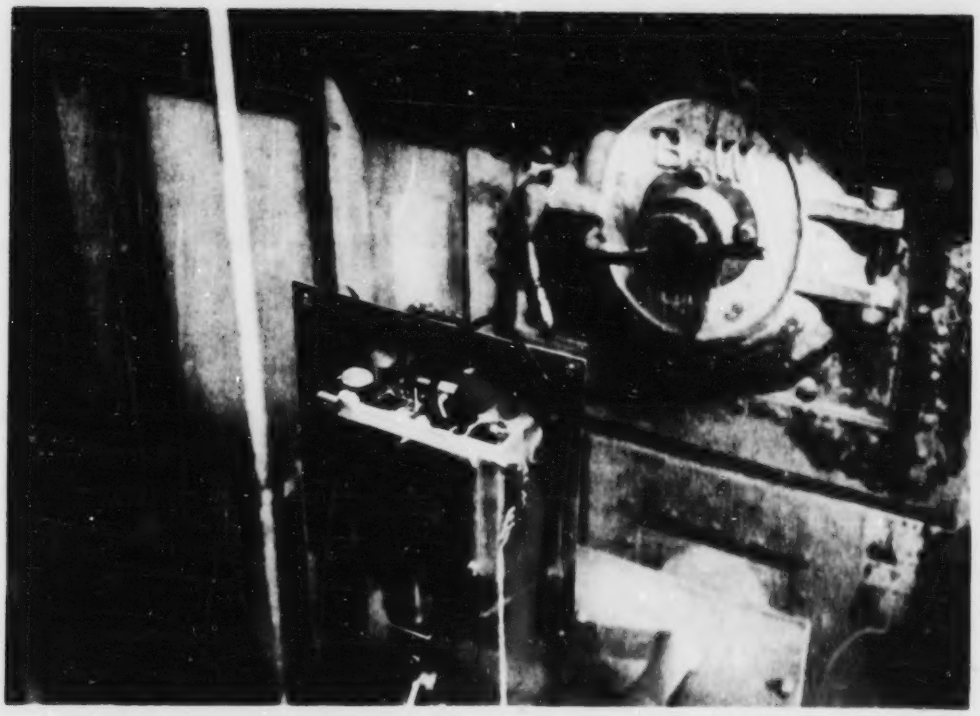

Figure 13. Photograph of shutter and plate holder placed in front of port on east side of Unit 10 superheater for Phase II tests

pulsed ruby laser. Two mirrors were used to subsequently direct the helium-neon gas laser beam through the ruby amplifier and then along the optical path of the pulse laser.[*]

With the gas laser operating, the ruby laser housing position was adjusted (using wedges) until the helium-neon beam passed through the opposed 4-inch-diameter boiler ports and was incident on the 4 by 5-inch format of the hologram film plate. Verification of the alignment was later made by observing the ruby laser optical pulse through a ground glass plate installed on the camera housing. Additional alignment checks were made with Eastman SO-243 cut film loaded in the camera back.

The camera consists of a holographic film plate holder, two shutter mechanisms and provisions for holding a Wratten No. 70 red gelatin filter to prevent fogging of the plate by flame or other extraneous light. The primary shutter was an adaptation of a focal plane shutter mechanism from a Graflex camera. The shutter is manually cocked against a preset spring tension using the large knob on the left-hand rear side of the camera assembly (Figure 13). Activation of the focal plane shutter is accomplished using a 28 vdc solenoid. A microswitch on the shutter winding shaft senses the open position of the focal plane shutter and remotely triggers the pulsed ruby laser. The nominal open time of the focal plane shutter is approximately 50 milliseconds during which the 50-nanosecond laser pulse occurs. The secondary "capping" shutter is also operated with a solenoid. This slow acting shutter is opened a convenient time prior to activation of the focal plane shutter and closed after the holographic recording has been made.

3.3 TWO-BEAM HOLOCAMERA

The Phase III holography studies conducted at the 365-foot elevation of Unit 10 utilized a two-beam transmission holocamera designed to record not the direct transmitted beam but instead, low angle forward scattered light. The two-beam holocamera differed from the Gabor setup in that the reference illumination was physically removed from the scene volume and passed around the outside of the boiler with the use of additional optics. The reference illumination, termed the "reference beam" is incident on the holographic plate in an unmodified state. As such, it is readily duplicated and facilitates reconstruction of the developed plate.

Application of a two-beam holographic technique proved absolutely essential in studying particulate matter dispersed over large distances in the operating boiler. Thermal gradients some indication of turbulence and the presence of large ensembles of particles, heavily attenuated the laser light (scene beam) passing through the boiler. Single-beam or Gabor holography is dependent upon a portion of the illumination passing through the scene in an unmodified state. This unmodified portion of the illumination serves as the reference beam which, when duplicated, reconstructs the recorded scene. In the case of the boiler studies, the heavy attenuation and modification of the laser beam encoded all of the illumination making it impossible to produce a meaningful reconstruction.

---

[*] The ruby laser used during the superheater test program was identical in function but different in form from the one described in Section 3.1. This earlier laser was a laboratory model provided by the Physical Electronics Laboratory of TRW. It was subsequently replaced by the newer illuminator described in this report.

The two-beam holocamera configuration eventually selected for work at the boiler is a modification of more conventional transmission holocamera arrangements. The particles contained within the recorded scene volume are not imaged directly onto the holographic plate. Rather, the presence of particles in the scene is detected by scattered light.

Verification of the low angle forward scattered light holocamera technique was first accomplished under the separate sponsorship of the TRW independent research program. The holographic arrangement used during these early tests is shown schematically in Figure 14. The arrangement utilized a 5-inch-diameter collimating telescope, two front-surface mirrors, a glass wedge beam splitter and a corner prism. The light beam from the pulsed ruby laser was directed through the beam splitter and corner prism and projected across a scene volume of approximately 45 feet. The unexpanded scene beam was purposely directed so as not to impinge on the holographic plate. The wedge beam splitter diverted about 4 percent of the light energy into the collimating telescope to form the 5-inch-diameter reference beam. The reference illumination was directed around the scene volume. The two front-surface mirrors directed the beam onto the hologram plate at an angle of nearly 10 degrees. In contrast, the scene beam (as seen in the diagram of Figure 14) consisted only of that portion of the light scattered at a low forward angle from objects placed to intercept the unexpanded laser beam. The technique is relatively independant of the temporal coherence of the ruby laser.

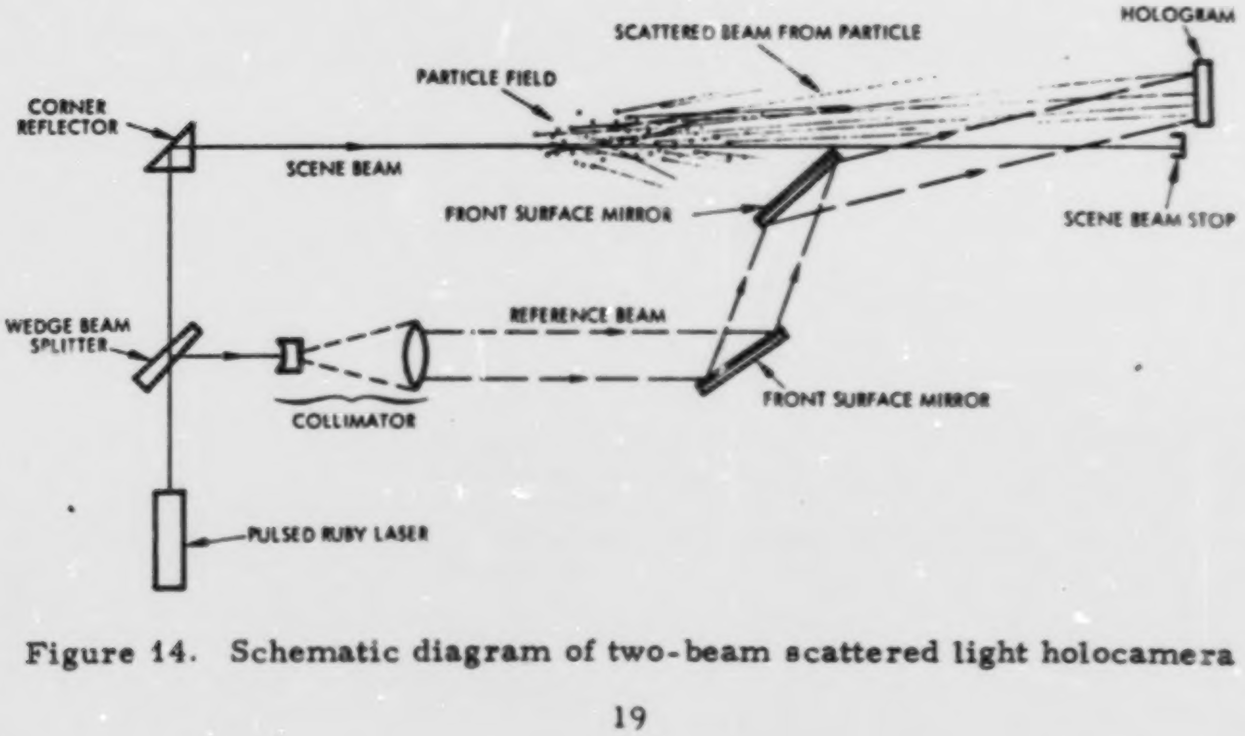

Figure 14. Schematic diagram of two-beam scattered light holocamera

The apparatus described above was used to demonstrate the feasibility of recording forward scattered light on holographic plates using a conventional Q-switched ruby laser. A series of tests was conducted in which scattered light from tufts of cotton, glass fibers and chalk dust was successfully recorded. The results of these tests are described in Section 4. Verification of the technique led to the design and installation of a scattered light transmission holocamera at elevation 365 feet on the Unit 10 boiler.

The holocamera optical component arrangement for the Phase III tests at elevation 365 feet on Unit 10 is shown in the plan view diagram of Figure 15a. The pulsed ruby laser illuminator for the holocamera was installed on a shelf positioned approximately 8 feet above the ground floor elevation of 345 feet. This installation is shown in Figure 16. The proximity of the laser to the boiler and holocamera components is shown in Figure 15b which is a perspective drawing of the test setup. From this illustration, it is seen that light was passed from the laser source to the beam splitter box (refer to Figure 15) by means of a periscope arrangement.

The laser input beam was directed into a horizontal plane at the desired boiler port elevation (~365 feet) by the periscope. The beam next entered the first optical package which consisted of a prism (No. 3), wedge beam splitter assembly and a collimating telescope. Referring to Figure 15, it will be seen that a portion of the laser input beam passed through the beam splitter assembly and proceeded directly across the front (south) side of Unit 10 to a prism box placed before the inlet port of the boiler. The laser beam is directed by the final reflector (prism No. 4) so as to enter the boiler and traverse the 24 feet of combustion volume. This last prism was set so that the light just missed the exit port on the far side or rear north wall. As in the Figure 14 test configuration, the laser beam did not fall directly on the holographic plate. Particles within the illuminating beam scattered light from the beam. Some of the light scattered at low angles in the forward direction emerged from the rear port and fell on the holographic plate to form the scene beam.

The reference illumination is formed by reflecting a portion of the laser light at the wedge beam splitter (Figure 15). The reference beam is passed through a negative lens and expanded to a 5-inch-diameter and then collimated. With the reference beam expanded to illuminate the holographic plate, it is passed by two front surface mirrors to the plate at an angle of 15 degrees with respect to the nominal axis of the emerging scene light. The angle of separation between the scene and reference beams is not critical. A design value of 10 to 30 degrees was selected as providing adequate viewing angle separation (on reconstruction) and at the same time simplify the tasks of camera and mirror mounting and of matching the optical path lengths of the scene and reference beams.

The camera and shutter assembly shown in Figure 17 is designed to accept standard 4 x 5 photographic film or plate holders. As described earlier in Section 3.2, it is fitted with two mechanical shutters, a slow-acting capping shutter which helps to protect internal parts from dust and

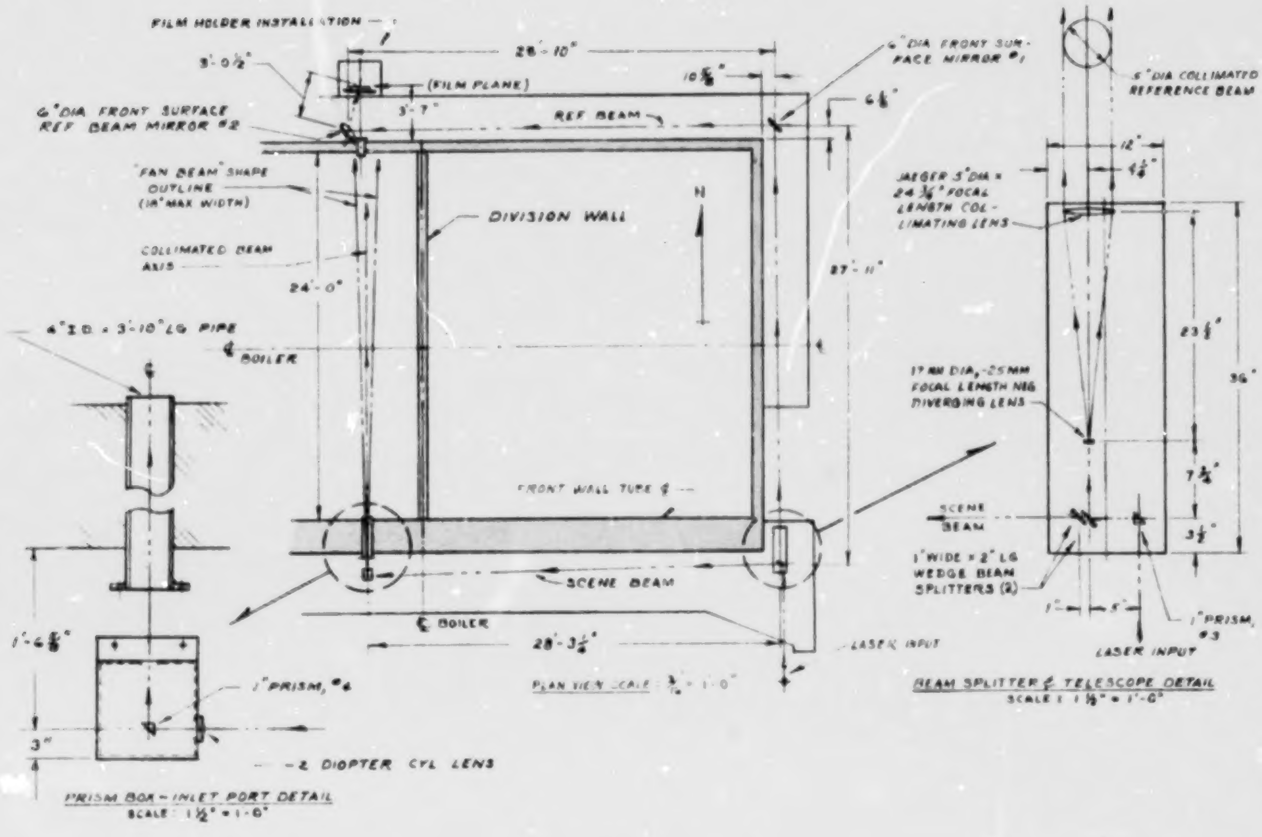
FILM HOLDER INSTALLATION
3'-0½"
(FILM PLANE)
28'-10"
10⅝"
6"DIA FRONT SURFACE REF BEAM MIRROR #2
3'-7"
REF BEAM
6"DIA FRONT SURFACE MIRROR #1
6⅛"
"FAN BEAM" SHAPE OUTLINE (18" MAX WIDTH)
DIVISION WALL
N
COLLIMATED BEAM AXIS
24'-0"
27'-11"
4"I.D. × 3'-10" LG PIPE
℄ BOILER
FRONT WALL TUBE ℄
SCENE BEAM
℄ BOILER
28'-3¼"
LASER INPUT
PLAN VIEW SCALE : 3/16" = 1'-0"
1'-6⅝"
1"PRISM, #4
3"
-2 DIOPTER CYL LENS
PRISM BOX - INLET PORT DETAIL
SCALE : 1½" = 1'-0"
5"DIA COLLIMATED REFERENCE BEAM
12"
4½"
JAEGER 5"DIA × 24 3/16" FOCAL LENGTH COLLIMATING LENS
23½"
36"
17 MM DIA, -25MM FOCAL LENGTH NEG DIVERGING LENS
7¾"
SCENE BEAM
3½"
1"WIDE × 2" LG WEDGE BEAM SPLITTERS (2)
1"
5"
1"PRISM, #3
LASER INPUT
BEAM SPLITTER ℄ TELESCOPE DETAIL
SCALE : 1½" = 1'-0"

Figure 15a. Plan view of two-beam holocamera installation at elevation 365 feet

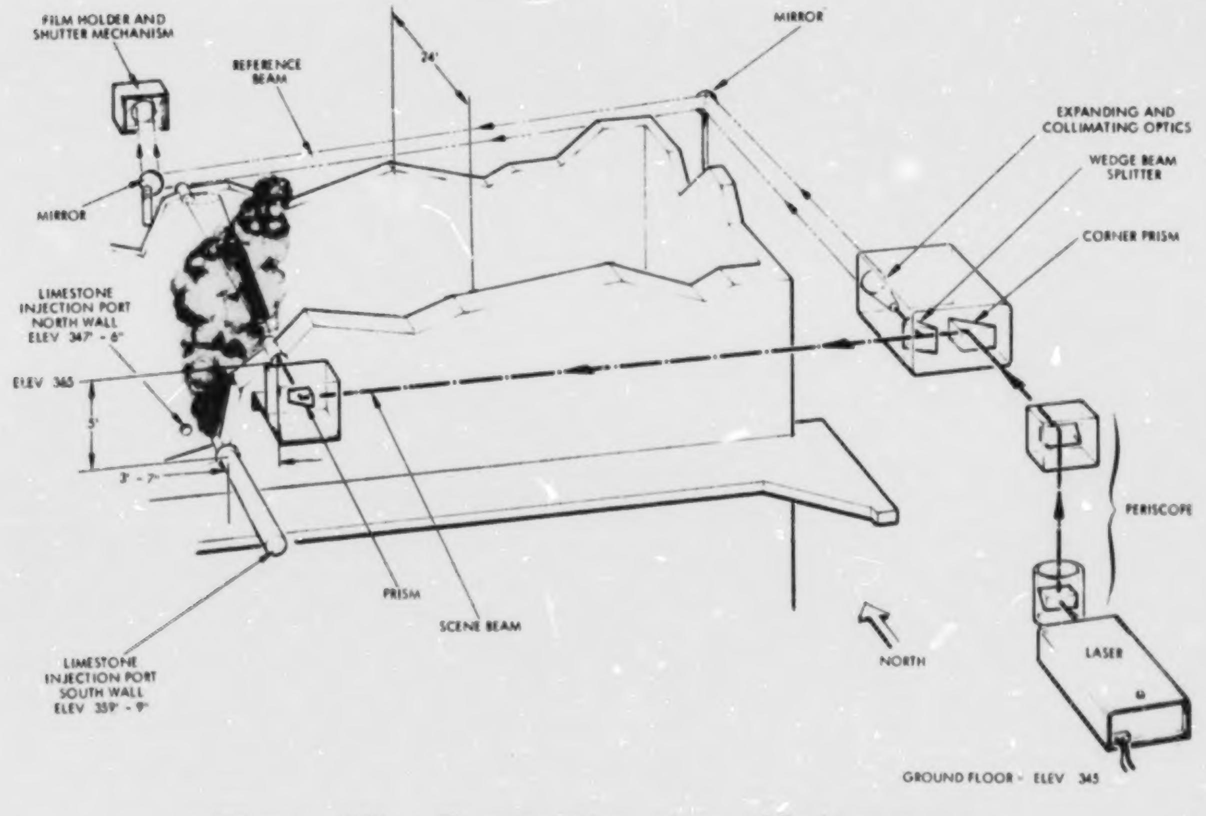
FILM HOLDER AND SHUTTER MECHANISM
REFERENCE BEAM
24'
MIRROR
MIRROR
EXPANDING AND COLLIMATING OPTICS
WEDGE BEAM SPLITTER
CORNER PRISM
LIMESTONE INJECTION PORT NORTH WALL ELEV 347' - 6"
ELEV 365
5'
3' - 7"
PERISCOPE
PRISM
SCENE BEAM
NORTH
LASER
LIMESTONE INJECTION PORT SOUTH WALL ELEV 359' - 9"
GROUND FLOOR - ELEV 345

Figure 15b. Perspective view of holocamera installation at Unit 10

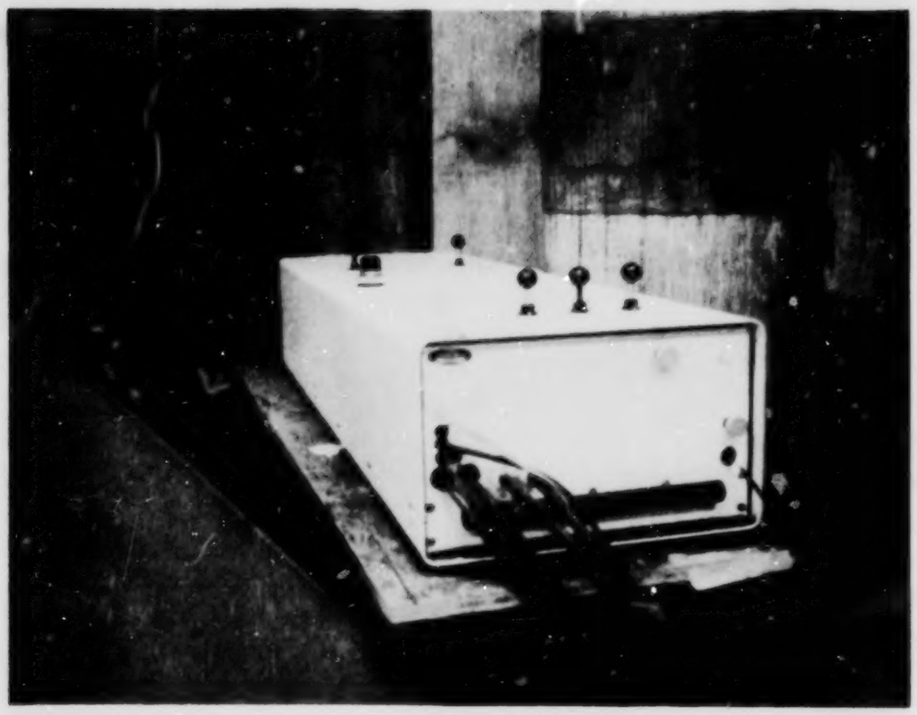

Figure 16. View of ruby laser illuminator installed adjacent to Unit 10 boiler at elevation 353 feet (approximately)

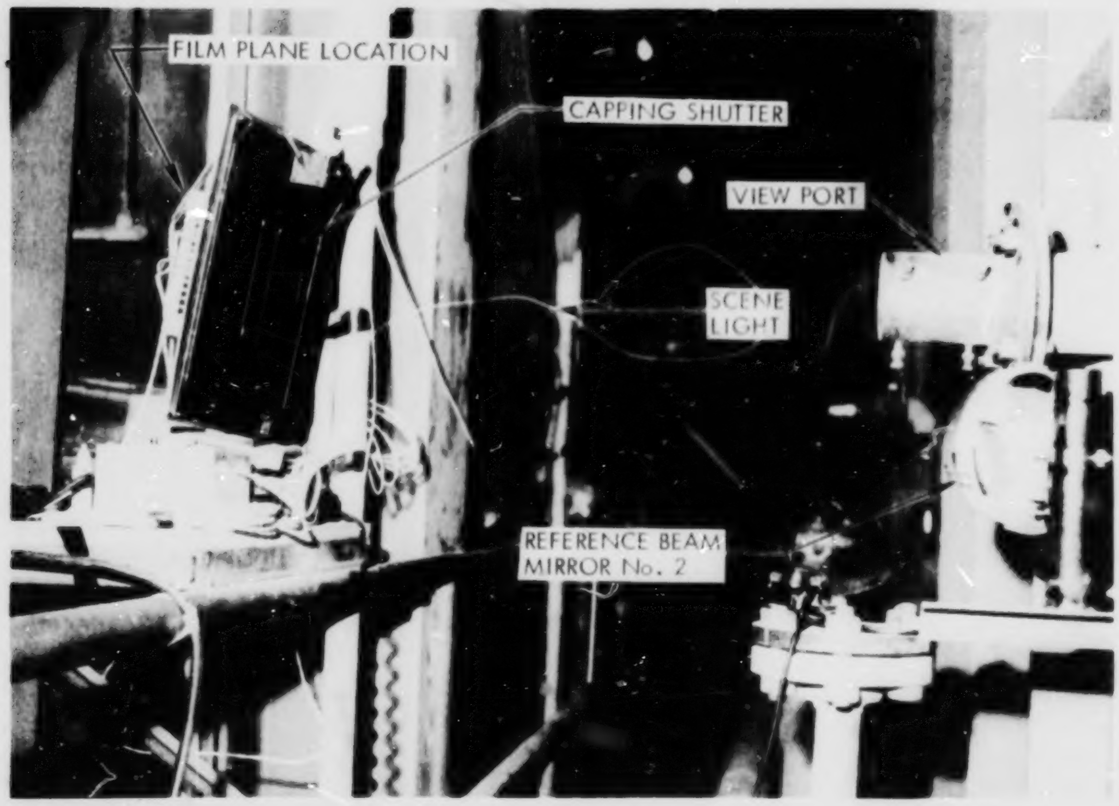

Figure 17. Holocamera shutter assembly

radiant heat, and a fast-acting "focal-plane" shutter. Each time an exposure is to be made, the following sequence of events is typical:

- The film holder is loaded into the shutter mechanism, and the dark slide pulled.
- The laser flashlamp capacitor banks are charged.
- The capping shutter is opened by energizing its electrical solenoid.
- The focal-plane shutter is tripped by energizing its solenoid. A microswitch operated from a cam on the focal-plane shutter mechanism sends a trigger pulse to the laser power supply at the instant the focal-plane shutter is fully open. Laser flash duration is approximately 50 nsec; total exposure of the film to flame light is approximately 50 msec before the focal plane shutter is completely closed again.
- The dark slide is replaced and the exposed film is either removed to the dark room for processing or stored for later processing.

3.4 RECONSTRUCTION APPARATUS AND TECHNIQUES

The scene volume recorded by a hologram is recreated or "reconstructed" by setting the holographic plate before a coherent monochromatic light source and illuminating it with a beam which closely duplicates the original reference illumination. To achieve the most accurate results, the original reference beam must be duplicated as nearly as possible with respect to wavelength and angle of divergence. A convenient continuous wave (CW) illumination source for reconstructing pulsed ruby laser holograms is a helium-neon gas laser which emits at a wavelength of 0.6328 micron. A Spectra-Physics Model 124 helium-neon gas laser of approximately 15 milliwatts power output is quite adequate for the task. Although there is a 10 percent difference in wavelength between the pulsed ruby laser ($\lambda = 0.6943$ micron) used to record the holograms, and the helium neon gas laser employed to reconstruct the scene, careful adjustment of beam divergence angle and orientation of the holographic plate before the reconstructing beam can eliminate or greatly minimize astigmatism and distortion.

When the developed holographic plate is properly illuminated in the reconstruction process, a virtual image of the recorded scene is observed behind the plate in the same physical location as the original scene. The holographic plate becomes a window through which the virtual image of the scene may be observed visually or with the aid of magnifying optics. A convenient means of obtaining a permanent reconstruction record is to photograph the virtual image. This technique was used to evaluate and reduce data contained in holograms recorded on the present program.

3.4.1 Reconstruction of Gabor Holograms

The similarities and differences between the recording and reconstruction geometries for single-beam holograms are illustrated in Figure 18. The hologram is formed as a recording of the stationary interference pattern between the collimated laser beam of wavelength λ and the diffracted light from the object at a distance d from the plate.

Upon illumination of the hologram with a collimated light beam of wavelength λ', four "beams" emerge from the hologram plate: (1) undeviated rays from the reconstruction beam, (2) "noise" rays from defects in lenses or in the hologram plate as well as from nonlinear and intermodulation effects, (3) diverging rays from the virtual image of the hologram, and (4) converging rays which come to a focus at some distance d_1 from the hologram plate, forming a real image. If $\lambda = \lambda'$, the focal distance d_1 will equal d also. The real image at d_1 can be observed by placing a viewing screen at that location, or it can be recorded directly on film. An auxiliary optical system (camera, eye, microscope or telescope) placed in the beam as shown in Figure 18 will form subsequent real images on film, retina or other sensitive material.

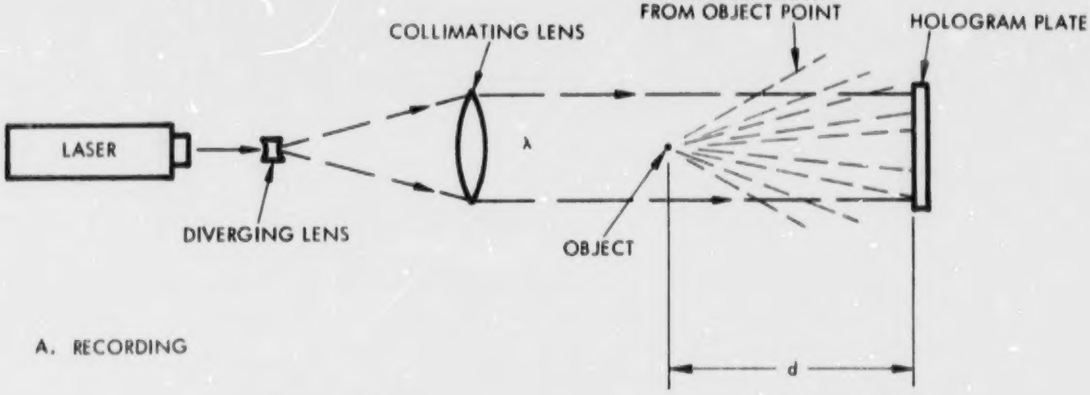

A. RECORDING

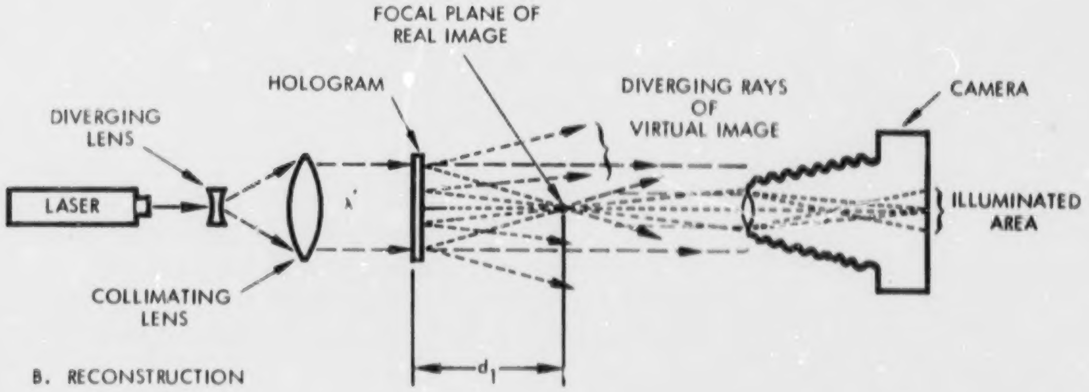

B. RECONSTRUCTION

Figure 18. Single-beam hologram recording and reconstruction geometries

3.4.2 Reconstruction of Two-Beam Holograms

The technique of reconstructing the two-beam holograms recorded during Phase III of the program is similar to that just described for the Gabor holograms. With single-beam or Gabor holograms, the scene and reference illumination are on a common axis. With the two-beam holocamera arrangement reported in Section 3.3, there is a separation in viewing angle between the scene and reference beams of 15 degrees. The viewing angle within the scene was limited by the size of the boiler viewing port to about 3 degrees. There is no overlap or confusion between reference and scene beams in the two-beam holograms.

To view the developed holographic plates made with the two-beam holocamera, it was necessary only to illuminate the plate with a CW gas laser beam which had been expanded and collimated to a diameter of approximately 5 inches and then to orient the plate at the proper angle with respect to the incident beam. In this manner, the entire plate is illuminated, and it is possible to view the recorded scene with full binocular perspective.

One of the unique characteristics of all of the holograms recorded during the program was the extreme length of the scene volume. During the Phase III tests at elevation 365 feet, the effective scene depth of field was 24 feet. In reality, the actual depth of field was greater since the holographic plate was physically located some 33 feet away from the corner prism on the far side of the Unit 10 boiler. To locate and measure axial distances to images within the scene volume, a range finding telescope was used. A medium power "astronomical" telescope was placed before the reconstructed hologram to observe the virtual image. Image distances could be read directly from a calibrated scale located on the focussing tube of this instrument which mapped the image field from 4 feet to infinity into a 4-inch scale.

To use the telescope distance measuring technique properly, the divergence angle of the reconstruction beam must be precisely set; otherwise, objects appear to focus at the wrong distance from the telescope. The easiest way to make this adjustment is to use the telescope as a standard. The laser and its expanding telescope are positioned to illuminate the hologram. The viewing telescope is then positioned to view the image, with the telescope at a fixed distance (say, 3 or 4 feet) from the hologram plate. This distance is added to the known distance from the hologram for the furthest visible object in the scene (in this case, the prism at the front of the boiler which deflects the scene beam for the last time, 33.25 feet from the hologram plate), and the focus scale is set to this value. The corresponding object is then brought into focus in the viewing telescope by adjustment of the focus of the expanding telescope on the laser. All scene distances as measured by the viewing telescope are then to scale.

Much of the data acquired from the limestone plume holograms of Phase III necessitated the production of a photographic negative of the reconstructed virtual image. An entirely different approach to hologram reconstruction was used in making most of the photographs and negatives reported subsequently. The objective of this approach was to maximize the depth of field of the reconstruction photographs. This was desired so that photometric studies could be performed on the resulting negatives. Information on images ranging across the entire 24-foot scene was required, hence the need for maximum depth of field in the reconstruction photograph.

Analogous to the reconstruction photographic technique used to obtain maximum depth of field is the old "pinhole" camera which has an infinite depth of field but admits a very small amount of light. With a hologram, it is possible to take advantage of the fact that each point (or pinhole) on the hologram has "information" from every point in the scene. By putting all of the unexpanded reconstruction laser light through a small portion of the hologram, it is possible to gain the depth of field advantage of a pinhole camera without its disadvantage of very limited light. The resulting reconstructed scene beam has remarkable depth of field properties and is quite bright in appearance.

Another phenomenon which must be contended with in the reconstruction process is laser "speckle" or granularity. The characteristic size of the granular pattern in the reconstructed image varies inversely with the size of the illuminated area of the hologram. If the illuminating beam is too small, the image may be severely compromised by the background noise level of the granularity. Accordingly, a practical setup which was used for photography of these holograms is shown in the sketch of Figure 19. The reconstruction helium-neon gas laser was located about 35 to 50 feet from the hologram so that the natural divergence of the beam allowed it to expand to a diameter of 3 to 4 mm at the hologram plane. The scene beam carrying the virtual image was brought to a focus by a 4-inch-diameter lens of 26-inch focal length such that the range of object distances in the scene occupied only about 1 inch in the real image field. A camera lens (with normal shutter) of 210 mm focal length brought the scene to focus again at the film plane, with the results shown in various photographs in Section 6.

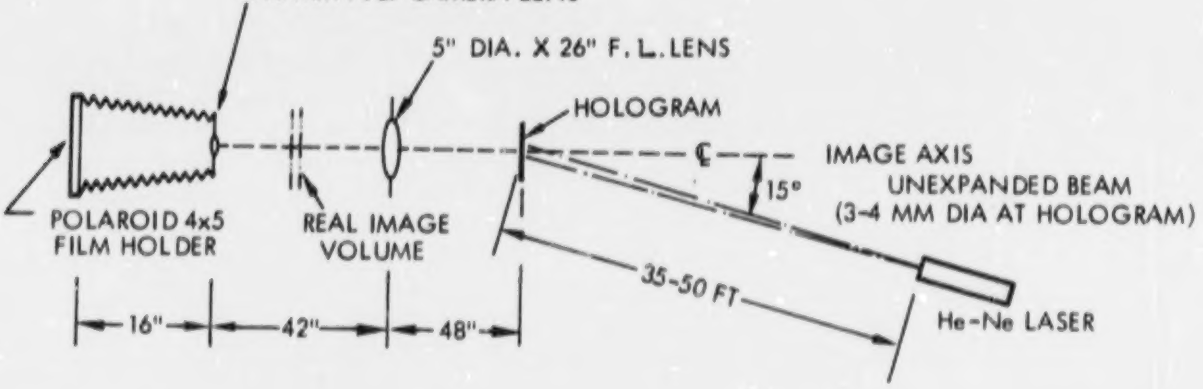

Figure 19. Reconstruction camera setup for maximum depth of field

3.5 RECORDING FILMS AND PROCESSING

The holographic film consistently used in all phases of the program was the Agfa 8E75 emulsion on 4- by 5-inch glass plates.* The plates incorporated an antihalation backing to absorb light reflected from the other surface of the plate.

The development of the plates was accomplished using Eastman HRP developer diluted 1:4 for most of the processing. Some work was done at stronger concentrations (to 1:1). Nominal development time for the plates was about 5 minutes at the rated dilution for the HRP developer. Each plate was sight developed to a density range of approximately 50 percent. After a water rinse, the plates were fixed using Eastman Kodak Rapid Fix. After a fixing period of 4 minutes, the plates were washed (for 10 to 15 minutes) and dried.

Some preliminary recordings were made using Eastman SO-243 cut film. Although it is possible to make holograms using this film, it is more difficult since the emulsion is not on a stable base thus making precise reconstructions a more rigorous task. For the most part, the SO-243 cut film used during this program was for the purpose of initial alignment of the laser and holocamera.

Reconstruction photographs were made exclusively using Polaroid Type 52 (positive) and Type 55 P/N (positive and negative) film in the 4- by 5-inch format.

---

*Product of Agfa-Gevaert, Antwerp, Belgium.

4. LABORATORY EXPERIMENTS

4.1 GABOR HOLOGRAMS

Of primary concern in the application of direct imaging single-beam holography was: (1) the resolving power of the holocamera and the degradation of resolution as a function of distance, and (2) the attenuation of the reference illumination such that reconstruction would be inhibited.

Resolution was investigated using USAF 1951 Resolving Power Test Targets.* The experimental test setup is shown in Figure 10 of Section 3.2. Using this Gabor holocamera arrangement, two sets of resolution target holograms were recorded, developed and subsequently reconstructed for examination with the aid of short working distance magnifiers. The resolution target or "object" was placed at various measured distances away from the holographic plate ranging from approximately 6 inches to more than 48 feet.

The single-beam resolution target holograms were recorded in two separate series, hologram series 10-3-69: 1-12 and series 10-8-69: 1-8. Data from each series are tabulated in Table 1. Prior to recording the second series of holograms (series 10-8-69), two refinements in the test setup were made to enhance resolution. A new USAF 1951 target was utilized since the previous example possessed defects thought to be responsible for a degradation in resolution. In addition, the Galilean telescope used to expand and collimate the ruby laser illuminator was modified to improve spatial coherence of the beam. These improvements contributed to an overall increase in measured resolution from the second set of holograms (series 10-8-69).

Data from both series of resolution chart holograms (10-3-69 and 10-8-69) have been plotted as a function of object distance in Figure 20. Note that a curve was generated for each of the two series of resolution chart holograms together with a third curve which represents the combined test data. For comparison, a fourth curve representing theoretical resolution (for any optical device) $R_{theo} = 1.22 \lambda F/D$, is also shown as a function of distance. In this equation, λ = wavelength of light, D is the diameter of the aperture and F is the distance from the test object to the hologram plate.

Linear and second degree curves were fitted to the data. The data from series 10-8-69 are thought to be most representative of what can be expected in the way of ultimate resolution over large distances using single-beam holography. Note that at a distance of 48 feet, there is an improvement in resolution by a factor of two over the earlier measurements. In summary, this is the best resolution of individual detail which one could hope to see in the boiler volume. In reality, turbulence, temperature gradients, etc., in the boiler environment would even further degrade resolution.

---

*A description of the USAF 1951 resolution target is given in Appendix B.

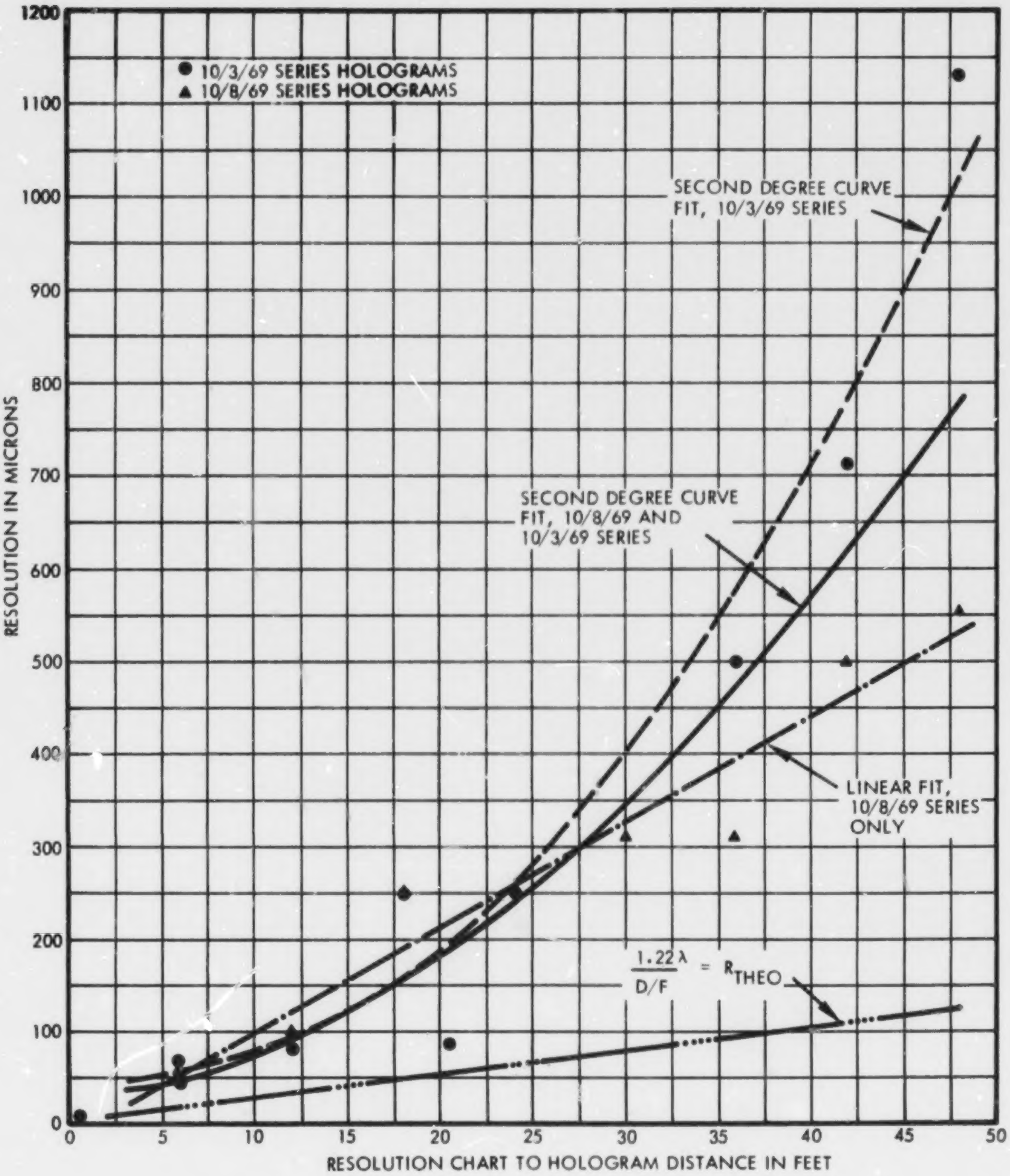

Figure 20. Single-beam holocamera resolution measurements

Table 1. Hologram Resolution Measurements - Gabor Technique
USAF 1951 Resolution Target

Series and Hologram No.	Object (target) Distance	Best Reading Lines (mm)	Equivelant Particle Size (microns)	Remarks
10-3-69: 0	0'-6 7/8"	55.0	9	
1	6'-0"	10.0	50	Laser not Q-switched
2	6'-0"	10.0	50	Laser not Q-switched
3	6'-0"	7.0	70	
4	12'-0"	6.0	83	
5	18'-0"	2.0	250	
6	24'-0"	2.0	250	
7	30'-0"	0.4	1250	This point omitted in curve fit
8	36'-0"	1.0	500	
9	42'-0"	0.7	715	
10	48'-0"	0.44	1130	
11	53'-10"	0.4	1250	
10-8-69: 1	6'-0"	9.0	56	
2	12'-0"	5.0	100	
3	18"-0"	2.0	250	Low contrast negative
4	24'-0"	-	-	Thin negative, no reading
5	30'-0"	1.6	312	
6	36'-0"	1.6	312	
7	42'-0"	1.0	500	Many confusing images
8	48'-0"	0.9	555	Many confusing images

In addition to the resolution target holograms, three sets of holograms of glass beads were recorded.* Two of these latter three sets of holograms used glass beads of 40 to 50 mesh and the third used beads of 120 to 170 mesh size. Size data for various mesh numbers are shown in the Table 2.

Table 2. U. S. Standard Sieve Series, 1940*

Mesh No.	Size (microns)	Sieve Opening (inches)
40	420	.0165
50	297	.0117
70	210	.0083
120	125	.0049
170	88	.0035
200	74	.0029
230	62	.0024
325	44	.0017

*Ref.: C. D. Hodgman, ed., Handbook of Chemistry and Physics, 43rd Edition, The Chemical Rubber Publishing Co., Cleveland, Ohio, 1961. p. 3401

---

*No. 831 titanium glass beads (high index of refraction) purchased from the Bavin Co., 2500 W. 6th Street, Los Angeles, California.

The procedure for recording holograms of glass beads was similar to that described for the resolution chart experiments. A fine stream of beads was dropped through the holocamera scene volume during the laser pulse. Recordings of the beads were made at 6-foot intervals along the optical path. The purpose of these tests was to record holograms of a scene similar to that which appears in the Unit 10 boiler superheater region. Reconstructions of these holograms were subsequently used to determine if one could focus on small distributed objects and determine where in the scene volume these objects were located. Resolution of known particle sizes at various object distances could also be compared with the earlier resolution target measurements.

In the first set of holograms of 40-50 mesh glass beads, well defined images (297 to 420-micron-diameter beads) could be observed at an object distance of 6 feet. In the reconstruction of the holograms recorded at object distances of 12 and 18 feet, respectively, bead images were visible but less well defined (i. e., the edges of the images were fuzzy). The holograms of beads located at distances greater than 18 feet exhibited even poorer reconstruction images. The results compared approximately with the resolution chart measurements (Figure 20) in that 300 to 400-micron particles are distinguishable at distances of 25 to 35 feet. At greater distances, the reconstructions appear only as blotches. Similar results were observed with the holograms sets of 120-170 mesh beads.

One of the glass bead Gabor holograms was selected for data reduction. The photograph of Figure 21 shows a helium-neon gas laser reconstruction of a dispersion of 40-50 mesh (297- to 420-micron diameter) beads located at a distance of 6 feet from the hologram plate. Bead images on three 1-inch- square areas of the film were measured. The resulting data were grouped into 25-micron intervals and counted. A computer program was used to calculate the cumulative volume fraction, $\Sigma ND^3/(\Sigma ND^3)_{total}$ where N is the number of beads for each 25-micron interval and D is the median diameter of the corresponding interval. A plot of these data is shown in Figure 22. Note that about 25 percent of the beads fall outside of the manufacturers nominal size range (297 to 420 microns) on both ends of the distribution.

The reconstructed scene in a Gabor hologram produces a negative image. This is seen in reconstruction photographs of glass bead holograms. In the real image produced by the holograms, the shadows of the beads show as bright spots against a dark background (Figure 21). Note also from this reconstruction photograph that the background is not uniformly dark, but is generally mottled and contains another set of less luminous spots. A similar effect is seen in the real image resolution target reconstruction photograph of Figure 23. In this figure, the spurious images look like three-bar chart elements out of place.

A real image of glass beads at a distance of 12 feet from the hologram is shown in Figure 24. This photo was made from hologram No. 2 of 7 October 1969. In a separate series of glass bead holograms made on 9 October, the number of beads within the scene volume was greatly reduced to avoid cross-modulation between images. Figures 25 and 26 are from holograms No. 1 and No. 2 of that series taken with the beads at 6 and 12 feet from the plate. Images of four beads are evident in

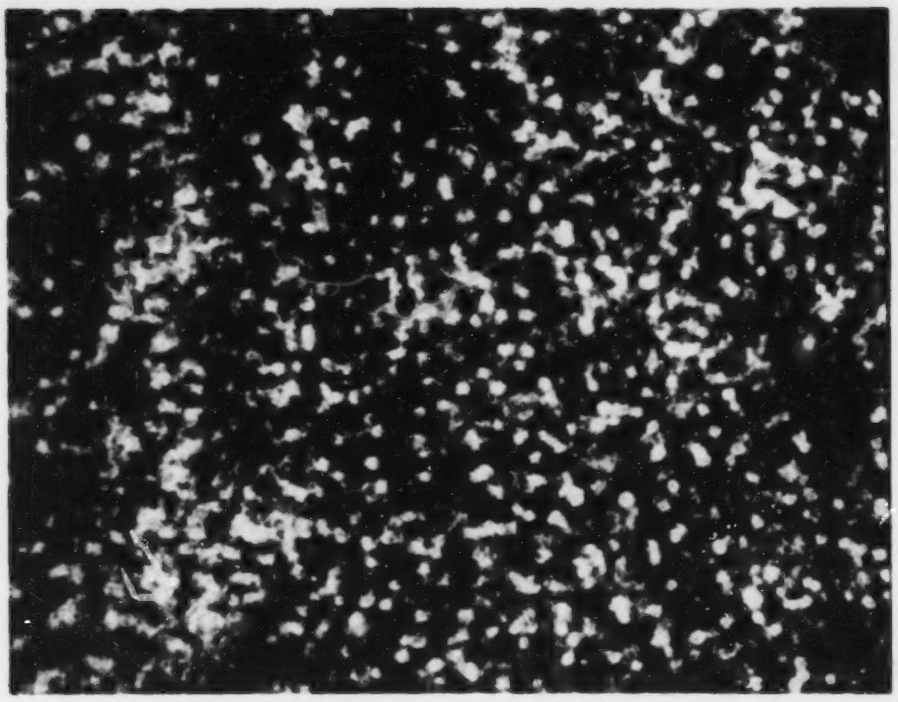

Figure 21. Helium-neon laser reconstruction of a pulsed ruby hologram. Reconstruction photo shows a distribution of 297- to 420-micron-diameter glass beads located a distance of 6 feet from the hologram plate. Beads are magnified by a factor of 5. 9.

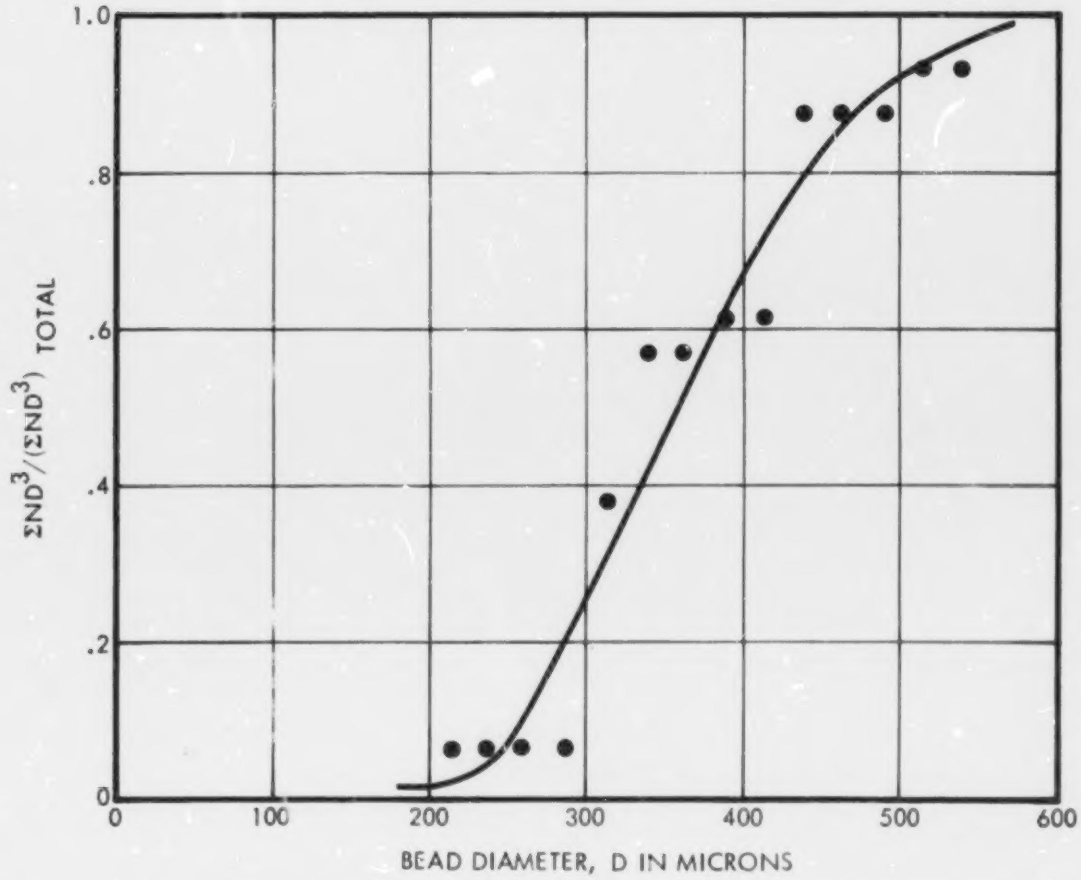

Figure 22. Cumulative volume fraction versus bead diameter. Distribution measured from bead images seen in Figure 19

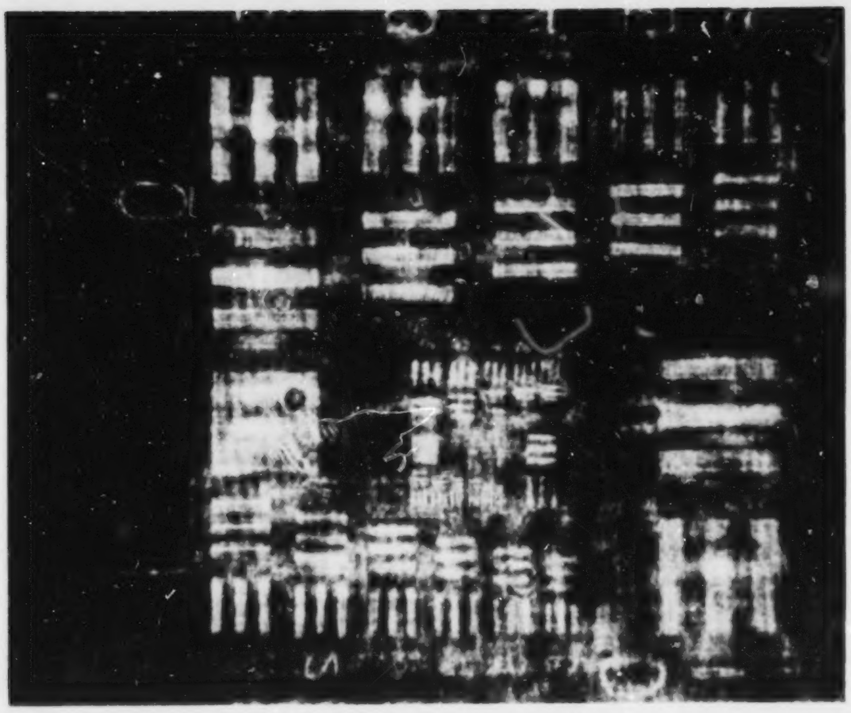

Figure 23. Real image from hologram No. 1, series 10-8-69. Image comes to focus at 6 feet from the hologram

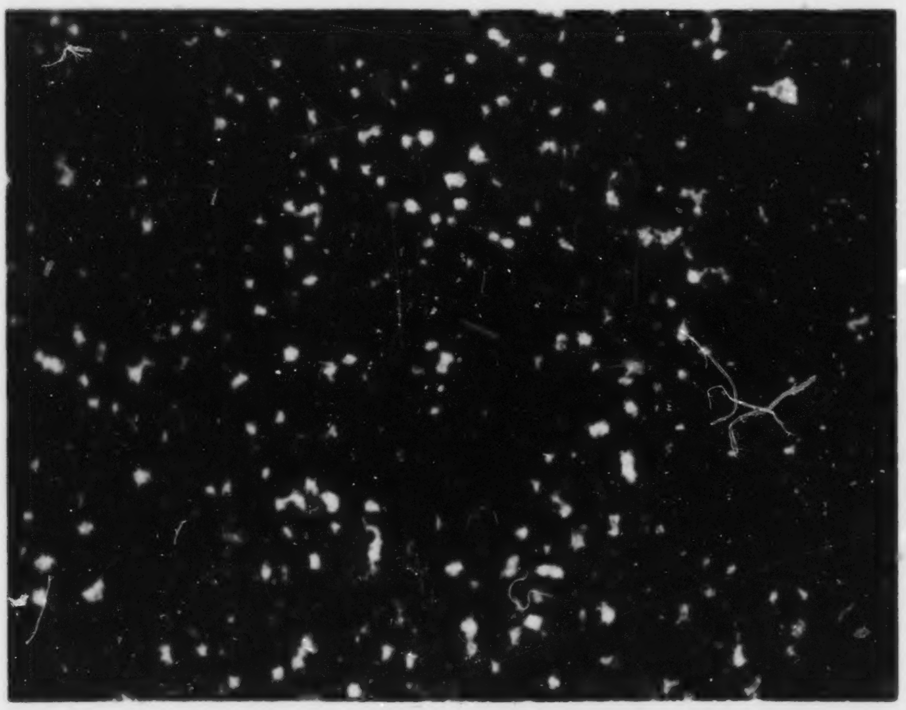

Figure 24. Reconstruction photo of stream of 40-50 mesh glass beads, holographed 12 feet from the film plate. Hologram 10-7-69:2

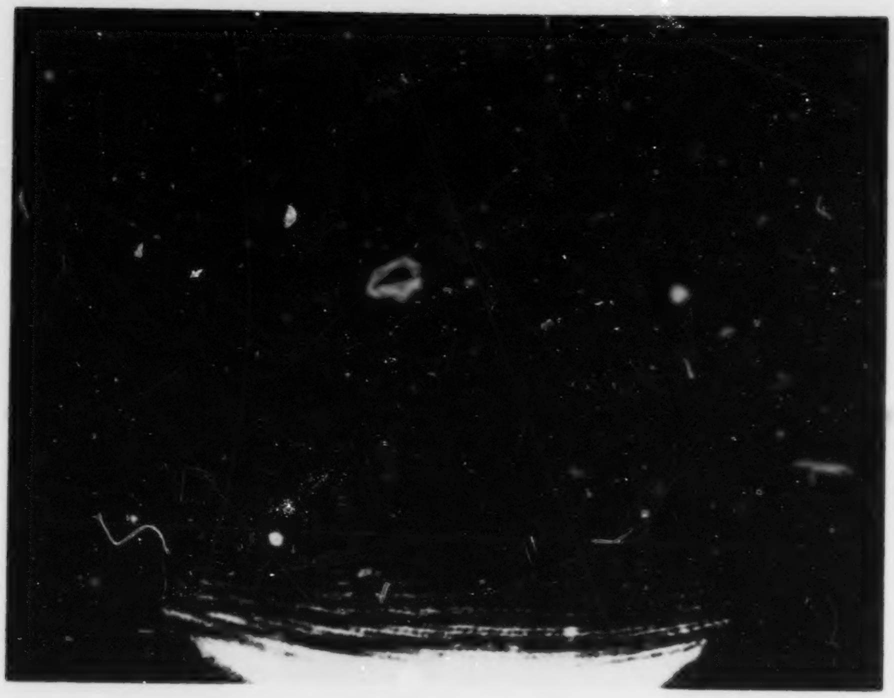

Figure 25. Reconstruction photo of stream of 40-50 mesh glass beads at 6 feet from hologram. Four bead images are visible. Number of objects in scene was reduced to reduce the number of spurious images.

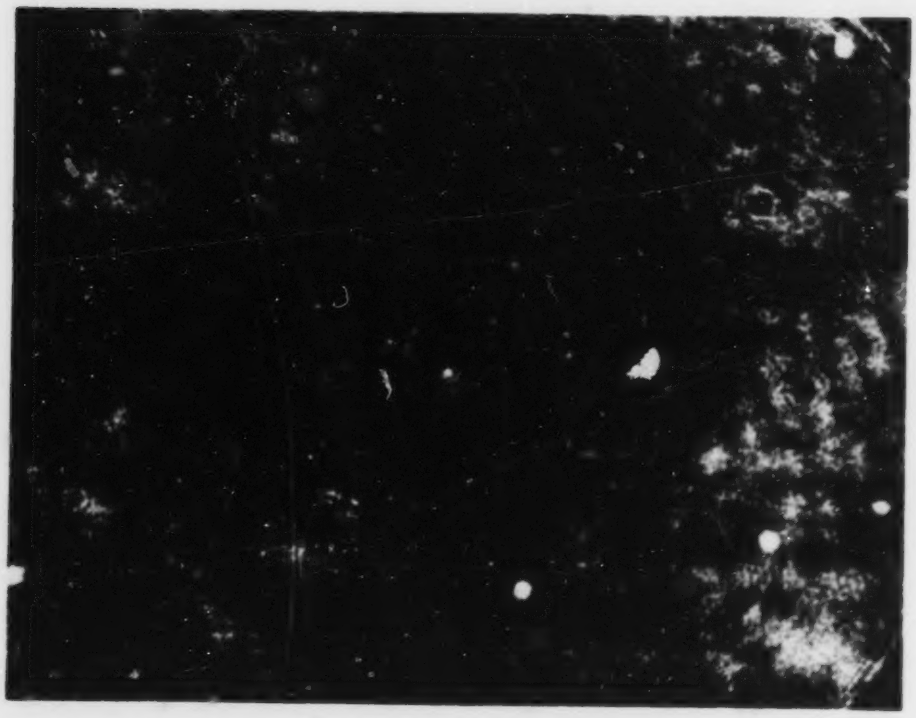

Figure 26. Reconstruction of images of 40-50 mesh glass beads at 12 feet from hologram. Five bead images are visible.

Figure 25 and five beads in Figure 26. In both instances, image sharpness is improved as the result of using fewer objects in the scene.

The reconstruction photographs and data reduction presented here have all centered on the holograms made using the more coarse (40-50 mesh) glass beads in the holocamera scene volume. No really satisfactory reconstruction photographs of hologram recordings of the smaller mesh size beads were made. In viewing the reconstructions of beads in the 120 to 170 mesh size range (nominally 125 to 88 micron diameter particles) individual bead images became indistinct at 18 feet and beyond.

4. 2 TWO-BEAM SCATTERED LIGHT HOLOGRAMS

For the application at hand, that of identifying, locating and measuring the boundaries of large ensembles or clouds of limestone particles across a 24-foot combustion volume, the technique of single-beam holography proved inadequate. Since the reference and scene beams of a Gabor hologram are coaxial, the reconstructions tend to be somewhat "noisy" and contain spurious images. Identification and location of objects in a complex scene becomes more difficult. A further handicap is the inherent degradation of size resolution with increasing distance. In the absence of a finite object on which to focus, it becomes impossible to achieve any spatial resolution. In the limit, the presence of very large ensembles of particles encodes the reference illumination of the single-beam hologram resulting in an inability to reconstruct a meaningful hologram scene. Such was the condition in the boiler at the Shawnee Power Plant.

Because of the inherent limitations of single-beam holography, an alternate approach was selected for evaluation. Under sponsorship of an independent research program at TRW, a method of recording low angle forward scattered light was tested. The concept of scattered light holography of clouds of particles had been conceived previously at TRW when it was realized that Gabor holography would not be adequate. Reduction to practice was accomplished concurrently with the Phase I effort of this program.

Basically, the scattered light holography technique is a modification of a more conventional TRW two-beam transmission holocamera system. The initial holocamera setup, used to demonstrate feasibility in a laboratory configuration, was described in Section 3. 3. A series of test scenes was recorded with the two-beam scattered light holocamera setup. These include tufts of cotton, glass wool fibers and dust from chalkboard erasers. The objects were placed at specific distances into the scene volume along the laser scene beam path. The depth of field for the holocamera was approximately 50 feet in length.

Reconstruction of the recorded holograms was accomplished using a continuous wave gas laser. The laser beam was expanded and collimated to approximate that of the original reference beam. The virtual image of each reconstructed scene was observed by looking through the hologram plate as through a window. Since the reference beam arrived at the hologram plate with an angular displacement relative to the scene beam, the reconstructed virtual image of the scene was made to appear against a uniformly dark background free from extraneous images. Upon viewing a typical reconstruction, the observer sees a bright point of light at a great distance into the scene (in reality, the laser light from the last corner prism some 50 feet away from the holographic plate), light scattered from various objects placed in the scene at corresponding distances (cotton, glass fibers, etc.), and innumerable bright points of light along the laser scene beam caused by low angle scattering from airborne dust particles.

Figure 27 is a typical reconstruction photograph made from a hologram (10-31-69:1) recorded during the scattered light tests. The photograph shows back lighted cotton tufts located at 6 and 12 feet from the holographic plate. The photo was made with a camera lens stopped to f/32 for maximum depth of field to simulate the view obtained with an observer's unaided eyesight. (In direct viewing, an individual's eyes compensate for angles and focus so unconsciously that everything in the scene seems in focus at once; with a camera, this is not so.)

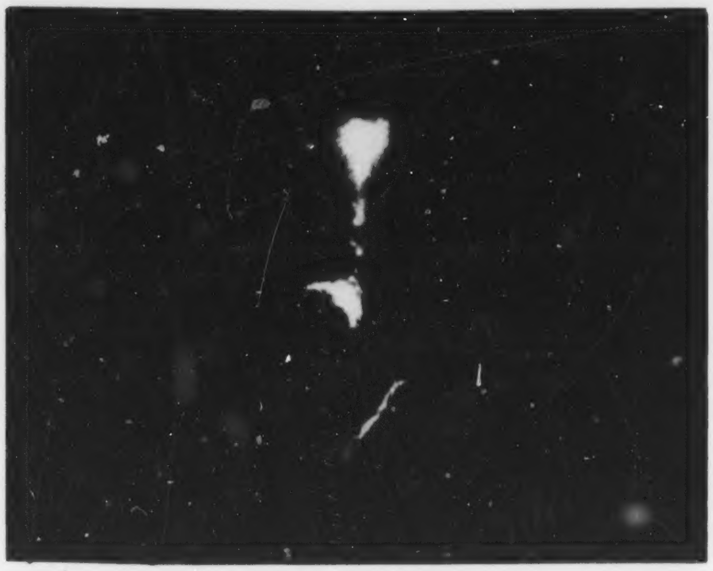

Figure 27. View of the virtual image of low-angle forward scattered light from cotton balls at 6 and 12 feet from the hologram. Light from airborne dust particles traces illuminating beam back to laser 50 feet away.

The image of this same hologram (10-31-69:1) was examined with a small astronomical telescope, and it was found that a great many objects in the scene could be brought into separate sharp focus. With this instrument the focal distance from 6 feet to infinity maps into about a 6-inch travel of the eyepiece focus adjustment so that a scale of distances is readily available for location of object distances in such a scene. An example of how such discrimination is made using the focus adjustment of the view camera is shown in Figure 28 which is a composite of three views at focal distances of 6, 12, and 35 feet beyond the hologram plane, and iris adjustment of f/8.

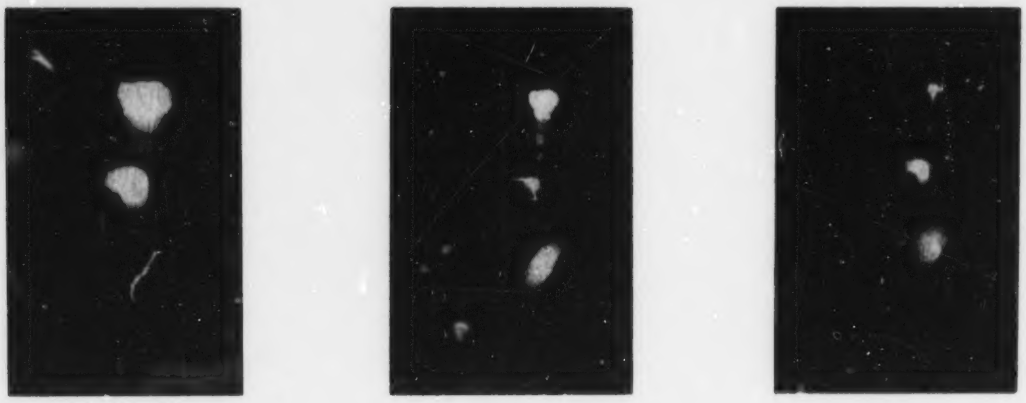

Figure 28. Composite views of a scattered light reconstruction at focal distances of 6, 12 and 35 feet

5. SHAWNEE UNIT 10 EXPERIMENTS

5.1 GABOR HOLOGRAMS—UNIT 10 SUPERHEATER

Gabor holographic recordings of fly-ash particles in the Unit 10 superheater (elevation 392 feet) were attempted during December 1969, using the holocamera apparatus described in Section 3.2. The limestone injection system was not operating during this initial holography work at the boiler.

Twenty-four holographic recordings were made of particulate in the superheater region. These are tabulated in Table 3. In addition to the initial six alignment tests, 23 more single-beam recordings were made using both Agfa 8E75 plate and Eastman S0-243 cut film. Laser light attenuation across the 47-foot optical path of the Unit 10 superheater (see Figure 11) proved more severe than originally estimated.[8] There was insufficient ruby light to expose the Agfa 8E75 emulsion. All efforts to obtain an exposure with Agfa 8E75 plate failed. The Eastman S0-243 emulsion, which has a sensitivity 100 times greater than the Agfa plate, could be adequately exposed such that 5 to 8 minutes development time in HRP developer (diluted 4:1) produced a negative of reasonable density and contrast.

Although exposures on S0-243 cut film sheets could be made, the results were not satisfactory. Upon reconstruction, no meaningful information could be abstracted from the hologram. In only a few instances, apparent real images could be brought to focus at various distances into the reconstruction field (for example, in holograms 1253 and 1254). The images appeared to be approximately 1000 microns in size. Examination of the holograms, however, failed to reveal any obvious corresponding fresnel diffraction patterns for these few images.

5.2 SCATTERED LIGHT HOLOGRAMS—UNIT 10 BOILER

Phase III scattered light holography tests at the Unit 10 boiler (elevation 365 feet) were divided into several series of experiments using the two-beam holographic test setup described in Section 3.3 and shown in the schematic diagram of Figure 15. The setup of the holocamera and the conduct of the test program required a total of 3 weeks during the month of February 1970.

A total of 79 holograms was recorded under a variety of operating conditions during the 3-week feasibility test program.* Figure 29 is a matrix of the various boiler and holocamera operating conditions. Test conditions are indicated around the periphery of the matrix diagram. Listed within each segment of the matrix are the record numbers of the specific holograms used for analysis and data reduction for the indicated test conditions.

---

*Appendix C presents basic holographic and boiler operating data and information on each of the 79 holograms. These holograms are currently on file at TRW Systems.

Table 3. Phase II Holograms — Unit 10 Superheater

Date	Hologram Number	Film Emulsion	HRP Dilution	Development		Laser Pulse Diode Output	Remarks
				Time, Min.	Temp., °F		
12-4-69	(1)	SO-243	4:1	4	65		Alignment check. Unexpanded beam, no Q-switch. Film saturated.
	(2)	"	4:1	2	68		Repeat of 12-4-69 - No. 1
	(3)	"	4:1	2	68		Alignment check with 4 in.dia. collimated beam. No Q-switch. Exposure non-uniform.
	(4)	"	4:1	2	69		Same as 12-4-69 - No. 3. Image contrast "soft."
	(5)	"	4:1	3	70		Same as 12-4-69 - No. 3. More contrast, exposure non-uniform.
	(6)	"	4:1	4	70		Same as 12-4-69 - No. 3. Good contrast, exposure non-uniform.
12-8-69	1232	8E75	4:1	8		0.16 volt	Dye cell Q-switch, 4 in.beam. Laser double pulsed. Plate fogged
	1233	"	4:1	9		0.21	Good laser pulse. No image. Plate accidentally fogged.
	1234	"	4:1	8		0.25	No image.
	1235	"	2:1	8		0.29	No image.
	1237					0.24	Visual beam alignment check. No film in camera.
	1238					0.25	Repeat of No. 1237.
	1239	SO-243	2:1	2	64	0.20	Very weak image, underdeveloped.
	1240	"	2:1	2.5	66	0.20	Weak image, underdeveloped.
	1241	"	2:1	2.5	66	0.21	Weak image, underdeveloped.
	1242	"	2:1	3	67	0.19	Underdeveloped.
	1243	"	2:1	3	69	0.15	Underdeveloped.
	1244	"	2:1	3.5	69	0.17	Weak image, underdeveloped.
12-9-69	1250	"	4:1	2	63	0.20	Weak image.
	1251	"	4:1	4	64	0.26	Moderate contrast.
	1252	"	4:1	8	66	0.22	Good contrast.
	1253	"	4:1	6	67	0.17	Good. Will reconstruct but with little apparent information.
	1254	"	4:1	5	67	0.19	Good contrast, but little apparent information.
	1255	"	4:1	5	67	0.21	Same as No. 1254.
	1256	"	4:1	5	69	0.34	Clear. No image on plate.
	1257	8E75					Laser accidentally pulsed early in sequence. No exposure
	1258	"	1:1	9	65	0.22	No image.
	1259	"	1:1	4	65	0.34	No image.
	1260	"	1:1	8	68	0.33	No image.

		No Limestone		Limestone	
		Coll. Beam	Fan Beam	Fan Beam	Coll. Beam
Power @ 140 MW	Rear Port	No. 1327(1) No. 1331 No. 1381(2) No. 1534	No. 1491	No. 1391 No. 1535	No. 1544 No's. 1547 thru 1549
	Front Port			No's. 1568 thru 1573	No's. 1562 thru 1567
Power @ 85 MW	Front Port	No. 1505	No. 1506		
	Rear Port				

Notes: (1) Reconstruction photograph to obtain scene beam "fingerprint" only.

(2) USAF 1951 target in scene. Reconstruction photos used to show extreme depth of field available

Figure 29. Matrix of Shawnee Unit 10 holographic tests and hologram numbers analyzed for information and limestone plume data

5.2.1 Operating and Test Conditions

With respect to the holocamera, two variables existed; namely, the use of a collimated scene beam or a flat "fan-shapped" scene beam. When a collimated scene beam was employed, an essentially cylindrical shaft of ruby light passed through the boiler. Some scene beam divergence did occur. The beam, initially about 1 inch in diameter at prism No. 4 (entering the boiler), was about 2 inches in diameter upon reaching the holographic film plate. The "fanned" ruby light scene beam was produced by placing a -2 diopter cylindrical lens ahead of prism No. 4 (Figure 15). This resulted in an essentially flat horizontally diverging scene beam in the form of a triangle normal to the boiler combustion gas flow. The fanned scene beam permitted somewhat more coverage of the phenomena occurring within the boiler. The two different scene beam geometries are shown in the schematic diagrams of Figure 30.

Of primary interest to the test program was the ability to discern and locate those portions of the limestone cloud passing through the scene beam of the holocamera. In this respect, holograms were recorded in the presence of limestone injected from the front (south) and from the rear (north) side of the boiler. Limestone injected from the front side of the boiler was accomplished using a row of injection ports at elevation 359 feet, 9 inches. The nearest injection port to the scene beam was approximately 3 feet, 7 inches west; and 5 feet below the scene beam inlet port at elevation 364 feet, 9 inches. On the rear or north side of the boiler, the nearest limestone injection port was in line with the scene beam exit port and 16 feet below it at elevation 348 feet.

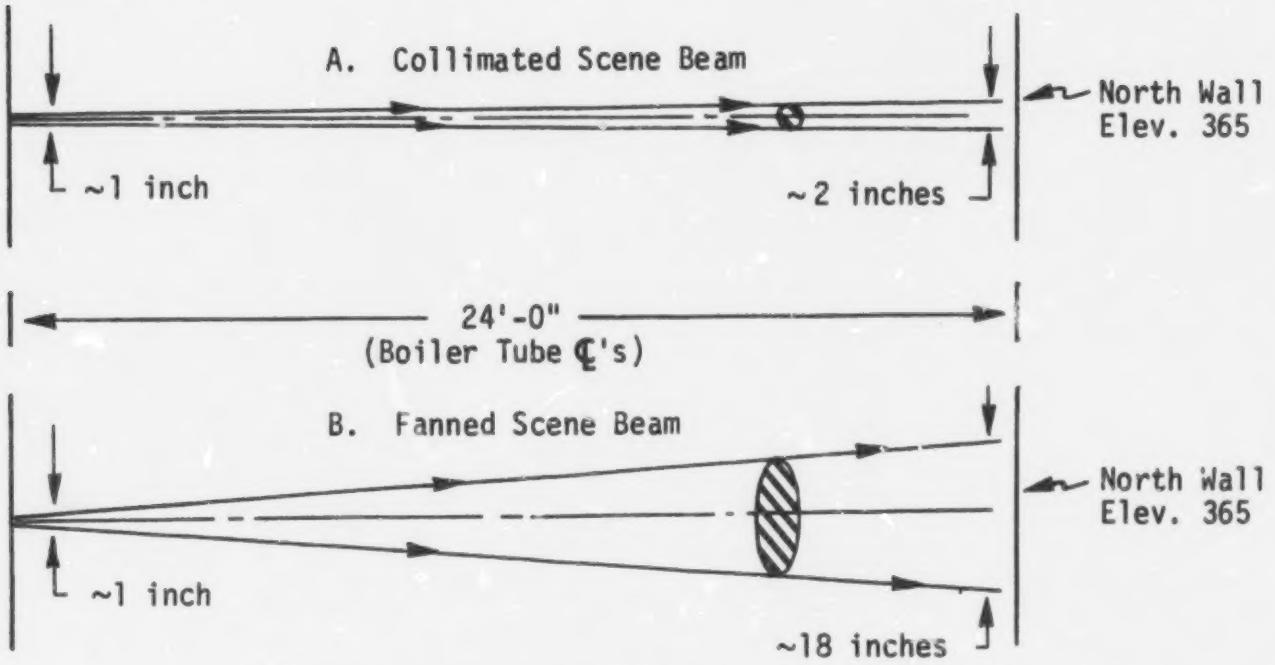

Figure 30. Schematic diagram of holocamera scene beam geometries used to record particulate in the Unit 10 boiler

During the holography test series, limestone injection rates through the front four ports (on 3-12-70) varied from approximately 7500 to 11,000 lb/hr or about 1870 to 2750 lb/hr through each port. Twelve holograms recorded while limestone was being injected through these front ports. All of these recordings were evaluated and reduced for limestone plume information.

Holography tests with limestone injected through the six lower rear side injection ports were conduction on 3-6-70 and on 3-12-70. Injection rates for the 3-6-70 series varied between 6000 and 7000 lb/hr or about 1000 to 1165 lb/hr per rear injection port (elevation 348 feet). During the latter series (3-12-70), injection rates ranged from approximately 3000 to 8000 lb/hr or 500 to 1330 lb/hr through each port. In all, 31 holograms were recorded of limestone injected through the rear set of injection ports. Of these, six were used for data acquisition.

In summary, 18 holograms, covering limestone plumes injected from both the front and rear side injection ports were evaluated.

The remaining operating variable was the power output of the boiler. This is a function of the pulverized coal and air feed rates. Hence, the particulate in the boiler (fly-ash) might be expected to vary approximately as the power outputs of the boiler. A series of holograms was recorded during a boiler power excursion on 3-11-70. The boiler was operated at power levels ranging from approximately 85 to 140 mw. Holograms from this series were qualitatively evaluated; however, no quantitative data were obtained.

5.2.2 Data Reduction from Holographic Reconstructions

The utility of the holographic method of detecting limestone plumes in an operating steam boiler is a function of the measurable quantities which may be obtained from the reconstructed images. With two-beam scattered light holograms, the quantities measured to date include:

- Axial distances between hologram and focusable images
- Angular distances between images
- Luminous intensity variations.

Axial distances between the hologram plate and images in the reconstructed scene have been measured with the ranging telescope. The method is described in Section 3.4 of this report. If the geometry of the boiler and holocamera arrangement are known, location of limestone clouds relative to the boiler walls can be determined.

Measurement of angular distances within the virtual image field using the wide depth-of-field reconstruction photographs has also been accomplished as part of the hologram data reduction process. From these measurements and the known geometry of the scene beam and boiler porting at elevation 365, a check on telescopic measurements of axial distances is possible. Good agreement between the results of the two methods was obtained.

Direct measurements of luminous intensity in the reconstructed holographic images were not accomplished. However, microdensitometer traces on photographic negatives of the reconstructions have been made and proved extremely useful. To date, the densitometer measurements of changes in negative intensity (relating to the presence or absence of clouds) have yielded only relative values since a suitable calibration or reference illumination on the original hologram is lacking. Qualitative comparisons have been made between negatives taken from similar holograms, for cases with and without limestone injection. Generally, the limestone traces show luminous intensity variations, often not discernible to the unaided eye, which reveal the presence of limestone clouds. In those instances where visible clouds are obviously present, the microdensitometer traces confirm the pronounced variations observed in the hologram reconstruction and measured with the ranging telescope.

6. RESULTS AND DISCUSSION

Although a significant amount of work was devoted to the technique of single-beam or Gabor holography, the only substantive results for in situ boiler studies were obtained with the two-beam holography technique of recording low-angle forward-scattered light. This section describes the scattered light holography results obtained during the 3-week period of Phase III at the Shawnee Unit 10 boiler.

Of the original 79 scattered light holograms made during Phase III, 25 were eventually selected as representative of the eight test condition categories listed in the test matrix of Figure 29 in Section 5. 2. 1.* Since the basic purpose of the holographic test program was to demonstrate a capability to record the presence of limestone plumes or clouds, 18 of the 25 holograms selected were recordings made during limestone injection tests. Much of the subsequent discussion centers on these latter 18 holograms.

6. 1 TESTS WITHOUT LIMESTONE INJECTION - 140 MW

Initial tests at Unit 10 were concerned with demonstrating the holographic technique and refining the test setup alignment. Holograms were made with a collimated scene beam and later, with a fan-shaped scene beam. Nominal boiler power output was 140 mw.

Holograms No. 1327 and 1331 are representative of these early tests (see Appendix C). Hologram 1327 was made with the scene beam light directly incident on the film plate. In addition to confirming alignment, it gave a direct measure of the scene beam divergence across the 24-foot scene volume. Figure 31 is a contact print made from this hologram.

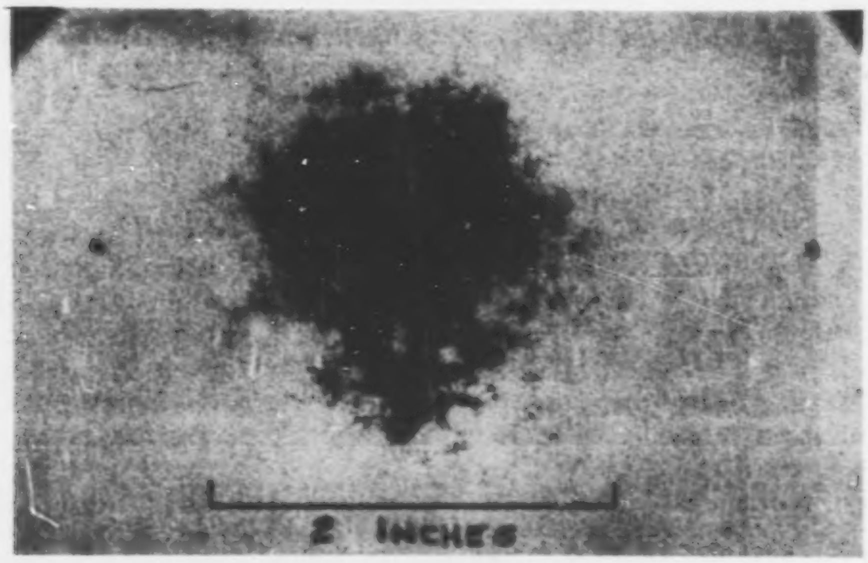

Figure 31. Collimated scene beam "fingerprint" on holographic plate after traversing 24-foot combustion volume of Unit 10 boiler

---

* See Appendix C for a complete listing of the 79 Phase II holograms.

Hologram 1331 was the first recording of scattered scene light made on the Agfa 8E75 emulsion. It provided an excellent reconstruction and exhibited numerous apparent discontinuities along the laser beam axis. These could be seen by viewing the reconstructed hologram's virtual image from varying positions and noting the nonlinearity or shimmering of the beam axis. These irregularities were termed "thermals" and were originally thought to be caused by strong temperature gradients and turbulence within the combustion gases. It was later found, however, that these so-called thermals were induced into the scene by a draft of cold air entering the boiler through the open viewing port at the recording station (Figure 17) of the holocamera setup.* A red glass filter (Corning CS-2-57) was subsequently used as a "window" to cover the open view port while recordings were being made. This technique eliminated the appearance of thermals in the reconstructed holograms.

Holograms 1331 and 1534 were reconstructed and (the virtual image) photographed. Single scan microdensitometer measurements were made with reconstruction negatives obtained from each hologram. An example densitometer scan is shown in Figure 32 for hologram 1331. Also shown is a reconstruction photograph of the laser scene beam which corresponds to the negative used in the densitometer measurements. The insert photograph is oriented in the direction of the scan trace. The observer is looking across a light beam spanning 24 feet with the near or north boiler wall at the right edge of the photographic image.

Densitometer measurements of hologram reconstruction photographs of fly ash (only) were characterized by a relatively straight line slope to the resulting traces. This may be seen in the illustration of Figure 32. Also, the intensity of the light scatter appeared uniform based on the nominal band width of the trace oscillations. These characteristics would imply that relatively uniform fly ash distribution across the boiler generally existed.

In another test (hologram 1381) during the first series, a USAF 1951 resolution target was placed before the open boiler port, a distance of 28.5 inches from the holographic film plate. Reconstruction photographs were made by focusing a view camera first on the virtual image of the resolution target (Figure 33a) and next on the scattered light from the scene beam (Figure 33b). In the upper photograph, the three-bar pattern of the resolution target located 2 feet, 4 inches from the holographic plate is in sharp focus while the scene beam scattered light is blurred in the background. The lower photo shows light scattered around the area of the 1-inch No. 4 prism (lower portion of the light image) some 33 feet, 3 inches from the hologram. In this illustration, the bar pattern of the resolution target is more grossly out of focus in the foreground.

The remaining two holograms in the tests at full boiler power output and without limestone injection represent demonstration of the technique using a collimated and then a fanned beam (holograms 1534 and 1491, respectively). These holograms, when reconstructed, exhibit a general characteristic of uniformity and brightness across the 24-foot scene length.

---

* A negative pressure gradient exists while the boiler is operating (1-2 inches of water) thus drawing ambient air into the open port.

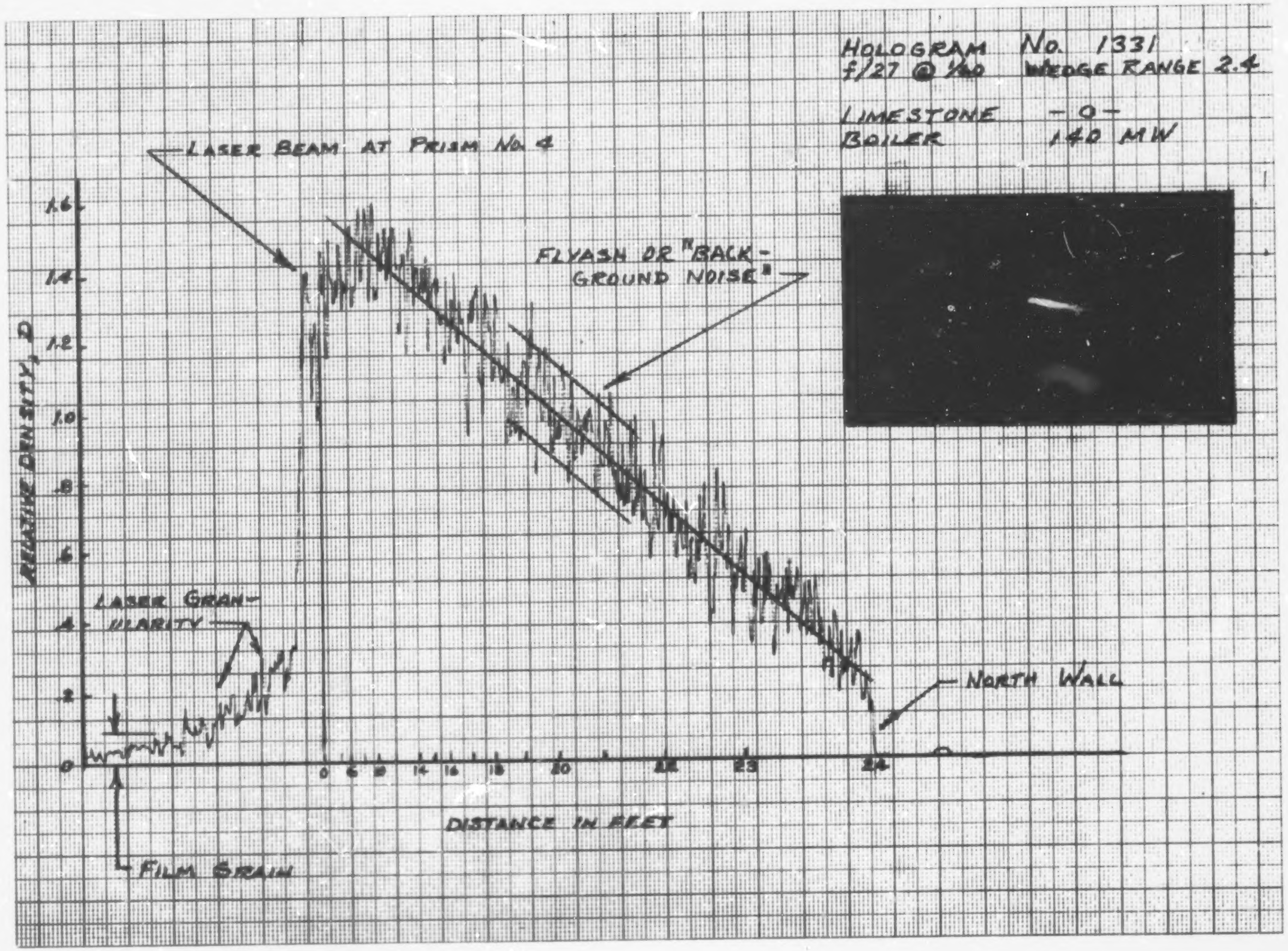

Figure 32. Densitometer trace for hologram No. 1331 reconstruction photograph

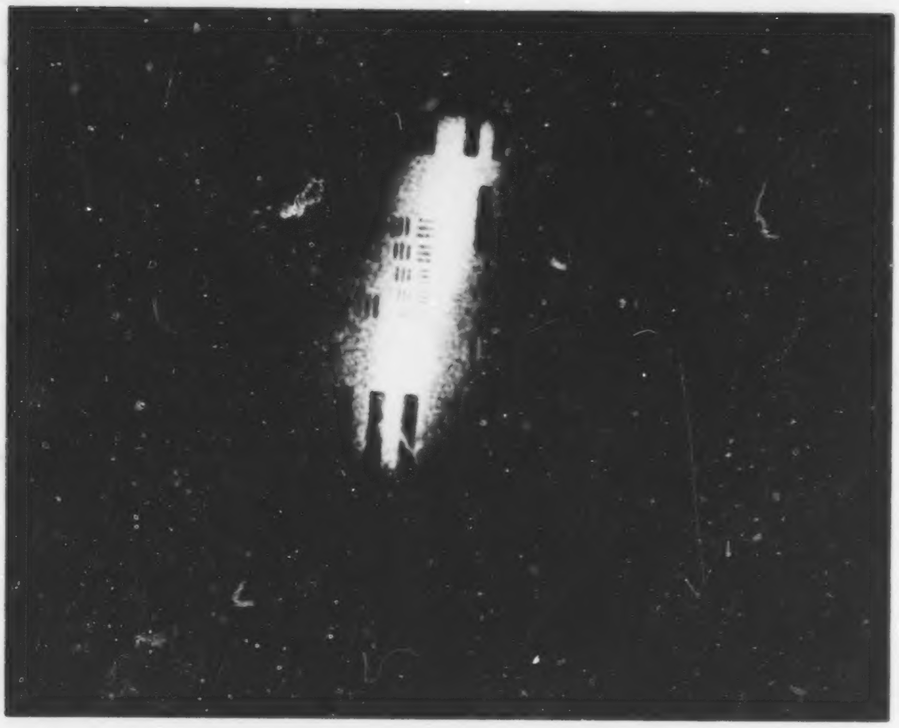

Figure 33a. Reconstruction photo of hologram 1381. Copy camera was focused on resolution target 28 inches from holographic plate.

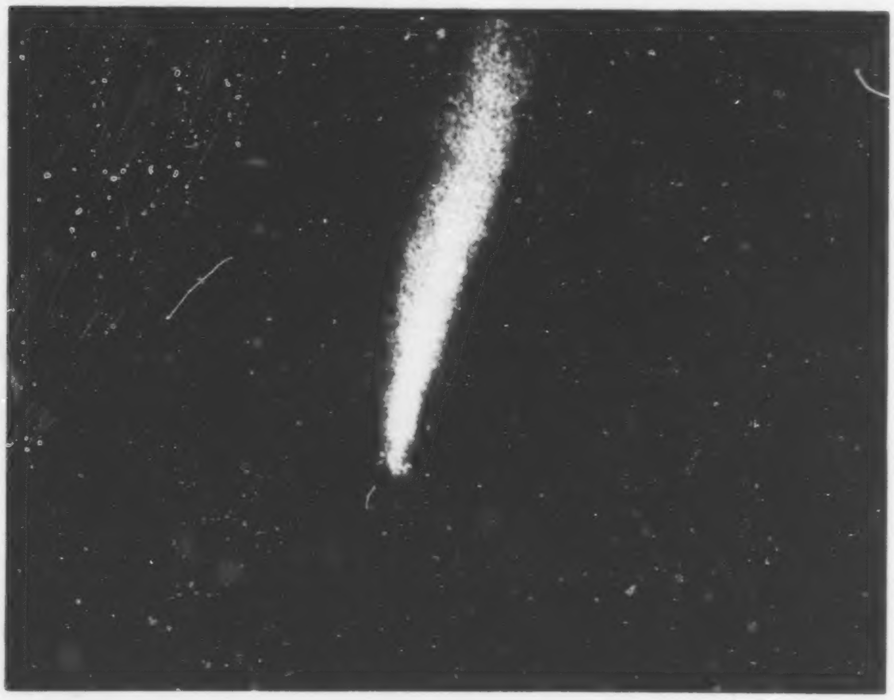

Figure 33b. Reconstruction photo of ruby scene beam light at the prism approximately 33 feet from the hologram plate (hologram No. 1381). The out-of-focus resolution target is barely discernible in the foreground of the scene.

It was concluded from this first series of tests that two-beam holography of scattered light in an operating boiler is entirely feasible. Each of the recordings possessed excellent three-dimensional qualities even though viewing was limited by use of a 4-inch inside diameter by 18-inch long boiler port on the observing or camera side of the test setup (see Figure 17). This had the effect of restricting one to viewing the large boiler combustion scene through a "knot hole." Holograms recorded in the initial series also served as a basis of comparison for subsequent tests with limestone present in the boiler.

6.2 TESTS WITHOUT LIMESTONE INJECTION - 85 MW

A series of holograms was recorded at various power levels of boiler operation. These were made during a power excursion with Unit 10 on 3-11-70 and are described in Lines 32 through 47 of Appendix C. It was thought that such a series of holograms would illustrate the sensitivity of the holography technique to changes in general particulate concentrations since at lower power settings, one would expect a corresponding reduction in fly ash.

No systematic data reduction was attempted of the power excursion series holograms. Rather, emphasis was placed on reducing holograms recorded in the presence of limestone. Holograms 1505 and 1506, however, are excellent examples of recordings made at low power (92 and 85 mw, respectively). The first hologram, No. 1505, was recorded using a collimated beam. The companion recording was made with a fanned scene beam. Both produced bright reconstructions and indicated that a very uniform scattering of the scene light occurred across the 24-foot width of the boiler. This in turn suggests a uniform distribution of fly ash.

The brightness of holograms 1505 and 1506 would further indicate that attenuation of the scene light was significantly reduced. This was physically confirmed by visually observing the combustion flame and opposite boiler wall during the power excursion tests. At the low power ratings, four of the 16 pulverized coal injectors were shut down and the flame was visibly more transparent to the red light from the continuous helium-neon ($\lambda = .6328\mu$) gas laser [illegible] the pulsed ruby illuminator. Turbulence was also reduced since gas laser beam flicker was almost nonexistent. Finally, the tube wall on the opposite side of the boiler was clearly visible at the lower power levels. This was in marked contrast to visual observations made at nominal power levels of 140 mw where the helium-neon sighting laser was barely visible and exhibited a considerable amount of flickering.

The holograms recorded during the power excursion could have been better. It was discovered that the reference beam was not perfectly aligned onto the hologram during part of the test series. This resulted in several weak reconstructions. Of significance, however, was the increase in laser light transmission which was visually observed at the low power setting of the boiler. This implies a substantial reduction in the number of particles per unit volume.

6.3 TESTS WITH LIMESTONE INJECTION - 140 MW

Eighteen holograms were selected for data reduction and evaluation in the test series where limestone was injected into the boiler. These are listed in Table 4 which is a compilation of data on boiler operation, the limestone injection system and limestone plume images recorded by the respective holograms. The hologram numbers correspond to those given in the test matrix of Figure 29, for the limestone injection tests (Section 5.2).

The first six holograms of Table 4 were recordings of portions of the limestone plumes or clouds produced by injecting through port No. 7A on the rear (north) side of the boiler at elevation 348 feet. The remaining 12 holograms (comprised of collimated and fanned beam recordings) are of limestone plume images from clouds formed by injecting through the front No. 2 port.

Evaluation of plume information in the various limestone holograms was made by: (1) visual observation of the reconstructed virtual images; (2) measurements of cloud images with a ranging telescope; and, (3) densitometer measurements of reconstruction photographic negatives. In the latter method, collimated beam hologram reconstruction negatives received a single scan with the densitometer instrument. Selected fanned beam reconstructions were "mapped" by making repeated adjacent scans until the entire image area was covered.

Reference to Table 4 shows that 28 percent of the holograms evaluated exhibited voids in the cloud structures. The voids could be measured and counted. The smallest void noted was approximately 3 inches (No. 1544), and the largest (No. 1571) was about 5 feet in width. In one example, hologram 1573, a void or striation in the horizontal plane (normal to the combustion gas flow) was observed. In effect, two parallel clouds existed which partially overlapped in the middle of the boiler.

The widest cloud noted (without voids) was approximately 19.5 feet and was seen in hologram 1562. The narrowest was about 4 feet (hologram 1573). Analysis of the cloud measurements for both front and rear injected limestone plumes showed that the average cloud width for each group was about 9.5 feet. This suggests that strong streamline flow conditions may exist in the boiler and that lateral mixing or dispersion of the clouds is limited with changing elevation. That is, once segments of the plume geometry are formed (upon injection) and some initial expansion is completed, the segments ascent through the boiler in stream tubes.

A factor which tends to reinforce this contention is the relative stability and similarity of the limestone plume centerline locations with regard to the side of the boiler from which the limestone was injected. For the six plumes recorded with limestone injected from the north side of the boiler, the mean centerline location was approximately 9.6 feet from the wall. Similarly, the mean centerline location for the 12 recorded clouds formed by injecting limestone through ports on the south side of the boiler

Table 4. Summary of data obtained from hologram recorded in the presence of injected limestone

			Boiler Data		Limestone Injection Data						Limestone Plume Data and Description				
Hologram No.	Date	Time Hrs.	Power MW	Air Flow M Lb/Hr(1)	Port No.	Port Elev. Ft.	Port Location	Rate Lb/Hr(2)	Air Meter Reading-%	SO_2 Conc. %(3)	Plume Location From S. Wall-Ft.	Plume Width in Ft.	No. of Voids	Width of Voids-Ft.	Comments
1391	3-6-70	1422	141	950	7A	348	Rear	1170	28	Unknown	3.0 to 17.0	14.0	0	---	Telescope measurements only. Uniform cloud with indistinct edges.
1535	3-12-70	0847	140	1000	7A	↓	Rear	500	30	19.0	12.0 to 20.0	8.0	0	---	Tele. meas. only. Bright spots (slag?) at 4.0 ft.
1544	↓	0920	141	1000	7A		Rear	1080	30	23.6	14.5 to 23.5	9.0	2	1.0/0.25	20-25% increase in scattered light intensity in plume regions.
1547		0925	141	1000	7A		Rear	1170	30	23.6	6.0 to 22.5	16.5	1	2.0	One bright cloud near far wall gradually dissipating to North wall. Maximum intensity increase 200%.
1548		0928	141	1000	7A		Rear	1080	30	23.5	10.0 to 19.5	9.5	0	---	Prominent cloud without apparent voids.
1549		0931	141	1000	7A		Rear	1000	30	23.4	8.0 to 17.0 22.7 to 23.8	9.0 1.1	0 0	--- ---	Major cloud - 80% increase in intensity. Secondary or minor concentration with 15% increase in intensity.
1562		1108	141	990	2	360	Front	2750	25	23.4	4.0 to 23.5	19.5	0	---	Apparent uniform intensity over ~19-20 ft of boiler. Presence of limestone questionable.
1563		1110	140	990	2	↓	Front	1870	25	22.7	7.0 to 16.0	9.0	0	---	Maximum increase in intensity is ~60%. One cloud and no apparent voids.
1564		1113	140	990	2		Front	1870	25	22.5	1.5 to 17.5	16.0	0	---	Major cloud, 100% increase in intensity. Possible minor cloud (+10%) in 21-23 foot region.
1565		1115	140	990	2		Front	1870	25	22.2	4.0 to 7.0 10.0 to 23.0	3.0 13.0	1 0	~3.0 ---	Low intensity, small cloud on far side. Major nearly uniform cloud over most of boiler with 50% intensity increase over background noise.
1566		1117	140	990	2		Front	1870	25	24.0	3.0 to 10.0	7.0	0	---	Tele. meas. only. Dark area casting shadow at approximately 10 ft. mark.
1567		1120	140	990	2		Front	1870	25	23.4	0.5 to 11.0	9.5	0	---	Major cloud with intensity increase of ~500%.
1568		1122	140	990	2		Front	2750	25	22.9	3.0 to 8.0	5.0	0	---	Tele. meas. only. Possible lateral structure in cloud (far beam).
1569		1124	140	990	2		Front	2750	25	24.5	2.0 to 9.0	7.0	0	---	Tele. meas. only. Lateral structure with possible void areas.
1570		1125	140	990	2		Front	2750	25	24.5	2.0 to 13.0	11.0	0	---	Tele. meas. only. Some lateral cloud structure noted.
1571		1127	140	990	2		Front	2750	25	24.0	0.5 to 13.0	12.5	1	~5.0	Telescope measurements verified with densitometer trace.
1572		1129	140	990	2		Front	2750	25	23.2	3.0 to 11.0	8.0	1	~1.0	Tele. meas. only. Small pocket or void at 5 ft. plus lateral structure.
1573		1130	140	990	2		Front	2750	25	23.6	2.5 to 11.0 (Down) 10.0 to 14.0 (Up)	8.5 4.0	0 0	--- ---	Tele. meas. only. Striation in horizontal plane forming 2 parallel clouds.

NOTES:
(1) Approximate average values taken from Unit 10 Log Sheets for 3-6-70 and 3-12-70.
(2) Average limestone injection flow rate per hour per injection port.
(3) SO_2 concentration in percent of 4000 ppm. Data obtained from D. T. Clay, NAPCA, and was obtained from the "B" side (West) of the Unit 10 boiler.

was about 7.5 feet from the (near) wall.* The 2-foot variation in centerline distance from the near wall for both injection locations may well be accounted for in the relative difference of injection port elevation with respect to the probing laser beam. In other words, those clouds detected near the north wall (rear injection ports) were more fully expanded into the flow field. Also of interest is the fact that the minimum and maximum centerline distances from the reference boiler wall were approximately 5 and 14 feet, respectively, for plumes injected from both the north and the south injection ports.

Densitometer measurements of reconstruction photographs (negatives) of limestone clouds were made of both collimated and fan-shaped scene beams. An example of a collimated beam reconstruction densitometer measurement illustrating a limestone plume is shown in the trace of Figure 34. The hologram used was No. 1564. The location and relative intensity of the existing limestone cloud is marked on the trace. The cloud extended from near the south wall of the boiler to a point approximately 7 feet away from the north wall. The cloud was reasonably well defined by the densitometer measurement and could also be located and measured using the ranging telescope.

In examples where a fanned scene beam is used, a single densitometer scan may not adequately characterize the plume. A multiple scan or "mapping" technique was used as an alternate. An example of this is shown in Figure 35 for hologram 1570. Successive densitometer scan traces were projected into a composite perspective sketch or map. The structure of the plume in terms of relative density D is readily seen. A photographic enlargement (5X) made from the reconstruction negative used in the densitometry mapping of hologram 1570 is pictured in Figure 36. The density structure in the photograph correlates well with the perspective map of Figure 35.

6.4 INTENSITY MEASUREMENTS AND CALIBRATION

In addition to physically locating and dimensioning a limestone cloud within the boiler, some assessment of the cloud particle number density is also desirable. With the present Phase III scattered light holograms of limestone clouds, it is possible only to infer changes in particle density through variations in light intensity of the reconstructed scene. The densitometer scans of reconstruction photographic negatives from these holograms provide a relative measure of light intensity as a function of distance across the boiler. In essence, the absolute intensity scale factor for the reconstructed images was lost during the sequence of hologram recording, processing and data reduction. Examples of how this loss occurs are discussed subsequently together with some thoughts on how the intensity scale factor could be preserved. Once such a calibration technique is established, it should be feasible to assess the particle number density of a given limestone cloud based upon a mathematical model of the phenomena under study and a measurement of the scattered light intensity of the reconstructed image.

---

*In holograms 1565 and 1573, two distinct clouds were observed. In determining the centerline values, only the initial cloud (closest to the near wall) was considered.

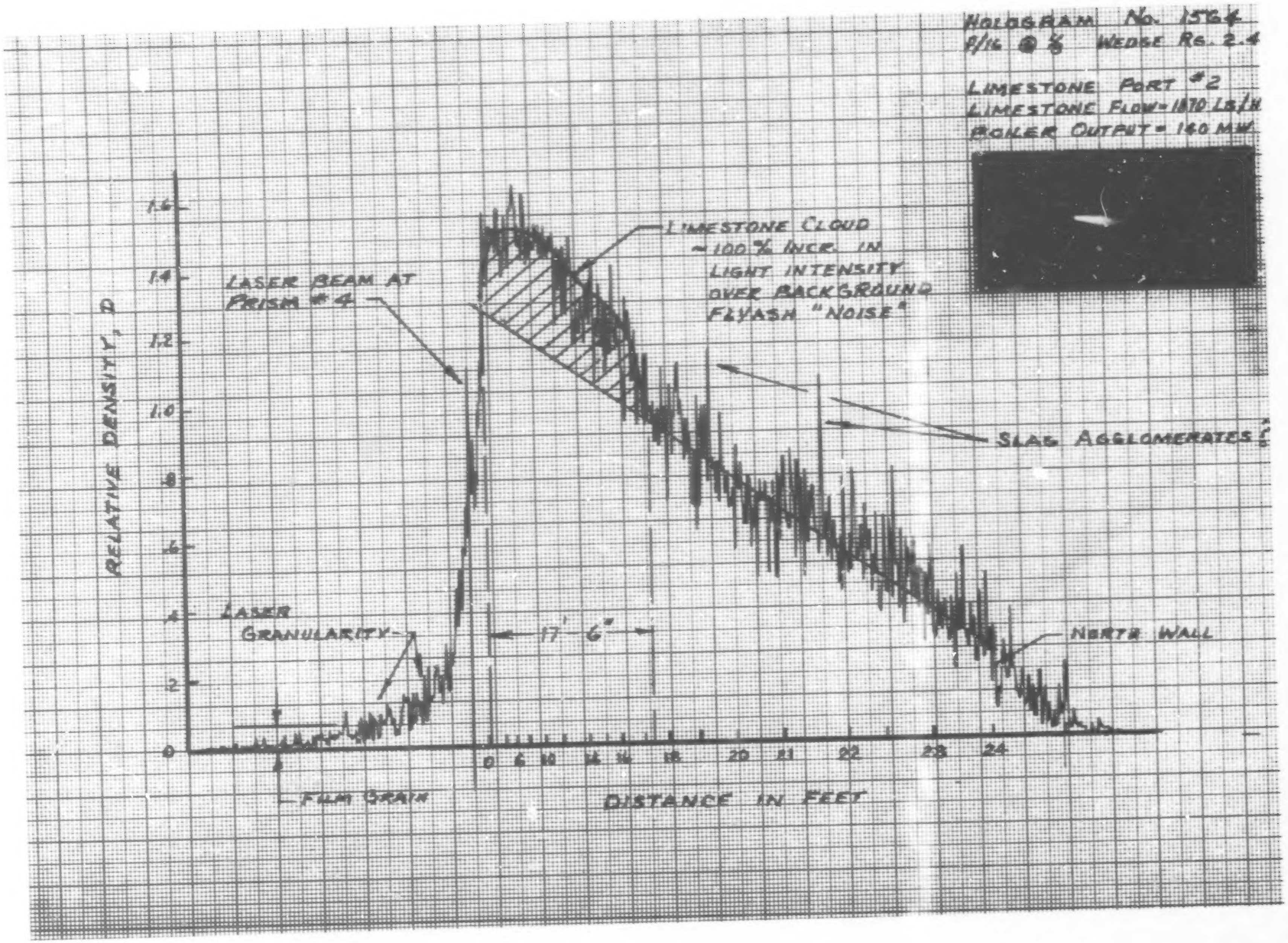

Figure 34. Densitometer trace for hologram 1564 reconstruction photograph

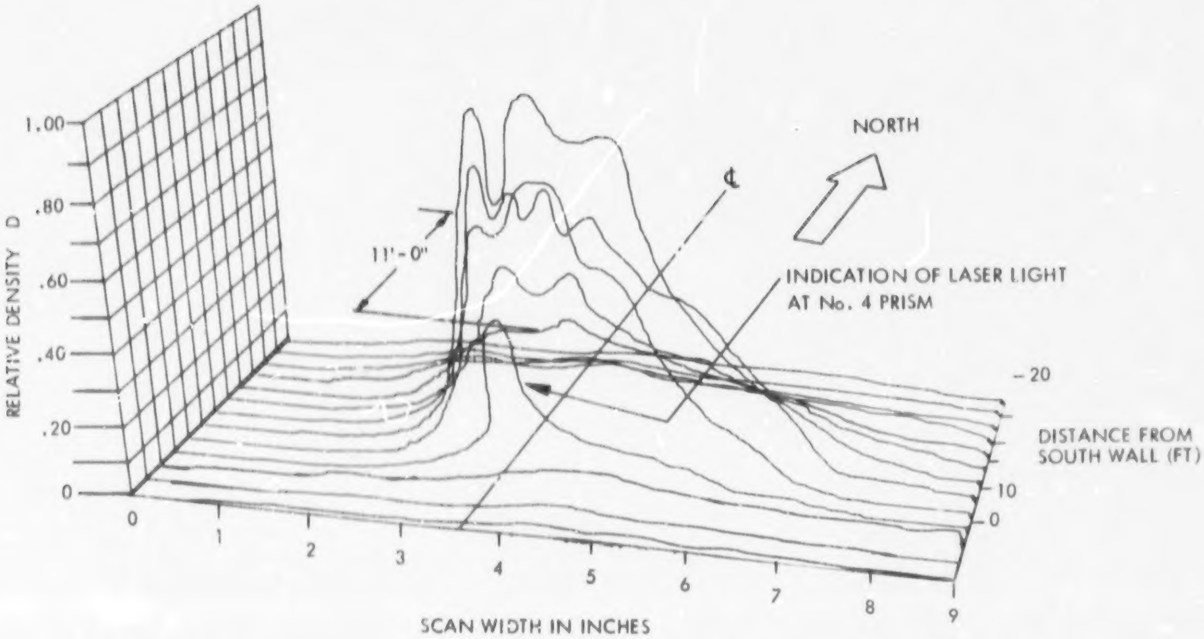

Figure 35. Densitometer Traces From a Mapping of Hologram 1570 projected into a composite perspective

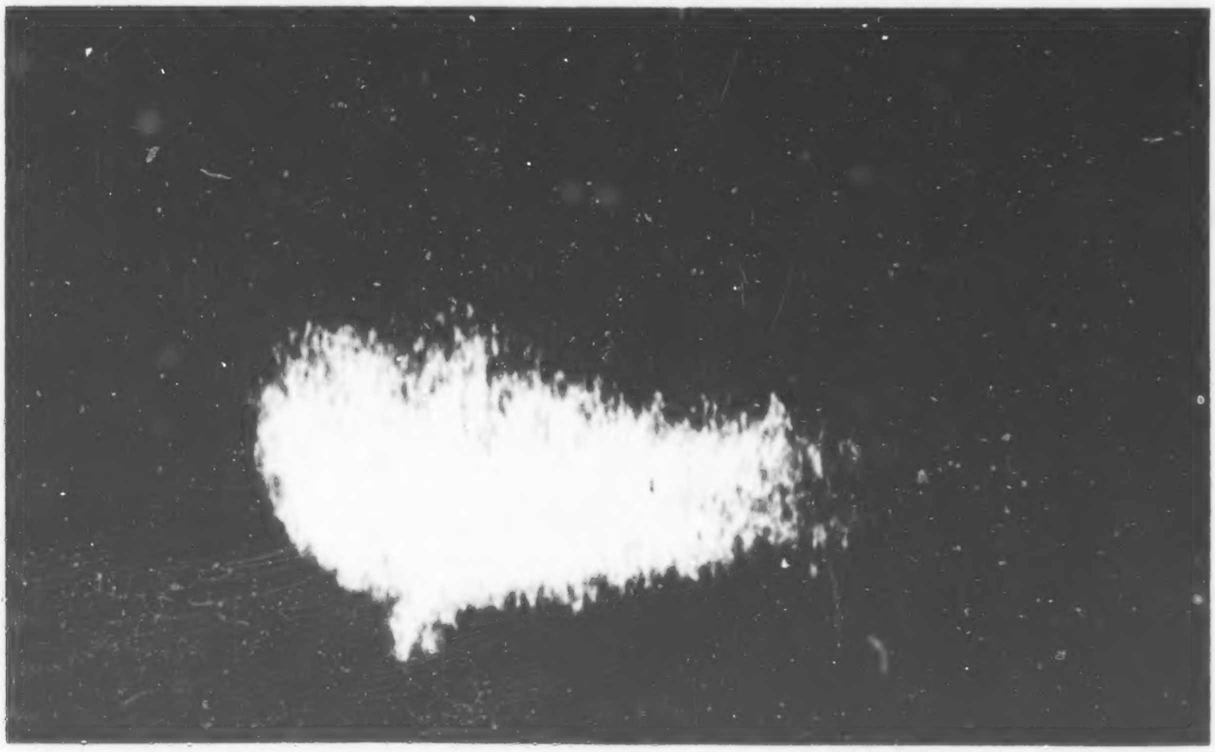

Figure 36. Photograph of reconstructed virtual image of fan beam scattered light from hologram 1570. Laser light from the prism 33 ft, 6 in. away is seen as a ball of light at the bottom of the photo. Note also the lateral cloud structure. The cloud width is ~11.0 ft.

The absolute brightness of the reconstructed image is proportional to the point-by-point efficiency of the hologram and to the intensity of the illuminating reconstructing beam. Accordingly, if the efficiency of each holographic plate were known, the illuminating beam brightness could then be adjusted to allow direct comparisons from one hologram to another. In addition, the intensity of the scattered light (as a function of distance coordinates within the scene volume) is proportional to the intensity of the probing laser scene beam. As will be seen, the overall process is not linear.

Variations in optical efficiency among several holograms in a series can be caused by variations in the energy content or coherence of the laser pulses as well as variations in dark-room processing technique (time, temperature, developer concentration or depletion, etc.). Although an optical intensity monitor was included in the laser used in the present studies, the location of the detector was not optimized in the sense used here.* For the purpose of quantitatively measuring the total plate exposure, a detector should be located in the reference beam path just in front of the film. A useful method for normalizing reconstruction beam intensities among several holograms consists of recording in every hologram an image point of reference intensity (e. g. , by illuminating a standard reflectance surface with a portion of the reference beam). On reconstruction, brightnesses within the scene can then be normalized to the reference intensity point, thus preserving an intensity calibration through the recording, processing, and reconstruction steps. Several types of photometers exist which could be used for making intensity measurements on the hologram.

Making reconstruction photographs of holographic images is another process in which the intensity scale factor is lost, inasmuch as the total exposure of the photograph is necessarily adjusted for best photographic results, depending on the particular photo materials being used. Accordingly, any negative or print provides only the function of relative intensities in the scene, at best. Again, the inclusion of a point of reference intensity would be an aid in preserving a scale factor through these photographic steps. A further degree in sophistication would be to make intensity measurements directly from either the real or virtual image of the hologram thus eliminating the intermediate step of producing photographic negatives of the reconstructed hologram.

The use of the densitometer typically involves discarding of the intensity scale factor, inasmuch as the instrument is a logarithmically measuring device, and hence preserves the shape of the relative density function for a given negative regardless of the absolute density value. Means exist (through somewhat tedious) for preserving the absolute density of a given negative; however, this has meaning relative to scene intensity only if the density function of exposure of the particular photographic material is known. Here, again, a reference intensity point could provide a calibration for at least one point on this function.

---

*The laser illumination is monitored using a photodiode to detect the output of the ruby oscillator. See Figure 6.

In the final analysis, one must always begin with a representation of the holographic image which at least displays the relative intensity function in the scene. In Section 6. 3, a great deal of information was obtained from the shape of the densitometer traces—evidence of limestone clouds was detected where it could not be readily seen with unaided eye. In other cases, a dense cloud of material near the entrance port attenuated the light beam to such an extent that the luminosity of fly ash near the exit port was noticeably reduced. Accordingly, it becomes obvious that the information content of the scene is encoded in the shape of the relative intensity function rather than in absolute local intensities.

What is needed at this point is a mathematical model (derivable from light attenuation theory and geometrical considerations) which predicts the shape of the densitometer traces, as function of the fly ash and limestone concentrations, with reasonable assumptions made as to size distributions of the two species. With this model, and using standard curve-fitting computer programs, the shape of the densitometer traces can be analyzed to yield nominal limestone concentrations as a function of distance across the boiler within the path of the probing light beam.

7. CONCLUSIONS

From the holography studies accomplished during this program, it has been conclusively established that two-beam scattered light holography of particulate in an operating boiler (nominal power output of 140 mw) is entirely feasible. In addition, photometric means of evaluating the reconstructed holographic images have been developed to the extent that quantitative data as well as qualitative impressions can be obtained. More specifically, the following may be stated:

(1) The presence of limestone plumes or clouds can be detected over (scene beam) distances of up to 24 feet of boiler combustion volume. Further, the technique appears applicable over much greater distances. For instance, two-beam holograms of scattered light across the 50-foot length of the Unit 10 superheater area would be entirely feasible.

(2) The recorded limestone clouds can be physically located within the scene along the laser beam axis. The clouds can be located using either a ranging telescope or via densitometer measurements scanning the virtual image of the reconstructed hologram.

(3) Cloud dimensions can be measured and the presence of voids established and also measured. Accuracy of measurement varies with distance into the reconstructed scene. It is estimated that at 24 feet (far wall of the boiler from the observer's station), accuracy is limited to approximately ±0. 5 feet. The greatest accuracy is obtained when making measurements close to the holographic plate (i. e., toward the near boiler wall) where ±0. 1 feet is feasible.

(4) The holography technique is sensitive to limestone plumes injected at elevations of 5 and 16 feet below the viewing (scene beam) ports. The intensity of the recorded clouds seen in holograms taken with limestone injected from either location appear similar. Evaluation of the cloud data suggests that stream tubes within the boiler may reduce significantly, the degree of plume dispersion once a basic plume geometry has been established following injection. In this regard, it is hypothesized that velocity profiles (normal to the flow) may strongly influence plume geometry.

(5) The limestone plumes or clouds generated by either the front or rear injection ports varied in overall dimension considerably. There did not appear to be any significant repeatability to the cloud size although, admittedly, the data sample size is limited. Remarkably more consistent, however, were the cloud centerline locations with respect to the wall through which the limestone was injected.

(6) A significant conclusion from the holographic data is that voids do occur in the limestone clouds as they ascend through the boiler. Voids were observed in 28 percent of the recorded limestone clouds which were reduced for data.

(7) The thermal cells which were originally observed in earlier holographic test series were artifically induced by cold air entering the boiler through the exit viewing port. When a window was used during later tests, the thermals were almost always eliminated from the reconstructed scene.

(8) With the present feasibility demonstration holograms, only relative changes in light intensity within a given hologram can be determined. Suitable calibration methods are lacking at present to make quantitative comparisons between different holograms. A method has been suggested, however, which should allow comparison of light intensity variations between two or more holograms (cloud images) and further, permit estimates of particle number concentrations.*

(9) During the recent test program, consecutive hologram recordings were made (at times) at a rate of one every 1-2 minutes using entirely manual techniques. This rate could be increased significantly if desired. Means of obtaining rapidly sequenced recordings are within the state of the art (to microsecond intervals if necessary) but require a more sophisticated camera setup.

(10) The nominal "turn around" time required to record, develop and reconstruct individual holograms made at the Unit 10 boiler was approximately 20 minutes. For the most part, however, recordings were made and processed in batches. The holograms were then leisurely examined at a later time. A reduction in turn around time to less than 8 minutes is entirely feasible without any appreciable difficulty.

The acquisition of quantitative hologram data was accomplished at TRW System facilities in Redondo Beach, California. Subsequent holography studies could incorporate means for interrogation of the hologram at the power plant site.

---

*Refer to discussion in Section 6. 4.

8. RECOMMENDATIONS FOR FUTURE WORK

Work accomplished during this program has demonstrated that holography is a viable technique for in situ measurements of limestone clouds injected into a full-scale (140 megawatt) operating steam boiler. The holographic apparatus and the techniques of operation are sufficiently flexible to permit the monitoring of limestone plumes from any set of opposed ports at the current (365-foot) boiler elevation. Further, the basic equipment may be installed at other elevations on the boiler provided that opposing ports are or can be made available. Specific recommendations based upon the results of this work are as follows:

- Holography should be utilized as one of the primary instrumentation methods during the formal limestone distribution study phase of the dry limestone process evaluation program at the Shawnee Unit 10 boiler.

- The holographic technique is most useful for obtaining instantaneous data concerning plume geometry and structural detail. Implementation of the technique during critical phases of the overall limestone distribution should be especially valuable.

- The acquisition of holographic data should be time coordinated with the simultaneous monitoring of other boiler and injection system operating parameters so that direct correlation of results can be made.

- Future holographic instrumentation at the Shawnee boiler should make provisions for using wider scene beam divergence (greater lateral coverage of the plume) or, as an alternative, multiple scene beams to probe more than one injected limestone plume at a time.

- Consideration should be given to developing a suitable technique for making rapid sequences of exposures on the holographic plate so that dynamic fluctuations in the injected limestone cloud may be observed.

- Subsequent holography studies at the boiler should incorporate a means of hologram calibration such that absolute light intensity measurements may be obtained to facilitate estimates of particle number concentrations in the recorded scattered light plume images.

A technique for estimating a particle number concentration based upon measuring the absolute intensity of a holographically recorded scattered light image of a limestone plume was discussed in Section 6.4 of this report. It is recommended that work in this area be continued in support of the basic holography study of limestone clouds injected into the Unit 10 boiler. Successful application of the proposed technique will provide further quantitative information from subsequent holograms recorded at the boiler.

It is entirely feasible to rapidly scan developed holograms and subsequently use the scan information as input to a computer program that would calculate the particle number concentrations and identify the location of the recorded plume images with respect to a reference wall in the boiler. The entire data acquisition, reduction and processing function could be initiated at the Shawnee plant. Formal presentation of the data in tabular or graphic form might be accomplished within approximately 24 hours for large quantities of holograms. Specific tests of interest could be accomplished in an even shorter period.

Because of the potential of the proposed holographic data reduction method and correspondingly large number of recordings which may be required in the process of evaluating the limestone distribution as a function of various (boiler) system parameters, it is recommended that development of an automated data handling technique be initiated in support of future work at the Shawnee Steam Plant.

REFERENCES

1. T. D. Womble, Jr. and J. T. Reese, "The Dry Limestone Injection Process for SO_2 Control, Part I - Equipment Description, Calibration and Operating Experience," paper presented at the NAPCA Dry Limestone Injection Process Symposium, Gilbertsville, Kentucky, June 22-26, 1970.

2. Ibid., "Part II - Preliminary Test Results."

3. H. W. Elder, "The Dry Limestone Injection Process for SO_2 Control, Part III - Test Program," paper presented at the NAPCA Dry Limestone Injection Process Symposium, Gilbertsiville, Kentucky, June 22-26, 1970.

4. Anon., "Sulfur Oxide Removal From Power Plant Stack Gas - Sorption by Limestone or Lime, Dry Process," Tennessee Valley Authroity Report prepared for the National Center for Air Pollution Control, 1968. p. 3.

5. G. H. McClellan, "Physical Characterization of Calcined and Sulfated Limestones," paper presented at the NAPCA Dry Limestone Injection Process Symposium, Gilvertsville, Kentucky, June 22-26, 1970. p. 18.

6. R. F. Wuerker, "Instruction Manual for Ruby Laser Holographic Illuminator," TRW Report No. 11709-6003-R0-00 (AFRPL Contract F04611-69-C-0015), February 1970.

7. Anon., Tymshare Super Basic 2245 "POLYCURV," Reference Series - Library Tymshare, Inc., Los Altos, California, February 1969.

8. B. J. Matthews, R. F. Wuerker and R. F. Kemp, "Holographic Determination of Injected Limestone Distribution in Unit 10 of the Shawnee Power Plant," Progress Report No. 1170. 69-001, NAPCA Contract CPA 70-4, September 1969. pp. 6-8.

APPENDIX A

THE TECHNIQUE OF HOLOGRAPHY

A single beam of coherent light scattered by small objects was the arrangement first used by Dennis Gabor to demonstrate the holographic principle.[1]

Fourteen years later, a second independent unmodified reference beam was added by Emmett Leith and Juris Upatnieks.[2,3] This rather significant improvement made possible the recording of scenes with large contrast ranges, and with large regions of opacities. The images, further, were positives of the original scene. Since the phase of the reconstructed wave front was not reproduced across the full area of the plate, interferometric comparisons between holograms recorded on the same or separate plates, or between a hologram recording and the real scene at a later time could be done for the first time.

The simplest form of holography is the version used originally by Gabor. A single beam of coherent light is typically passed through the scene and allowed to fall on a photographic plate. The plate records the intensity distribution due to the interference between the transmitted beam and light scattered by the objects in the beam. Although only a single beam is used, the photographic plate records the superposition of two wave fronts; namely, the transmitted and the scattered light. This version is known as "single-beam" or Gabor holography, to distinguish it from the more improved form in which a separate reference beam is employed.

Even recently, the single beam technique has been used to successfully measure tenuous, distributed microscopic high speed phenomena.[4,5] Rather than the filtered light from a mercury arc (used originally by Gabor), a pulsed ruby laser of 20-50 billionths of a second duration has been used to illuminate the hologram. The short duration of the laser source makes possible the freezing of high speed microscopic phenomena.

Both "single beam" and double beam holography are described by the same basic mathematical equations.

One specifies the unmodified or reference wave via complex notation,* as:

$$\psi_r\ (x,\ y,\ z,\ t) = A_r(x,y)\ \{\exp j[\omega t - kz + \phi_r(x,y)]\} \qquad (1)$$

where

$A_r(x,\ y)$	is the amplitude of the right traveling wave specified in equation 1.
exp	is the exponential function of the base of the natural system of logarithms. $(e = 2.71828)$
j	is $\sqrt{-1}$
ω	is the angular frequency of wave in radians per second $(\omega = 2\pi f)$.
k	is the wave number (i.e., $k = 2\pi/\lambda$) .

and

$\phi_r\ (x,\ y)$ is the phase of the wave.

Equation 1 describes a wave traveling in the positive z Cartesian direction with a velocity of ω/k.** Ideally, the reference is a plane

---

* Equation (1) is a solution of a wave equation or differential equation of the form:

$$\frac{\partial^2 \mu}{\partial x^2} + \left(\frac{k^2}{\omega^2}\right)\frac{\partial^2 \mu}{\partial t^2} = 0$$

This type of equation specifies the propagation of electromagnetic radiation (i.e., light) in free space, as well as propagation acoustic energy.

** The wave travels to the right with a velocity found by setting the argument of the exponential equal to a constant and differentiating, namely, $\frac{dz}{dt} = \frac{\omega}{k} = C$, where C for electromagnetic radiation C is the velocity of light.

wave of constant amplitude and phase. For such a case,

$$\psi_r(z, t) = A_r \exp j[\omega t - kz] \qquad (2)$$

The scene beam is represented similarly, but will in most cases consist of amplitude and phase terms which are functions of the x, y position, namely:

$$\psi_s(x, y, z, t) = A_s(x, y) \{\exp j[\omega t - kz + \phi_s(x, y)]\} \qquad (3)$$

Holography is concerned with the superposition of these two coherent waves on top of one another and the recording of the resultant stationary interference pattern on a piece of film or photosensitive material. At the plane of the photographic plate, the two waves are superimposed one on top of the other.

$$\psi_s + \psi_r \qquad (4)$$

The intensity in this region of superposition is simply:

$$I = (\psi_s + \psi_r)\ (\psi_s + \psi_r)^* \qquad (5)$$

where * denotes the complex conjugate of the sum of ψ_s and ψ_r. Thus, in complex notation, the intensity at the plate is simply:

$$I = \psi_s\psi_s^* + \psi_r\psi_r + \psi_r\psi_s^* + \psi_r^*\psi_s \qquad (6)$$

which on expansion can be shown to reduce to the following real expression:

$$I = \left|A_s(x, y)\right|^2 + \left|A_r\right|^2 + A_rA_s(x, y) \left\{\text{Cos } \phi_r - \phi_z(x, y)\right\} \qquad (7)$$

which is a mathematical expression for the fact that the superposition of two traveling waves results in a stationary distribution in space.

One next assumes an ideal photographic plate; namely, one in which the amplitude transmission is proportional to the exposure. For such a recording media,

$$T_a = K_o - K_1 \, It \qquad (8)$$

where K_o and K_1 are constants of the film, I is the intensity of the light, and t is the exposure time.

After exposure to the intensity pattern given by either Equation 6 or 7, the film will have a transmission (substitution of Equation 6 into 8) of

$$T_a = K_o - K_1 \, [\psi_s\psi_s^* + \psi_r\psi_r^* + \psi_r\psi_s^* + \psi_r^*\psi_s \,]t \qquad (9)$$

If the developed photographic plate is next reilluminated by a beam that is a duplicate of the original beam ψ_r then the following light distribution pattern will emerge from the other side.

$$\psi_{out} = \psi_r T = K_o\psi_r - tK_1[\psi_s\psi_s^*\psi_r + \psi_r\psi_r^*\psi_r + \psi_r\psi_r\psi_s^* + \psi_r\psi_r^*\psi_s \,]\psi_r \qquad (10)$$

Gathering terms, one can identify the following:

(a) $[K_o - tK_1\psi_r\psi_r^*]\psi_r$ as the reference wave transmitted through the hologram (11)

(b) $- tK_1[\psi_s\psi_s^*]\psi_r$ as noise transmitted in the direction of the reference beam (12)

(c) $- tK_1[\psi_r\psi_r]\psi_s^*$ as the complex conjugate of the original scene, and (13)

(d) $- tK_1[\psi_r\psi_r^*]\psi_s$ as the reconstructed wave, i.e., the one which is identical in phase to the original and of amplitude proportional to the original. (14)

Thus, the mathematical argument predicts that the hologram will reconstruct a wave proportional to the original scene wave whenever the hologram is reilluminated by a duplicate of the original reference wave front. Recent experiments have verified the truth of this Aristotelian argument.[6,7]

In the case of the Leith-Upatnieks configuration, the two beams pass through one another at different angles. Mathematically, this is equivalent to the addition of a linear phase factor. One could write for the scene the following expression:

$$\psi_s = A_s(x, y) \{\exp j[\omega t - kz + \phi_s + \alpha x]\} \qquad (15)$$

where the quantity αx gives a phase which increases uniformly in the x direction. The reference is the same as before (i.e., equation 1). Summing the two waves, taking the intensity (as in equation 5), multiplying by the transmission of the film, and multiplying again by the reference, yields the same equation (i.e., equation 10). Collecting terms, one obtains the two that are of interest, namely, the virtual image:

$$- tK_1[\psi_r\psi_r^*]\psi_s\epsilon^{j\alpha x} ,$$

and the conjugate image

$$- tK_1[\psi_r\psi_r]\psi_s^*\epsilon^{-j\alpha x} .$$

The quantity $-\alpha x$ is interpreted as a wave propagating at minus the angle of the original wave.

The two beam arrangement has the feature that it separates the real and conjugate wave constructed from the hologram. In the case of Gabor or single beam holography, the "scene" is created by scattering of the reference beam by objects within the beam and between the source and the photographic plate. In the two beam hologram arrangement, the reference is separately supplied.

In the Gabor case, the scattering scene, however, modifies the reference beam so that the phase and amplitude of the reference no longer are simple functions. The theory says that to identically recreate the original scene beam, the plate must be reilluminated by a beam identically equal to the reference beam at the time that the hologram was recorded. If the reference is a complex function of both amplitude and phase, the hologram is somewhat encoded, with the result that resolution suffers.

Two beam holography does not suffer from this difficulty.

The operation and resolution of a simple Gabor hologram arrangement can be understood from the schematic shown in Figure A-1. The upper picture shows the recording of the hologram of light scattered from a point source (ψ_s) by a parallel reference wave, (ψ_r). If the extreme rays scattered by the point source cross those of the reference at an angle θ, then the hologram will have a numerical aperture of Sin θ.[8]

The schematic in Figure A-1 also shows the reconstruction of the real ($tK_1[\psi_r\psi_r^*]\psi_s$) image and the conjugate image ($tK_1[\psi_r\psi_r\psi_s^*]$) from the

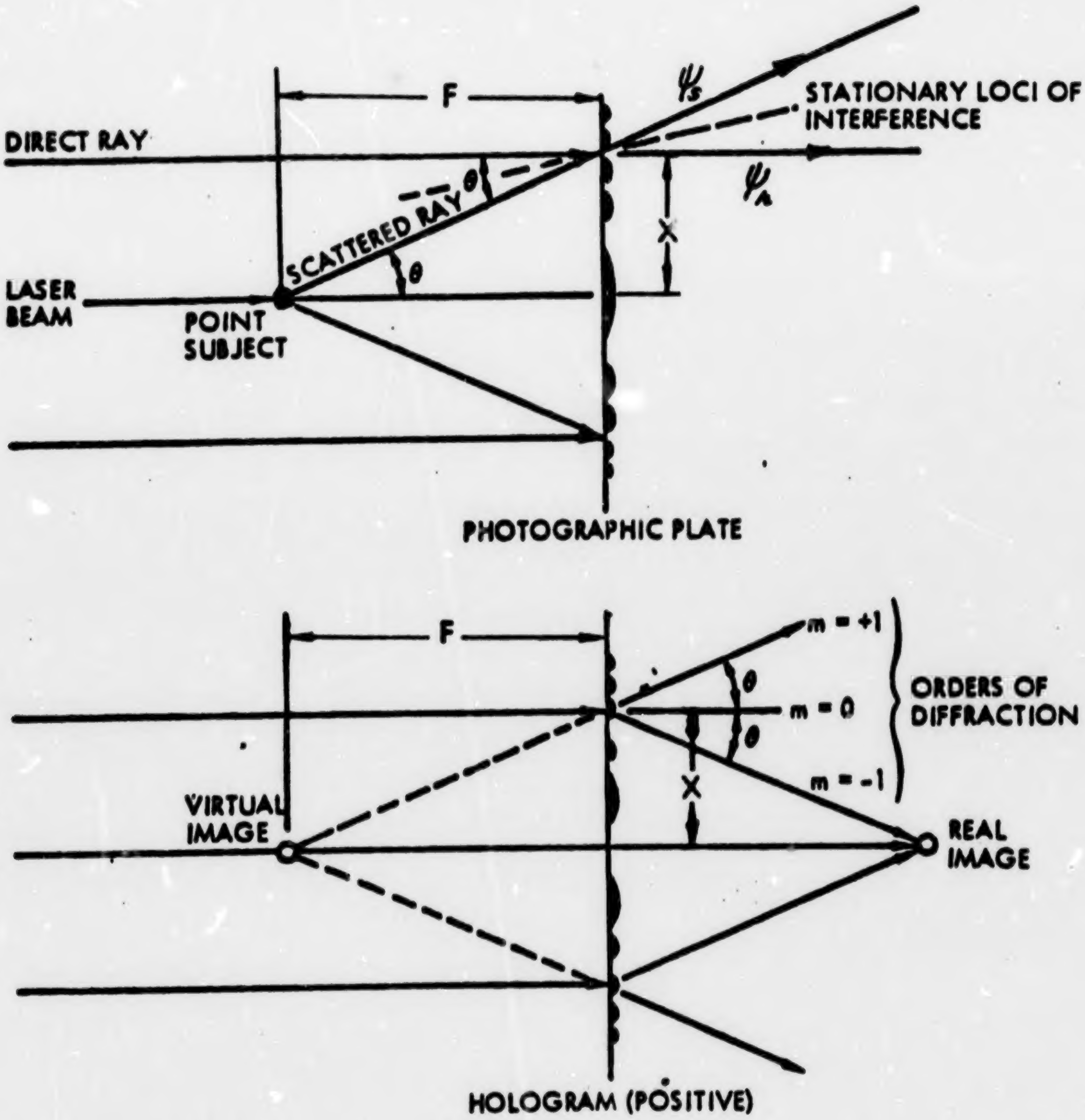

FIGURE A-1. - Single beam (Gabor) hologram of a point subject, showing the recording of the hologram in the upper schematic and the reconstruction of the virtual and real images from the hologram in the lower schematic. The angle θ determines the numerical aperture of the hologram and the resolution of the reconstructed images.

hologram. In terms of diffraction from periodic gratings, the former is known as m = 1 order while the latter is m = -1. The resolution of the reconstruction is determined by the angle subtended by the virtual and real image, provided the phase of the reference is recreated exactly over the full aperture. Thus, for this ideal situation, the resolution is the same as with any other optical apparatus,[9] namely:

$$R = \frac{\lambda}{2 \operatorname{Sin} \theta} \quad . \tag{16}$$

In the case of the original hologram, the superposition of the scene and reference rays creates stationary regions of constructive and destructive interference. These can be shown to be separated by an amount equal to:

$$\Delta = \frac{\lambda}{2 \operatorname{Sin} \theta/2} \quad . \tag{17}$$

Thus, in the ideal case, the resolution

$$R = \Delta \frac{\operatorname{Sin} \theta/2}{\operatorname{Sin} \theta} \quad , \tag{18}$$

which in the limit of small angles $\approx \Delta/2$, namely the resolution of the reconstruction is equal to half the resolution of the photographic film.

The arguments are highly idealized in that it was assumed that the reference beam used to reilluminate the hologram was identically equal to the one originally used in the recording. It can be seen that as the scene becomes more and more complicated, the reference beam becomes increasingly encoded. Duplication is only possible across a small aperture. Refractive index changes also complicate the background wave by the same process. The net result is that the reference beam can only be reproduced over a small aperture. This, in turn, reduces the resolution. To appreciate this, one can rewrite the resolution (Equation 16) as:

$$R = \frac{\lambda}{2X} \sqrt{F^2 + X^2} \quad , \qquad (19)$$

in terms of aperture diameter 2X and the object distance F. In the limit of small aperture,

$$R_{D \ll F} \sim \frac{\lambda F}{2X} \quad . \qquad (20)$$

For example, for 0.69μ, the wavelength of a ruby laser, and a hologram object-distance of 100 centimeters and aperture diameter of 1 centimeter, resolution is 69 microns. A reduction to 1 millimeter gives a resolution of 694 microns! Thus, maximum resolution requires the maintenance and integrity of the reference beam.

For situations where the beam transmitted through the scene volume is heavily attenuated, a two beam arrangement is clearly warranted. The reference beam can then be piped around the scene and kept simple and reproducible.

REFERENCES - APPENDIX A

1. D. Gabor, "A New Microscopic Principle," Nature, 161, 777-778 (1948).

2. E. N. Leith and J. Upatnieks, "Reconstructed Wavefronts and Communication Theory", J. Opt.Soc. Am., 52, 1123-1130 (1962).

3. E. N. Leith and J. Upatnieks, "Wavefront Reconstruction with Continuous Tone Objects", J. Opt. Soc. Am., 53, 1377-1381, Dec. 196

4. B. J. Thompson, "Fraunhofer Holography", Proceedings SPIE, Seminar in Depth on Holography, Volume 15, Society of Photo-Optical Instrumentation Engineers, 1968.

5. C. Knox, "Holographic Microscopy as a Technique for Recording Dynamic Microscopic Subjects", Science, 153, 989-990, 26 August 1966.

6. L. O. Heflinger, R. F. Wuerker, and R. E. Brooks, "Holographic Interferometry", Journal of Applied Physics, 37, 642-649, Feb., 1966.

7. R. L. Powell and K. A. Statson, J. Opt. Soc. Am., 55, (612A), 1965, p. 1956.

8. F. A. Jenkins and H. E. White, Fundamentals of Optics, McGraw Hill Book Co., 1950, p. 298.

9. Ibid.

APPENDIX B

USAF 1951 RESOLVING POWER TEST TARGET

The resolution of an optical instrument is basically its capacity for imaging fine detail. Stated another way, resolution is concerned with the ability to measure differences based upon the comparison of two very close sources of light. Ultimate resolution is the measure of the closest distance two points of light can be placed and still be recognized as being individual points.

The linear resolution for an optical system may be numerically expressed in terms of lines per millimeter. Resolution devices or targets for evaluating optical systems often consist of geometric patterns which may be "read" or interpreted. A commonly accepted patterned target is the U.S.Air Force 1951 Resolving Power Test Target, which is defined by Military Standard 150-A. This resolution target, shown in Figure A-1, consists of an array of three-line "patterns." The width of a line is equal to the width of the spacing between lines in each pattern. Further, the length of each line is five times its width.

A grouping of two patterns set at right angles to each other is termed an "element" of the test target. The elements are arranged in increasingly smaller sizes. These elemental size changes in the USAF 1951 Target are defined by a geometric progression based upon the sixth root of 2, or $\sqrt[6]{2}$. Stated another way, the number of lines per millimeter doubles every sixth target element.

The target elements are arranged in columnar form. Each column is numbered (from -2 to 7) and each element within a given column is identified by another number (1 to 6). Therefore, an element on the target is described by a column number and a "row" number. The accompanying table (see Figure B-1) provides a listing of the number of lines per millimeter for each element. For the 1951 target, the largest element corresponds to 0.250 lines per millimeter while the smallest is 228 lines per millimeter.

In reading a resolution chart, one identifies the smallest element in hich the three-line pattern can be distinguished. The column and row numbers of this element (for example, column 3, row 1 or 3-1) are noted and he corresponding number of lines per millimeter for the element is then onveniently obtained from the Table in Figure B-1. For element 3-1, the alue is 8.00 lines per millimeter.

It is also possible to assign an equivalent particle width (or diamter) from the resolution target. Remembering that the width of each line nd adjacent space are equal, and taking the reciprocal of the measured esolution in lines per millimeter, the period of the line spacing is obtained (millimeters per line). One-half of the period then, is the smallest bject which may be discerned. Thus, if a USAF 1951 target can be "read" to column 3, row 1, the line spacing is 8 lines per millimeter. This is equivalent to 1/8 = 0.125 millimeters per line. One-half of this value is 0.0625 millimeters (width of the line only) or 0.0625 millimeters x 1000 microns per millimeter = 62.5 microns. This would be the smallest width or diameter of an object which could be individually identified by the optical system in question.

Element No. (Row No.)	Group Number (Column Number)									
	-2	-1	0	1	2	3	4	5	6	7
1	0.250	0.500	1.000	2.00	4.00	8.00	16.0	32.0	64.0	128.
2	0.280	0.561	1.12	2.24	4.49	8.98	17.95	36.0	71.8	144.
3	0.315	0.630	1.26	2.52	5.04	10.1	20.16	40.3	80.6	161.
4	0.353	0.707	1.41	2.83	5.66	11.3	22.62	45.3	90.5	181.
5	0.397	0.793	1.59	3.17	6.35	12.7	25.39	50.8	102.	203.
6	0.445	0.891	1.78	3.56	7.13	14.3	28.51	57.0	114.	228.

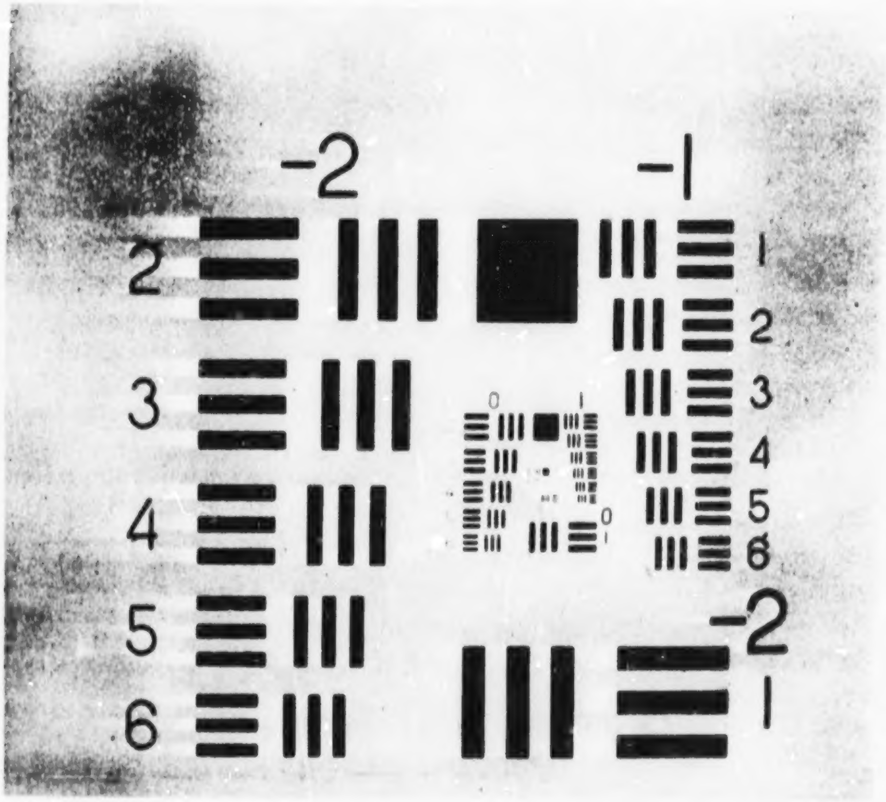

Figure B-1. Photograph of a USAF 1951 Resolving Power Test Target. The table above the photograph indicates the number of lines per millimeter for each element on the target.

APPENDIX C

DATA SUMMARY SHEETS
UNIT 10 LIMESTONE INJECTION TEST HOLOGRAMS

Line No.	Date	Time	Power Output MW	Limestone Injection lb/hr	Remarks	Record No.	Hologram Recording Data							Test Conditions & Remarks	Line No.
							Filters Used			Development		Laser Pulse			
							No. 70	CS-2-58	N.D.	Time Min.	HRP Ratio	Output mV	Quality		
1.	3-4-70			No Limestone		(SO-243) 1322	No Filter	None	None	4	4:1	155		No Filter. Scene beam centered on port. SO-243 saturated. Checkout test only.	1.
2.	↓			↓		1325	X	↓	↓	8	↓	135		Direct scene beam onto plate. Good "fingerprint" of scene beam. Light flame fogging of film plate.	2.
3.	↓			↓		1327	↓	↓	↓	4	↓	135		Scene "fingerprint" plus scattered light all around.	3.
4.	↓			↓		(SO-243) 1330	↓	↓	↓	2	↓			Scattered light. SO-243 film. Film saturated - hologram barely visible.	4.
5.	↓	1700	140	↓		1331	↓	↓	↓	3.5	↓	160		Best of series on 3-4-70. (Possible thermal cells)	5.
6.	↓			↓		1339	↓	↓	↓	2.0	↓	185		Multiple camera shutter operation. Hologram not as bright as #1331.	6.
7.	3-5-70		138	↓		1378	X	↓	0.3	4	↓	-	Multiple Pulse	N.D. Filter - partially covers reference beam. Conclusion - Severe fog.	7.
8.	↓		138	↓		1380	↓	↓	0.3	5	↓	175		N.D. Filter partially covers scene beam. Can focus on edge of filters. Test not conclusive.	8.
9.	↓		138	↓		1381	↓	↓	None	5	↓	185		USAF 1951 target in scene 28.5" from hologram, back-lighted by scattered light. Good to Col. 3, Row 2.	9.
10.	3-6-70	0925	141	↓	Limestone started at 0902 hrs. System failed at 0907 hrs.	1385	↓	↓	↓	5.5	↓	150		Ground glass over inlet boiler port, 32'-3" from film plate.	10.
11.		0935	140	↓		1386	↓	↓	↓	5	↓	135		Duplicate of #1331. Scattered light. Very bright hologram.	11.
12.		1422	141	~ 7000	Rear injection ports (28%)	1391	↓	↓	↓	5.5	↓	170		Bright hologram. Some thermal distortion of beam near exit. No visible plume.	12.
13.	↓	1425	~140	~ 7000	" " "	1392	↓	↓	↓	5.5	↓	220		Scene beam distortion near right edge. No plume of limestone can be discerned.	13.
14.	↓	1433	<140	~ 6000	" " "	1393	↓	↓	↓	5.5	↓	187		Many "thermals". No apparent plume.	14.
15.	↓	1435	<140	~ 7000	" " "	1394	↓	↓	↓	7	↓	165		No image. Plate fogged.	15.
16.	↓	1435	<140	~ 7000	" " "	1395	↓	↓	↓	6	↓	145		Weak hologram. Periodic incoherence?	16.
17.	↓	1442	~135	~ 7000	" " "	1396	↓	↓	↓	6	↓	185		Focusable light and dark spots. Many "thermals" under scene beam.	17.

Line No.	Date	Time	Power Output MW	Limestone Injection lb/hr	Remarks	Record No.	Hologram Recording Data							Test Conditions & Remarks	Line No.
							Filters Used			Development		Laser Pulse			
							No. 70	CS-2-58	N.D.	Time Min.	HRP Ratio	Output mV	Quality		
18.	3-6-70	1455	~132	~6000	Limestone Injection through rear ports (34%	1397	X			5.5	1:4	170		Uniform but weak exposure. No distinct limestone cloud. Lots of "thermals".	18.
19.	↓	1458	132	~6000	" "	1398	↓			5.5	↓	195		Same as #1397	19.
20.	↓	1459	132	~6000	" "	1399	↓			5.5	↓	170		Same as #1397	20.
21.	↓	1510	132	~6000	" "	1400	↓			2.0	↓	180		Changed scene beam to hit closer to port. No image. Plate fogged.	21.
22.	↓	1512	~133	~6000	" "	1401	↓			7.2	↓	162		Faint image. Image of particle can be seen thru lower left-hand corner (slag?).	22.
23.	↓	1513	~133	~7000	" "	1402	↓			6.2	↓	168		Several "rays", both light and dark. Lots of scattering. Good hologram.	23.
24.	3-11-70	1617	140	-	No limestone on 3-11-70 test series.	1474		Glass filter as window		Unknown	↓	125	Osc. & Ampl.	Cyl. ("spreader") lens installed at entrance to last prism box before boiler. Amplifier removed for repair - new flash lamp. Weak image.	24.
25.	↓	1620	↓			1475		↓		↓	↓	170	↓	Same as #1474. Slightly stronger image.	25.
26.	↓	1626	↓			1476		↓		↓	↓	200	↓	Spreader lens removed. Slightly weak image. Scattered light can be observed.	26.
27.	↓	1629	↓			1477		↓		↓	↓	135	↓	Same as #1476. Weak image.	27.
28.	↓	1724	↓			1488		↓		↓	↓	170	Osc. & Ampl.	Spreader lens again installed. Amplifier installed in laser. Ref. beam alignment on plate is somewhat off.	28.
29.	↓	1732	↓			1490		↓		↓	↓	160		Spreader lens out. Moderately good image. Beam scatters light entire distance (24').	29.
30.	↓	1816	141			1491		↓		5.0	1:4	150		Spreader lens in. Soot blower 1K-1 going. Moderately good fan shaped image. Light scattered across 24'.	30.
31.	↓	1820	141			1492		↓		9.0	1:2	160		Spreader lens out. Soot blower 1K-1 going. No image. Heavy fog.	31.
32.	↓	1829	128		Start Unit 10 Power Reduction Tests	1493		↓		13.0	↓	150		Spreader lens in. Soot blower 1K-1 going. No image. Flamelight fogging of plate.	32.
33.	↓	1838	105		" "	1494		↓		Unknown	↓	180		Plate missing.	33.
34.	↓	1852	100		" "	1502/ 1504		↓		↓	↓	~150		Double exposure? Lens out. Weak image.	34.

Line No.	Date	Time	Power Output MW	Limestone Injection lb/hr	Remarks	Record No.	Hologram Recording Data							Test Conditions & Remarks	Line No.
							Filters Used			Development		Laser Pulse			
							No. 70	CS-2-58	N.D.	Time Min.	HRP Ratio	Output mV	Quality		
35.	3-11-70	1855	92	No Limestone	Unit 10 Power Reduction	1505	X					180		Spreader lens out. Good image. Uniform scattering of light across beam.	35.
36.	↓	1906	86	↓	84 MW = Min. Power 4 coal burners Lean O/F.	1506	↓			9.0	1:1	160		Lens in. Good bright hologram. Apparently uniform particulate (fly ash) distribution. Some "rays" visible	36.
37.	↓	1915	85	↓	Flame Transparent	1513	↓			3.5	1:2	160		Lens in. Plate fogged by accident. No image.	37.
38.	↓	1921	85	↓	Opposite boiler tube wall clearly visible.	1516	↓			7.0	1:2	160		Lens in. Good image. Many "rays". Scattering over 24 ft.	38.
39.	↓	1923	85	↓	↓	1517	↓		0.3	6.0	1:1	140		Lens in. Weak image.	39.
40.	↓	1926	85	↓	↓	1518	↓			6.0	1:2	150		Spreader lens out. Reconstructs but image is somewhat weak.	40.
41.	↓	1928	84	↓	↓	1519	↓		0.3	6.0	↓	140		Lens out. Moderately good image even with N.D. 0.3 filter.	41.
42.	↓	2006	84	↓	↓	1524	↓		1.0	18.0	↓	150		Lens out. Fair image. N.D. 1.0 filter in scene.	42.
43.	↓	2010	84	↓	↓	1525	↓	Glass filter as window		20.0	↓	170		Lens out. Bright image, uniform scattering, no "thermals".	43.
44.	↓	2012	84	↓	↓	1526	↓	↓		15.0	↓	170		Lens out. Same comments as for #1525.	44.
45.	↓	2013	88	↓	↓	1527	↓	↓		20.0	↓	150		Lens out. Same as #1525.	45.
46.	↓	2027	138	↓	↓	1528	↓	↓		17.0	↓	180		Lens out. Same as #1525.	46.
47.	↓	2028	140	↓	↓	1529	↓	↓		15.0	↓	140		Lens out. Same as #1525.	47.
48.	3-12-70	0835	~140	No Limestone	Opposite boiler tube wall barely visible.	1534	↓	↓		13.0	↓	170		Lens out. Bright reconstruction with uniform scattering. No thermals.	48.
49.	↓	0847	↓	~ 3000	Limestone thru rear ports at 0845. Air meter at 30%.	1535	↓	↓		11.0	↓	150		Lens in. Good, bright reconstruction. A lot of scattering.	49.
50.	↓	0850	↓	8000	↓	1536	↓	↓		10.0	↓	150		Lens in. Same as #1535.	50.
51.	↓	0858	141	7500	↓	1537-1538	↓	↓		10.0	↓	~170		Lens in. Moderate fog. Will reconstruct but not as bright as #1535-1536.	51.

Line No.	Date	Time	Power Output MW	Limestone Injection lb/hr	Remarks	Record No.	Hologram Recording Data							Test Conditions & Remarks	Line No.
							Filters Used			Development		Laser Pulse			
							No. 70	CS-2-58	N.D.	Time Min.	HRP Ratio	Output mW	Quality		
52.	3-12-70	0902	~141	7500	Limestone thru rear ports only. Tests #1535-1560. Air meter at 30%.	1539	X	Glass filter as window		11.0	1:2	140		Lens in. Very good, bright hologram. Uniform scattering.	52.
53.	↓	0910	↓	6000	↓ ↓	1542	↓	↓		11.0	↓	150		Lens in. Very good hologram and uniform scattering.	53.
54.	↓	0918	↓	6500	↓ ↓	1543	↓	↓		5.5	↓	175		Lens out. Bright reconstruction. Uniform.	54.
55.	↓	0920	↓	6500	Opposite boiler tube wall not visible.	1544	↓	↓		5.5	↓	170		Lens out. Same as #1542.	55.
56.	↓	0922	↓	7000	↓ ↓	1545		↓	1.0 in top of scene	5.5	↓	160		Lens out. Bright as #1542. Can focus on edge of N.D. filter.	56.
57.	↓	0925	↓	7000	↓ ↓	1547		↓	↓	5.5	↓	140		Lens out. Same as #1545.	57.
58.	↓	0928	↓	6500	↓ ↓	1548		↓	1.0 & 2.0 in top of scene	12.0	↓	165		Lens out. Same as #1545.	58.
59.	↓	0931	↓	6000	↓ ↓	1549		↓	↓	12.0	↓	150		Lens out. Same as #1545.	59.
60.	↓	0948	↓	6000	↓ ↓	1550		↓		7.0	↓	150		Lens in. Bright reconstruction. Apparently uniform scattering. Many "rays".	60.
61.	↓	0951	↓	6000	Limestone supply nearly out.	1552	X	↓		10.0	↓	140		Lens in. Same as #1550.	61.
62.	↓	0953	↓	6000	↓ ↓	1553	N-70 in top of scene only	↓		8.0	↓	175		Lens in. Same as #1550. Rays appear uniformly spaced.	62.
63.	↓	0954	↓	6000	↓ ↓	1554	↓	↓		8.0	↓	150		Lens in. Same as #1550.	63.
64.	↓	0956	↓	6000	↓ ↓	1555		↓		12.0	↓	160		Lens in. Very good, bright hologram. One of best quality of series.	64.
65.	↓	0958	↓	~5000	↓ ↓	1556	X	↓		13.0	↓	180		Lens in. Very good reconstruction. Similar to #1555.	65.
66.	↓	1005	↓	4000	↓ ↓	1558-1559	↓	↓		3.0	↓	170		Double exposure (lens in.). Plate fogged but will reconstruct.	66.
67.	↓	1008	↓	5000	Some limestone feed thru bottom rear ports only.	1560	↓	↓		6.0	↓	140		Lens in. Very bright hologram. Little evidence of limestone.	67.
68.	↓	1108	↓	11,000	Limestone injected thru front 4 ports only. Air at 25%.	1562	↓	↓		7.0	↓	150		Lens out. Gas laser beam barely visible and extinguished at times when visually observed.	68.

Line No.	Date	Time	Power Output MW	Limestone Injection lb/hr	Remarks	Record No.	Hologram Recording Data							Test Conditions & Remarks	Line No.
							Filters Used			Development		Laser Pulse			
							No. 70	CS-2-58	N.D.	Time Min.	HRP Ratio	Output mV	Quality		
69.	3-12-70	1110	~140	~7500	Limestone injected thru front 4 ports only. Air meter 25%	1563	X	Glass filter as window		11.0	1:2	160		Lens out. Bright hologram. Evidence of a cloud at front of boiler.	69.
70.	↓	1113	↓	↓	↓ ↓	1564	↓	↓	1.0 in top of scene	13.0	↓	150		Lens out. Similar to #1563. Good hologram reconstruction.	70.
71.		1115				1565			↓	12.0		155		Lens out. Bright reconstruction but difficult to define limestone cloud edges. Similar to #1563.	71.
72.		1117				1566			1.0 & 2.0 in top of scene	10.0		170		Lens out. Similar to #1563.	72.
73.		1120				1567				10.0		165		Lens out. Bright reconstruction but difficult to precisely identify cloud.	73.
74.		1122		~11,000		1568				6.0		140		Lens in. Cloud visible - has structure and limits. Rays also visible. Good hologram.	74.
75.		1124		↓		1569				5.5		155		Lens in. Very thin limestone cloud. Bright rays seen in reconstruction in foreground. Good hologram.	75.
76.		1125				1570				7.5		120		Lens in. Dense limestone cloud. Edges can be defined. Cloud appears to have some structure. Good hologram.	76.
77.		1127				1571				5.5		130		Lens in. Bright cloud with edges and structure. This is one of the best holograms of this series.	77.
78.		1129				1572				7.0		150		Lens in. Similar to #1570. Note the one predominate "ray" of light in scene. Good hologram.	78.
79.		1130	<140			1573				6.5		160		Lens in. Cloud visible and has structure and boundaries. Good hologram.	79.

STANDARD TITLE PAGE FOR TECHNICAL REPORTS

1. Report No. APTD-0594

2. Govt. Accession No.

3. Recipient's Catalog No.

4. Title and Subtitle

Holographic Determination of Injected Limestone Distribution in Unit 10 of the Shawnee Power Plant

5. Report Date June 1970

6. Performing Organization Code

7. Author(s)

Matthews, B. J. and R. F. Kemp

8. Performing Organization Rept. No.

9. Performing Organization Name and Address

TRW Systems Group
One Space Park
Redondo Beach, California

10. Project/Task/Work Unit No.

11. Contract/Grant No.

CPA 70-4

12. Sponsoring Agency Name and Address

DHEW, PHS, EHS, NAPCA
Division of Process Control Engineering
5710 Wooster Pike
Cincinnati, Ohio 45227

13. Type of Report & Period Covered

14. Sponsoring Agency Code

15. Supplementary Notes

16. Abstracts

Pulsed ruby laser holography was applied as a technique for detecting the penetration and dispersion of limestone plumes injected into the Unit 10 boiler operating at nominal conditions. The experimental equipment, the laboratory experiments, and the test programs are described. Two-beam scattered light holography of particulate in an operating boiler (nominal power output of 140 mw) is entirely feasible. Photometric means of evaluating the reconstructed holographic images have been developed to the extent that quantitative data, as well as qualitative impressions can be obtained.

17. Key Words and Document Analysis. (a). Descriptors

Air pollution
Holography
Air pollution control equipment
Limestone
Distribution (property)
Thermal power plants
Sulfur oxides
Ruby lasers
Penetration
Superheaters

17b. Identifiers/Open-Ended Terms

Shawnee power plant

17c. COSATI Field/Group 13/02, 14/05

18. Distribution Statement

Unlimited

19. Security Class (This Report) UNCLASSIFIED

20. Security Class. (This Page) UNCLASSIFIED

21. No. of Pages 89

22. Price

FORM NBS-867(1-70)

This report was furnished to the National Air Pollution Control Administration by the TRW Systems Group in fulfillment of Contract No. CPA 70-4.